BGC ENGINEERING INC.
AN APPLIED EARTH SCIENCES COMPANY

TOWN OF CANMORE

COUGAR CREEK

DEBRIS FLOOD HAZARD ASSESSMENT

FINAL

PROJECT NO.:	1261-001	DISTRIBUTION:	
DATE:	March 7, 2014	RECIPIENT:	5 copies
DOCUMENT NO.:	TC13-010	BGC:	3 copies

BGC ENGINEERING INC.
AN APPLIED EARTH SCIENCES COMPANY
Suite 800 - 1045 Howe Street
Vancouver, BC Canada V6Z 2A9
Telephone (604) 684-5900
Fax (604) 684-5909

March 7, 2014
Project No.:1261-001

Mr. Andy Esarte, P.Eng.
Engineering Services
Town of Canmore
902 7th Avenue
Canmore, Alberta T1W 3K1

Re: Cougar Creek Debris Flood Hazard Assessment – FINAL

Please find attached our above referenced final report dated March 7, 2014.

It has been a pleasure working on this stimulating project. Should you have any questions or comments, please do not hesitate to contact me at the number listed above.

Yours sincerely,

BGC ENGINEERING INC.
per:

ISSUED AS DIGITAL DOCUMENT.
SIGNED HARDCOPY ON FILE WITH
BGC ENGINEERING INC.

Matthias Jakob, Ph.D., P.Geo.
Senior Geoscientist

EXECUTIVE SUMMARY

This report describes the methods and results for a debris flood hazard assessment of Cougar Creek, located in Canmore, Alberta. The primary objectives of this assessment are to establish a relation between the magnitude (sediment volume and peak flow) and frequency of debris floods and to identify representative debris flood scenarios that could potentially lead to damages and loss of life. These scenarios were modelled numerically using a two-dimensional flood routing model which allows for variable sediment concentrations and rheologies to assess potential impacts on the fan. The results of this assessment will form the basis for an assessment of debris flood risk, which will be provided in a separate report.

Hydro-geomorphic Processes

BGC's analyses indicate that significant sediment movement on Cougar Creek derives from two distinct data populations.

The first population is interpreted as debris floods where sediment concentrations (bedload and suspended sediment) increase in response to extreme rainfall and elevated bank erosion rates. Such debris floods are believed to be triggered by decadal to perhaps century scale return period rainfall likely in conjunction with late spring or early summer snowmelt. The change from normal bedload transport and debris flooding is likely transitional. Given the low channel gradient (~5%) along Cougar Creek, sediment entrainment is largely through the tractive forces of water, rather than mass channel bed mobilization as can be observed on steeper channels.

The second data population is interpreted to consist of debris floods triggered by hillslope processes (debris flows, slumps, ravels) feeding sediment to the main channel as well as landslide dam outbreaks from either tributary debris-flows or rock slides of variable size. Evidence of such events was observed at numerous locations along the channel and may be associated with prevalent paired terraces that are observed in the field and verified by LiDAR-generated shaded relief imagery. Rockslides were found to be abundant, largely along dip and overdip slopes in the sedimentary rocks of the Cougar Creek watershed.

BGC also documented matrix-supported sediment facies[1] on the fan with clay contents up to 11% in test trenches and along natural channel exposures that may suggest a mass movement (landslide dam outbreak flood) origin rather than bedload entrainment. Further support for this hypothesis is gained through the observation of an overall convex fan slope. This shape may be expected as mass movement processes (landslide dam outbreak floods) preferentially deposit the majority of their sediment load in the proximal fan portions where channel confinement is lost and flow depth abruptly decreases. Last not least paired

[1] Sediment facies are a body of rock or soil with specified characteristics

terraces were encountered along the channel of Cougar Creek suggesting past outbreak floods and subsequent fluvial incision.

Frequency-Magnitude[2] Analysis

The frequency – magnitude analysis in this study is based on two independent approaches. The first relies on physical evidence of previous debris floods deciphered from the stratigraphy in test trenches on the Cougar Creek fan. This work was supplemented with dendrochronological investigations and measurements of debris flood inundation areas using historical air photographs in combination with empirical formulae relating inundation area to debris volume. Detailed cross-section measurements at paired terraces flanking Cougar Creek assisted in estimating peak flows of past debris floods interpreted as resulting from landslide dam outbreaks. The second approach applies an empirical formula derived from a comprehensive Swiss dataset that correlates sediment transport volumes to runoff volumes. Combining all data allowed the construction of a frequency-magnitude relationship (Table ES-1-1). According to this analysis the best estimate debris flood volume of a 3000-year event could reach some 260,000 m^3, while the 10,000-year return period event may reach up to 320,000 m^3. The best estimates were used for numerical modeling and fed into the risk assessment. The volume and peak discharge values presented herein should not be viewed as exact but as reasonable approximations for the respective return period class.

Table ES-1-1. Debris flood frequency – magnitude relation for Cougar Creek.

Return Period (T) (yrs)	Annual Probability (1/T)	Volume Best Estimate (m^3)	Peak Discharge (m^3)	Dominant Hydro-Geomorphological Process
1-10	1-0.1	< 6,000	-	flooding
10-30	01-0.03	30,000	30	flooding/debris floods
30-100	0.03-0.01	40,000	50	flooding/debris floods
100-300	0.01-0.003	60,000	60	debris floods
300-1000	0.003-0.001	160,000	700	landslide dam outbreak floods
1000-3000	0.001-0.0003	260,000	1000	landslide dam outbreak floods

On the basis of the above table, the 2013 debris flood at Cougar Creek is estimated to correspond to approximately a 400-year return period.

Despite the combination of several analytical techniques, substantial uncertainty persists in the temporal and volumetric reconstruction of previous events and it is not possible to claim that a continuous record of large debris floods for the 3000 years of observation has been

[2] The term "magnitude" is used in this context because it may be interchangeably used for debris flood volume and peak discharge.

reconstructed. Nonetheless, the combination of analytical techniques and an independent of fan volume against the frequency magnitude relationship test allows an approximation as a suitable basis for numerical modelling.

Numerical Modeling

Based on the frequency-magnitude analysis, the event scenarios in Table ES were simulated with the two-dimensional flood routing model FLO-2D. Debris flood scenarios with a return period of less than 10-years were not modeled, as those are very likely to remain in the present channel under consideration of the proposed short-term mitigation measures. Pertinent results from the modelling exercise include:

- Debris floods of return periods up to 30 years and corresponding sediment volumes of up to 30,000 m^3 are expected to remain confined in the channel of Cougar Creek. Avulsions are unlikely at Elk Run Boulevard and at Highway 1. Due to the low culvert capacity and low channel gradient, avulsions are still considered to be possible at Highway 1A and the CPR.
- Debris floods of higher return periods and thus higher volumes are more likely to block the existing culverts, especially those at Highway 1, Highway 1A and CPR.
- Debris floods of return periods exceeding approximately 300 years are likely to avulse at Elk Run Boulevard particularly onto the eastern fan segments.
- At the present time (e.g. with the currently designed channel crossing), avulsions at Elk Run Boulevard are more likely to affect the eastern fan sector than the western fan sector.
- The presently constructed mitigation measures (channel widening and armoring, grade control structures and a debris net with an approximate storage capacity of 20,000 m^3) are significantly reducing debris flood risk for flows up to a 30-year return period, and provide some risk reduction for flows up to 300 years. For flows exceeding a 300-year return period, the short-term mitigation measures currently under construction will have little effect on reducing the potential of fan inundation, but will reduce erosion along the banks of Cougar Creek.

The major conclusions of the numerical modeling are that:

- Inundation of the eastern and western fan sectors becomes increasingly likely for event magnitudes in excess of the 2013 debris flood.
- Portions of the east fan sector would likely have become inundated during the 2013 event if not for the efforts by the Town of Canmore to keep the Elk Run Boulevard culvert free of debris.

Debris Flood Hazard Mapping

For each return period class as listed above, debris-flood hazard intensity maps were prepared (Drawing 11). For areas with higher velocity (>1 m/s) flows, these maps display an impact index calculated as flow depth multiplied by the square of flow velocity. Flood depths are shown where velocities were below 1 m/s (e.g. where inundation depth becomes the controlling factor for flood damage)[3]. These intensity maps provide a measure of the destruction potential for a given debris flood scenario and form the basis to assess debris flood risk. This risk assessment, which considers both the probability and consequences of debris flood impact, can then form the basis to optimize risk reduction planning. Methods and results of the risk assessment, as well as additional hazard and risk maps, will be provided under separate cover in a forthcoming report.

[3] This 1 m/s velocity threshold should be considered preliminary and may be adjusted during the risk analysis.

TABLE OF CONTENTS

LIST OF TABLES

LIST OF FIGURES

LIST OF APPENDICES

LIST OF DRAWINGS

LIMITATIONS

BGC Engineering Inc. (BGC) prepared this report for the account of the Town of Canmore. It presents the results of a frequency-magnitude analysis for debris floods on Cougar Creek.

The material in this memorandum reflects the judgment of BGC staff in light of the information available to BGC at the time of report preparation. Any use which a Third Party makes of this memorandum or any reliance on decisions to be based on it is the responsibility of such Third Parties. BGC accepts no responsibility for damages, if any, suffered by any Third Party as a result of decisions made or actions based on this report. In particular, BGC accepts no responsibility for changes in real estate values that may occur as a consequence of this report.

As a mutual protection to our client, the public, and ourselves, this report is submitted for the confidential information of the Town of Canmore. Authorization outside of this use for publication of data, statements, conclusions or abstracts from or regarding this report and drawings is reserved pending our written approval.

Anyone outside of the Town of Canmore receiving a copy of this report ought to recognize that these documents represent an interim step in the risk management process as defined by Canadian Standards Association Guidelines.

1.0 INTRODUCTION

1.1. Background

The southwestern Alberta mountain front was affected by a high intensity/duration rainstorm between June 19 and 21, 2013. Direct runoff, coupled with meltwater released from rain-on-snow, caused sudden and prolonged high flows in the Bow, High, and Ghost Rivers and their tributaries originating in the Rocky Mountains. These flows resulted in high rates and volumes of sediment transport, bank erosion and avulsions on alluvial fans[4].

Almost all of the steep gradient tributaries to Bow River within the municipal boundary of the Town of Canmore (Town) were affected by the combined storm and snowmelt runoff, including Cougar Creek, the focus of this report. Major damage was sustained on Cougar Creek fan due to sediment deposition and bank erosion along the principal channel which is flanked by dense development. Economic damages were in excess of $13.5 million for emergency assessments and reconstruction costs alone (pers. comm., Alberta Transportation and ISL Engineering and Land Services Ltd., 2013), although these do not include many additional costs such as services provided by the fire department (e.g. time, food, or equipment), town staff (e.g. overtime, benefits, food, clothes, and equipment), or any costs associated with flood relief accommodations. They also do not include estimates of direct damage costs to impacted development and infrastructure (e.g. roads, buildings, property, water/sewer system, gas, or power transmission), costs of professional services to assess hazard and risk (e.g. this assessment), or costs of long-term risk reduction measures.

The Town retained BGC Engineering Inc. (BGC) to complete a forensic analysis of the June 2013 debris flood event on Cougar Creek (BGC, 2013). Information contained in that report includes the following:

- Details on the Cougar Creek watershed, channel and fan reaches
- A systematic summary of previous studies as they related to Cougar Creek hydrology and geomorphic processes
- A chronological description of the June 2013 debris flood with a characterization of damages
- A summary of hydroclimatic conditions that led to the storm event
- A preliminary frequency analysis based on air photograph interpretation
- Conceptual short and long-term mitigation options.

BGC also authored a second report that provides additional details on the rainfall, snowpack and streamflow characteristics of the June 19-21 storm (BGC, 2014).

[4] Alluvial fans are fan-shaped deposits of water-transported material (alluvium). They typically form at the outlet of tributary streams into a main valley where there is a marked break in slope.

1.2. Hazard and Risk Assessment

The two forensic reports represent a staged approach (Stage 1) to the analysis of debris floods at Cougar Creek with the ultimate objective being the implementation of mitigation options that protect the residents on Cougar Creek fan from future debris floods, which could potentially be of larger magnitude than the 2013 event.

For creek hazards, Canadian practice has been to estimate the discharge of a 100-year or 200-year return period flood[5] and design protection to defend against the associated flood stage. This hazard-based method, while based on sound assumptions, does not account for severity of consequences to assets at risk. For example, a purely hazard-based approach cannot identify changes in risk due to changes in vulnerabilities of certain elements at risk. An increase in vulnerability results, for example, by an increase in development in areas subject to debris floods. As such, international best-practices have generally moved towards a risk-based approach that explicitly and systematically evaluates the consequences of flooding. This approach facilitates objective determination of the optimal approach to risk reduction. Such approaches allow a transparent and repeatable evaluation of potential flood mitigation alternatives, allow comparison of flood risk to other risks faced by society, and help define thresholds for the tolerance of flood risk.

As an example, a decision might be made to protect a community against flooding for a return period of 200 years. The hazard-based approach would then be to construct or raise an existing dike so that the dike was constructed to the 200-year flood level plus an appropriate freeboard allowance. In contrast, a risk-based approach would assess the probability of flooding and associated consequences for a range of return periods and evaluate options for flood risk reduction. This evaluation could be made from a purely economic perspective or based on flood risk tolerance thresholds for loss of life.

Through consultation with BGC, the Town has adopted a quantitative flood risk assessment (QFRA) approach to debris floods at Cougar Creek. A staged approach has been adopted for such an assessment, as follows:

- Stage 1 was a forensic analysis of the 2013 debris flood event and providing conceptual recommendations for short-term mitigation (BGC, 2013).
- Stage 2, the focus of this report, is establishing the frequency (i.e. return period) and magnitude (i.e. peak flow and sediment volume) of debris floods arriving at the fan apex. Stage 2 represents a hazard assessment of debris floods on Cougar Creek.
- A QFRA will be completed in Stage 3. The primary objective of the QFRA is to establish the optimal risk reduction benefit from a combination of engineering measures, early warning, contingency plans in case of a landslide dam outbreak flood and passive measures as per future zoning regulations.

[5] In this context “floods” are referred to as clearwater floods with minor bedload movement and wash load.

Design and construction of debris flood mitigation measures would then follow these assessments.

1.3. Study Scope and Objectives

This report provides a detailed debris flood hazard assessment on Cougar Creek fan (Stage 2). The study objectives are to:

- Summarize scientific and engineering studies with respect to hydrology and flood/debris flood hazard management that have been conducted on Cougar Creek fan
- Determine the frequency and magnitude of debris floods originating from the watershed and arriving at the fan apex
- Complete hydraulic modelling to assess the intensity (destructive power) of various return period debris floods.

This report was written by BGC and has been reviewed by the Town, as well as a Peer Review Group consisting of Drs. N. Morgenstern (University of Alberta), J. Pomeroy (University of Saskatchewan) and M. Church (University of British Columbia). Results from this report form the hazard basis for the subsequent QFRA.

The two BGC (2013, 2014) reports should be read in conjunction with this debris flood hazard assessment to provide the relevant context.

1.4. Report Organization

This report is organized as follows:

- Section 2 provides background on the geology and Quaternary history of the area and Cougar Creek watershed. This information is important to understand fan evolution, watershed processes, and the potential of landslide dams. This latter mechanism drives the risk for the low frequency – high magnitude events.
- Section 3 discusses the processes that generate debris floods on Cougar Creek.
- Section 4 details the analytical methods used to decipher debris flood frequency and presents results.
- Section 5 focuses on the estimation of debris flood volume and peak discharge using a variety of analytical methods.
- Section 6 combines the results from Sections 4 and 5 into a frequency-magnitude relationship and presents five return period classes from 10 to 30 years to 1000 to 3000 years.
- Section 7 provides the results of two-dimensional hydraulic modelling for the return period classes identified in Section 6.
- Section 8 summarizes the major conclusions of the assessment.
- Appendix A summarizes BGC's review of the available engineering reports on Cougar Creek.

- Appendix B summarizes BGC's review of archived regional newspapers.
- Appendix C provides the stratigraphy logs from the test trench field program.
- Appendix D provides the results from the radiocarbon dating of samples retrieved during fieldwork.
- Appendix E provides the results of the dendrochronology analysis of tree samples retrieved from Cougar Creek channel.
- Appendix F provides a graph showing historical Bow River discharge at Calgary (from "The 2013 Great Alberta Flood: Actions to Mitigate, Manage and Control Future Floods" prepared by Alberta WaterSMART Water Management Solutions Ltd. August 2013.

2.0 GEOLOGY

An understanding of the bedrock geology in the study area is important for two reasons. First, it provides an understanding of the geologic groups eroding and forming sediment sources to Cougar Creek, which is important from a sediment balance perspective. Secondly, it provides an engineering geologic interpretation of landslides that have dammed Cougar Creek in the past and may do so in the future. This chapter commences with a brief description of the regional geology and then focuses on the engineering geology that is important with regard to sediment delivery into Cougar Creek. The section concludes with a brief description of the Quaternary geology of the area, in as far as it relates to sediment processes at Cougar Creek.

2.1. Regional Geology

The Canadian Rocky Mountains (CRM) are a fold and thrust belt, where thick units of more erosion resistant Paleozoic carbonates were folded and thrust progressively in a north-westerly direction over more friable Mesozoic sandstones and shales. Four main sequences of rocks can be characterized in the Canmore region.

The oldest unit at the base is referred to as the basement rocks of the North American cratonic plate (30 – 50 km thick), which bears no relevance to this present study. The next unit is the Pre-Cambrian to Lower-Cambrian clastic and minor carbonate rock unit (~10 km thick) composed of weathered rock from the Canadian Shield (further east). The ~ 6.5 km thick middle carbonate unit (Middle-Cambrian to Upper Jurassic, 540 – 155 M[6]a) consists of marine carbonates (limestone and dolostone) and shale. The upper unit (~ 5 km thick) is composed of a young Jurassic to Tertiary (155 – 1.9 Ma) unit of sandstone, shale, conglomerate and coal. This final unit consists of eroded sediments from an uplifting landscape into a foreland basin to the east (Gadd, 1995; Henderson *et al*, 2009).

Osborn *et al.* (2006) describe the final stages of the mountain building stage as being associated with differential erosion of various units. The softer Mesozoic rocks led to rounded mountain tops exposing the underlying Paleozoic and Proterozoic rocks that can support steeper and higher slopes.

2.2. Bedrock Geology

The geologic exposures within the Cougar Creek drainage are primarily composed of thick Carboniferous and Devonian successions. Most of the rock units are of Lower Carboniferous (Mississippian) origin with some representation of Upper Carboniferous (Pennsylvanian) and Devonian units (Drawing 1).

Most of the rock formations are sedimentary (carbonates and siliciclastics) with minor metamorphic components (i.e. calcite). Geologic formations that are more resistant to

[6] Ma stands for million years

erosion are more conducive to the formation of cliffs, while more recessive units tend to form sloping ledges. This concept is illustrated well by the most resistant, cliff-forming rock units such as the Palliser, Pekisko, Shunda, Livingstone and Mount Head formations. More erosive units such as the shale-dominated Banff and Exshaw formations are gently sloping ledges (Figure 2-1).

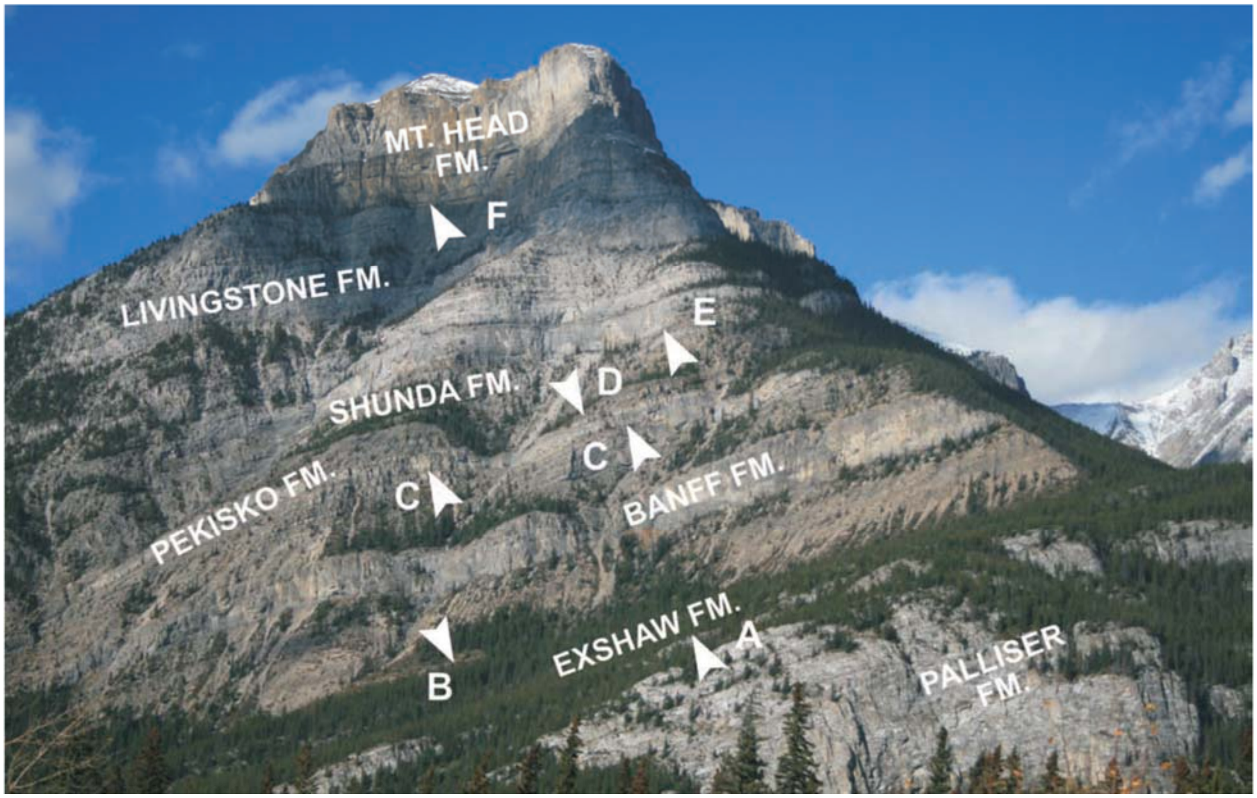

Figure 2-1. Grotto Mountain looking northwest from Exshaw, Alberta. This image gives a good general overview of the Upper Devonian and Lower Carboniferous formations that exist in the Cougar Creek drainage. A- top of Palliser Formation; B – top of Exshaw Formation and base of Banff Formation; C – base of Pekisko Formation; D – Base of Shunda Formation: E – base of Livingstone Formation; F – base of Mount Head Formation. Modified from Henderson *et al.* (2009).

2.3. Engineering Geology

This section describes BGC's interpretation of relations between bedrock structure and stratigraphy, mass movements and weathering rates in the Cougar Creek watershed. It is discussed in some detail because it is postulated later in this report that landslide damming and subsequent dam outbreak represent a significant hazard to fan residents.

2.3.1. Overview

Thrust faults and folds in the region strike in a northwest to southeast direction. Two common joint sets can be differentiated: strike joints parallel to the orientation of bedding planes and dip joints that are perpendicular to bedding. Conjugate joints occur on rare occasions (Cruden and Hu, 1999). The main channel of Cougar Creek drainage is oriented approximately at a right angle to the main thrust fault belt.

The lower reaches of Cougar Creek (A to B in Drawing 1) cross the Spray River Group and Ishbel and Spray Lakes Group. These rock types consist largely of quartz sandstone, dolomitic sandstone, silty dolomite, and chert. Because these groups that trend northwest-southeast only occupy very small sections of the lowermost watershed, they are of negligible importance with respect to mass movement processes.

From C to D (Drawing 1), the Cougar Creek watershed crosses the Etherington, Mount Head and Livingstone Formations with interbedded limestone, dolomite, sandstone, shale and siltstone. These formations are important as they supply rock-fall derived sediment to the lower tributaries of Cougar Creek from where they are remobilized as episodic debris flows. These episodic debris flows are the principal geomorphic process delivering tributary sediment to the mainstem of Cougar Creek. On the southeast flank of Mount Lady MacDonald, rocks of these groups expose steeply (~ 35º) southward dipping limestone beds, some of which lack buttressing against the opposing strike slope. The steep dips, in combination with lack of lateral confinement on the east side, make such beds candidates for large rock slope failures. For example, Figure 2-2 shows a location in the lower (western) Cougar Creek watershed where this process could result in a failure of up to 300,000 m^3.

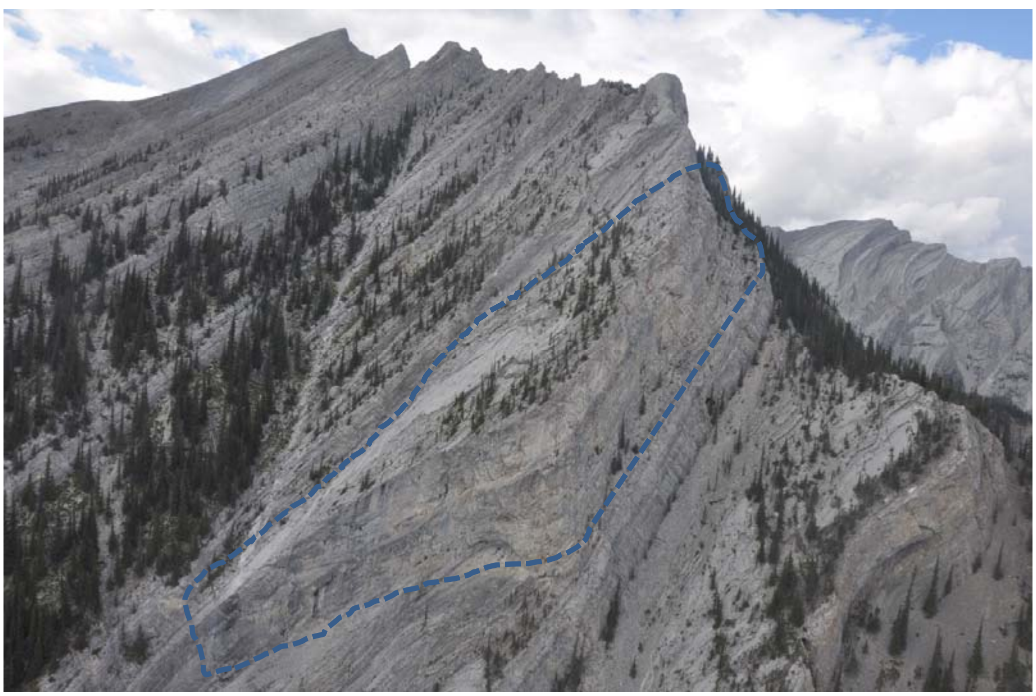

Figure 2-2. Large, potentially unstable rock mass in the lower (western) Cougar Creek watershed in steeply dipping limestones. The unbuttressed rock mass (dashed blue line) in mid photograph is approximately 180 m long, 80 m wide, 10-20 m thick and approximately 35º steep. BGC photograph of August 7, 2013, looking west.

A rock slope failure of this magnitude would quickly narrow in the downstream gully likely bulking in volume through erosion of surface sediments. In this case, the travel distance would be approximately 1 km over a relief of approximately 600 m (from the landslide toe). By the time the rock slide reached the valley bottom, it is conceivable that the mass movement would create a landslide dam.

Despite the abundance of limestone in the Cougar Creek watershed, karst[7] was observed in only a few cases (Figure 2-3). No correlation could be drawn between known landslide occurrence and karst development.

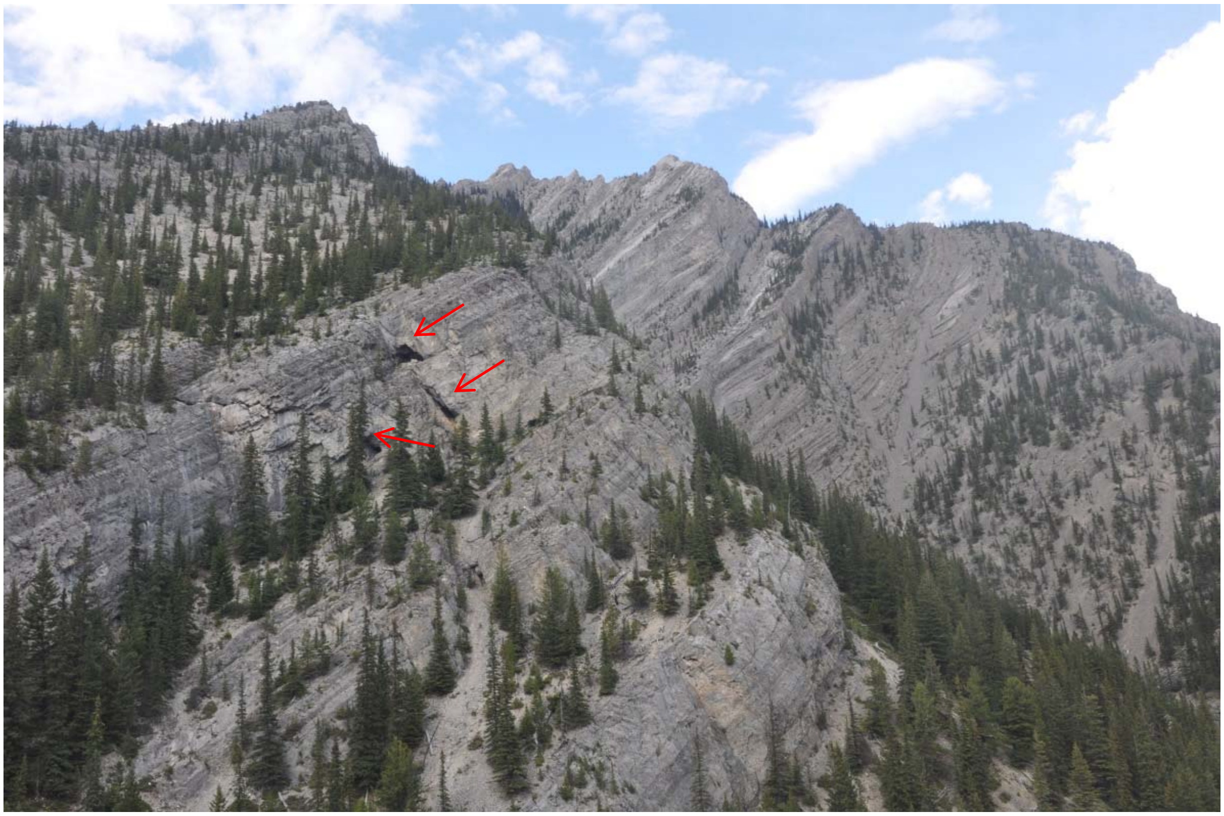

Figure 2-3. Outcrops of the Etherington Formation with karst formation (caves) in the lower (northern) portions of the Cougar Creek watershed. Red arrows denote caves. BGC photograph of August 7, 2013, looking north.

Between points E and F (Drawing 1), Cougar Creek traverses rocks of the Shunda, Pekisko and Exshaw and Banff formations as well as at least two northwest-trending thrust faults, including the Inglismaidie Thrust fault.

In the northwestern portions of the watershed, slivers of parallel trending outcrops of the Spray River, Ishbel and Spray Lakes Group are encountered (e.g. Figure 2-4). At high

---

[7] Karst describes a landscape underlain by limestone which has been eroded by rock solution, producing ridges, towers, fissures, sinkholes and other characteristic landforms

elevation, outcrops of these sedimentary rocks are susceptible to heavy frost weathering and have formed largely smooth talus slopes. Unlike the more competent limestone and dolostones of the adjacent Etherington and Mount Head formations, these Triassic sedimentary rocks are less prone to cliff formation and thus have lower susceptibility to rockfall.

Figure 2-4. Outcrops (circled in yellow) of the Triassic Spray River and Ishbel and Spray Lakes Group Rocks on the eastern flanks of Mount Lady MacDonald. Google Earth image.

The northwestern portions of the Cougar Creek watershed expose Paleozoic sedimentary rocks that are members of the Exshaw and Banff Formations. These rocks consist of thinly bedded limestones, shales, siltstones as well as calcarenitic limestone and argillaceous dolomites. Due to the higher erosion susceptibility of these more fissile rock units, ridges composed of these groups have become smooth. In the periglacial belt[8] (see Section 2.4), gelifluction[9] lobes can be observed sporadically. Current sediment production rates from these rocks are believed to be significantly less than those of the more competent limestones due to the lack of rockfall-producing cliffs and a lower areal abundance. In one instance, a rock slide deposit was interpreted as originating from the Exshaw Formation (Figure 2-5). This rock slide does not appear to have evolved into a long-runout rock avalanche as evidenced by its lobate appearance near its source zone.

[8] The periglacial belt is subject to conditions (environment), processes and landforms associated with cold, non-glacial environments that are affected by sub-zero temperatures and frost action.

[9] Gelifluction is the slow downslope flow of unfrozen earth materials on a frozen substrate.

Figure 2-5. Rockslide in the northernmost portion of the Cougar Creek watershed. The landslide is delineated in yellow. Mount Townsend (2820 m) is seen in the background. The lighter-coloured rocks in the foreground belong to the Palaeozoic Livingston Formation. Google Earth image.

2.3.2. Rock Structure, Friction Angles and Landslide Susceptibility

Cruden and Eaton (1987) mapped 228 rockslides in the Kananaskis (south of the Cougar Creek watershed) and developed a hierarchy of regional rock formations in terms of landslide susceptibility. The Devonian Palliser Formation was found to have the highest susceptibility to rock slides followed by the Permo-Carboniferous Rocky Mountain Group (i.e. Ishbel and Spray Lakes Groups) and Lower Carboniferous Rundle Group (i.e. Mount Head Formation).

With respect to rockslides and rock avalanches in the Cougar Creek watershed, the following principal rock units and failure mechanisms can be differentiated:

- Overdip and dip slope rock slides along steeply inclined bedding planes (Figure 2-6 and Figure 2-7), primarily in rocks of the Livingstone Formation
- Topples along daylighting dip slopes (Figure 2-8)
- Rock fall from toppling from anaclinal[10] slopes (Figure 2-10).

The first two factors are the primary kinematic factors associated with larger scale instability, particularly where such failures would connect directly to the mainstem of Cougar Creek (Figure 2-10). Large scale failures of this type can and have travelled into the valley bottom

[10] Having a downward inclination opposite to that of a stratum.

where they can dam Cougar Creek creating a sizable impoundment given the low overall creek channel gradient (5%).

Figure 2-6. Rock slide deposits in the northernmost headwaters of Cougar Creek along a pronounced southeast-trending syncline that roughly defines the valley bottom. Note the steeply dipping and daylighting joint sets on both side of the valley. The slope of the limestone beds on the right (east) is approximately 40º, while on the left (west) it is approximately 35º. BGC photograph, Aug. 7, 2013, looking north.

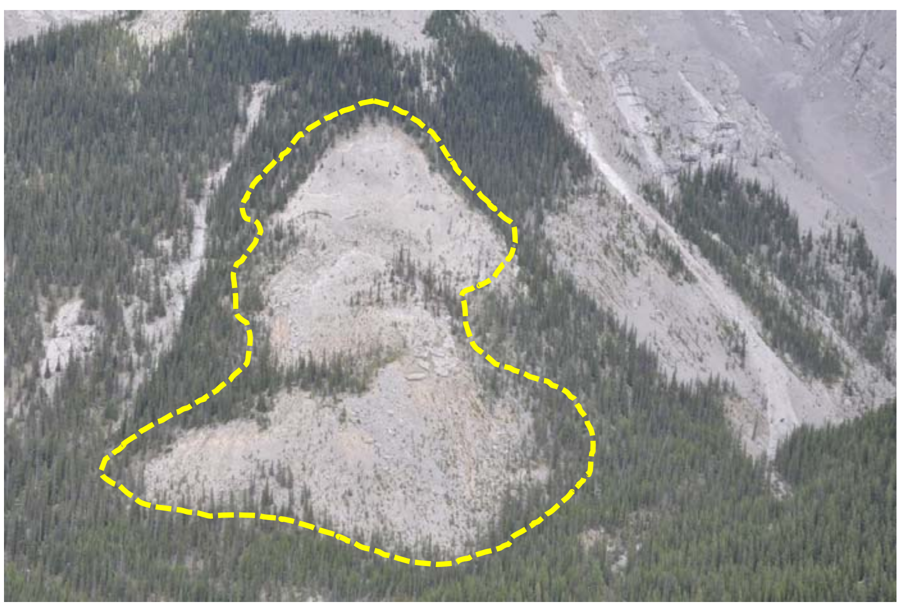

Figure 2-7. Large rockslide complex in the upper, northern headwaters of Cougar Creek in the upper Devonian Palliser Formation. The rock slide, as delineated in yellow, is approximately 400 m long, 150 m wide and perhaps 10-30 m thick. The slope angle of the upper, exposed failure surface is approximately 37º. BGC photograph of August 7, 2013, looking east.

Figure 2-8. Large-scale toppling of limestone beds in an eastern tributary of Cougar Creek. The individual topple towers are approximately 20 m high. Note tension cracks indicated with a white arrow. BGC photograph of August 7, 2013, looking SE.

Figure 2-9 shows a recent rock slope failure of approximately 3000 m^2 and an estimated average thickness of 10 m which resulted in a rock slide of approximately 30,000 m^3. It travelled some 600 m and some of the rocks ran into a tributary east of Cougar Creek. This failure is of interest in that it happened sometime between 30th of September, 2010 and April 27, 2012 and is thus likely the most recent rock slide in the Cougar Creek watershed.

Figure 2-11 illustrates a steeply dipping rock stratum in the Exshaw formation. Unlike the case in Figure 2-9 an abrupt failure of this rock mass that encompasses an area of approximately 70,000 m^2 and an estimated thickness of 20-30 m would most likely travel to and dam Cougar Creek.

Figure 2-9. Recent (between Sept. 30, 2010 and April 4, 2012) rock slide in the central Cougar Creek watershed. The upper failure scarp is indicated by a white arrow. The average slope in the failure zone is 42º. Google Earth 2010 and 2012 imagery. North is to the top.

Figure 2-10. Rock fall producing cliffs on the strike slope of Grotto Mountain, primarily composed of the Mount Head and Livingstone Formation. BGC photograph of August 7, 2013, looking south.

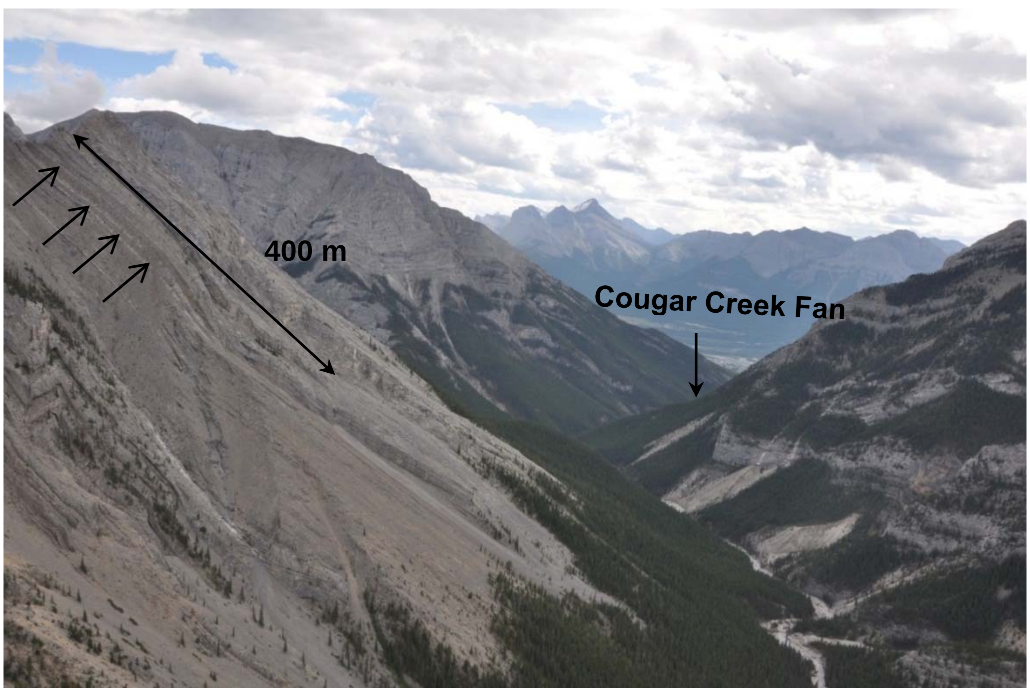

Figure 2-11. Photograph of steeply dipping strata of the Exshaw Formation outcropping above the mainstem of Cougar Creek with discontinuities daylighting slightly above treeline. Weaker rock units (black arrows) are preferentially eroded. The average dip angle is 33º. BGC photograph of August 7, 2013, looking southwest.

2.4. Periglacial Processes and Landforms

Periglacial processes are defined in this report as processes associated with cold, non-glacial environments that are affected by sub-zero temperatures and frost action. In Cougar Creek these zones are preferentially located on north-facing slopes from 2300 m elevation, and on the other aspects, above 2600 m elevation. Periglacial landforms identified in upper Cougar Creek include gelifluction lobes and rock glaciers.

Figure 2-12 shows one such rock glacier, located in a northern tributary of Cougar Creek. The rock glacier is raveling into the creek and a recent failure in the active layer of the rock glacier was described in BGC (2013). The presence of active rock glaciers is relevant to this assessment as an indicator of alpine permafrost. However, rock glaciers themselves do not constitute a landslide hazard, as their dominant form of mass movement is slow creep, typically along one or more shear zones.

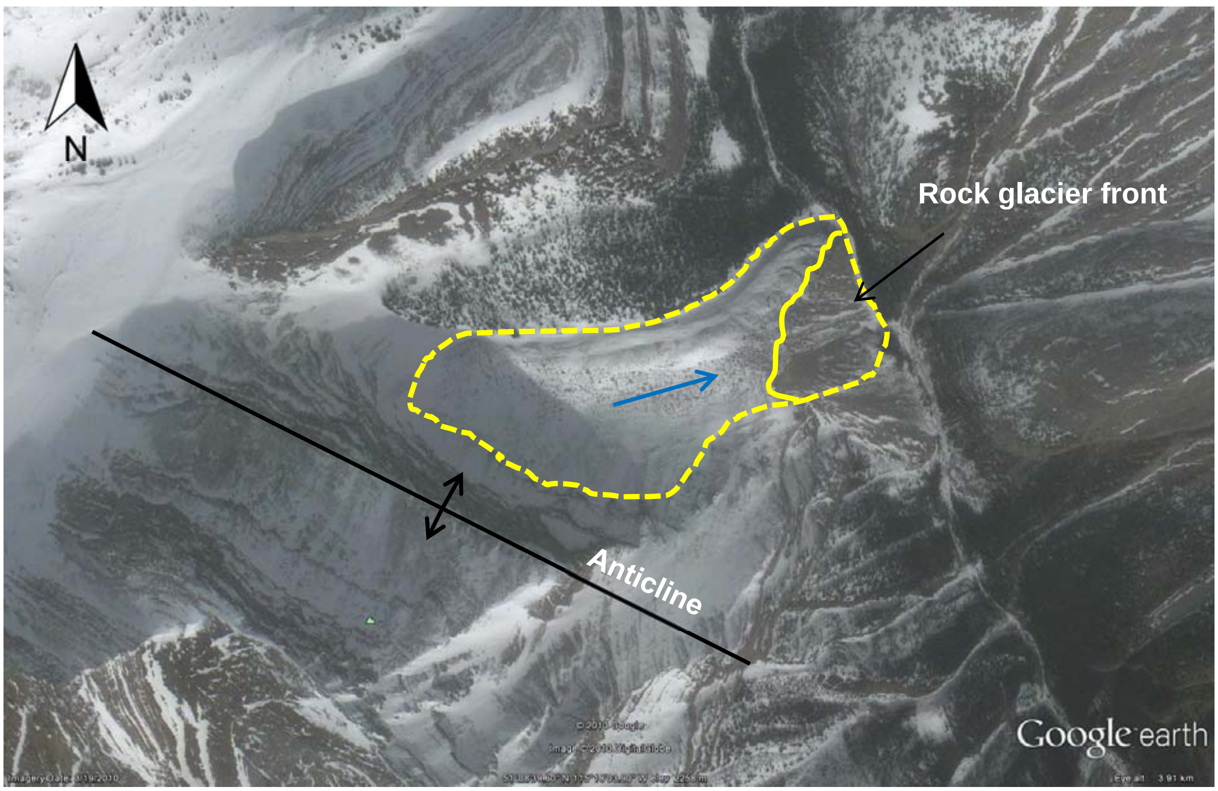

Figure 2-12. Rock glacier southeast of Mount Charles Stewart (2809 m) that was likely generated from failure along a southeast trending anticline whose axis forms the ridge to the west. The rock glacier front is now ravelling into the mainstem of Cougar Creek. The creep direction is indicated by a blue arrow. Vertical Google Earth satellite image.

2.5. Quaternary Geology

The late Pleistocene era (past 126,000 to approximately 11,700 years) of the Bow Valley and Cougar Creek fan development must be considered for any detailed fan study because geomorphic processes particularly during the latter part of the late Pleistocene supplied sediment to the channel system and influenced fan formation processes that followed the retreat of ice. Some late Pleistocene deposits are likely still providing sediment to the channel system.

The Cougar Creek watershed is located in a region that was affected by phases of glaciation and de-glaciation during the Holocene period (11,700 years BP to present).

The Late Pleistocene and Holocene epochs of the Quaternary Period in the Canadian Rockies represent a period of changes in climate due to a transition from extensive glaciation to de-glaciation. During this period, the final stages of major glacial erosion and deposition occurred and the establishment of the present day Quaternary sedimentation in the Bow Valley was initiated. In order to understand the relations between the Quaternary sediments, this section will first describe the paleo-climatic conditions that existed, the specific glacial advances that occurred, and then will address the sedimentation that resulted.

2.5.1. Late Pleistocene and Holocene History of the Canmore Area

The Late Pleistocene and Early Holocene (127,000 years BP to present) are the latter epochs of the Quaternary geologic time period. The Quaternary period experienced alternating colder periods, with extensive glaciation and short interglacial periods in which temperatures in the mid-latitudes were higher than they are presently.

Late Pleistocene glaciers reached their maximum extent in the Canadian Rockies around 16,500 years BP after which significant climatic warming led to the decay of the extensive mountain ice sheets (Menounos *et al.*, 2009). During the Holocene there have been some minor periods of glacial advance and retreat that were restricted to the high elevation icefields and cirques (Reasoner *et al.,* 1994). Such advances provided sediments in the form of moraines to the channel system and likely locally oversteepened some slopes. The lack of morainal deposits in the watershed can likely be explained by the high rates of geomorphic activity that eroded or obliterated evidence of Holocene glacial advances.

It is likely that the tributary valleys were ice-free when there was still a sizable glacier in Bow Valley. This glacier would have created a dam against which ponding would have occurred in the principal tributary valleys. Particularly in low gradient valleys such as Cougar Creek, glaciolacustrine[11] sediments indicate the development of glacially dammed lakes that may have persisted for many years or even centuries. Eventual drainage of these lakes and subsequent erosion has exposed thinly bedded lacustrine sediments in soil outcrops such as along Cougar Creek channel (Figure 2-13). At times, such lakes would have overtopped the

[11] Sediments deposited at the bottom of lakes dammed by glaciers

main trunk glacier in the Bow Valley or drained through subglacial conduits. The frequency of such events is unknown. The principal significance of the occurrence of lacustrine sediments is that they serve to estimate the rate of geomorphic activity since their deposition.

Figure 2-13. Fine-grained (clayey silts) lacustrine beds outcropping along Cougar Creek channel and underlying debris flow deposits. Beds are 30 cm to 100 cm thick and thinly varved[12]. BGC photograph of August, 2013, looking downstream along west side of channel.

The early Holocene experienced a period of drought called the Hypsithermal that caused the lowering of lake levels, higher treelines and almost complete ablation of glaciers between 10,000 years BP and 9,400 years BP. According to studies in lake sediment cores, the glaciers did not re-establish until 6,800 years BP (Beierle, 1997; Beierle and Smith, 1998).

The term “Little Ice Age” is used to describe the late Holocene cooling time period beginning in approximately the 1200s and terminating in the mid-1800s with the present day warming trend. Summit Icefields, valley glaciers and cirques reached their Holocene maximum extent during this period of time (Luckman, 2000). As discussed above, there is little evidence of Little Ice Age moraines in the upper watershed of Cougar Creek where landslides and erosion may have removed such evidence over the past century and a half.

[12] Varving describes the seasonal layering of fine sediments in the stratigraphy that is due to changing grain size input between the flow season (spring, summer and fall) and winter.

2.5.2. Bow Valley Glaciation

There have been several studies on the Quaternary geology of the Canadian Rockies that contain information on Pleistocene and Holocene glaciation. The first series of detailed studies of the region were completed by Rutter in the 1960s and 1970s who originally described four glacial events (Rutter, 1965, 1966a, 1966b, 1972). The events are the Pre-Bow Valley Advance, Bow Valley Advance, Canmore Advance and Eisenhower Junction Advance. Rutter later discarded the notion of the Pre-Bow Valley Advance (Bobrowski and Rutter, 1992) and it will be excluded from the discussion.

Bow Valley Advance

The timing of the Bow Valley Advance (BVA) is not conclusive, but was interpreted by Rutter (1972) and Clague (1989) as occurring between 25,000 and 21,000 years before present. The BVA is represented by breaks in slope due to glacial erosion as well as thick accumulations of till overlying glaciofluvial outwash gravels. The BVA extended into the foothills of the Rockies and retreated to the area of the Banff town site (Rutter, 1972). This advance likely deposited significant amounts of sediment at the mouth of Cougar Creek and into the lower watershed that was subsequently eroded by creek processes.

Canmore Advance

Following the retreat of BVA, the Canmore Advance included glacial advance to a position near Mount Yamnuska. Rutter (1972) determined the thickness of the ice by observing the break in slope due to glacial erosion (Table 2-1). Jackson (1980) concluded that the ice from the Canmore Advance was in retreat by 12,000 years BP. As for the BVA, this glacial advance likely supplied ice marginal sediments and morainal material in the vicinity of the Cougar Creek outlet but was the quickly eroded by fluvial processes.

Table 2-1. Estimated ice thickness of the Canmore advance (modified from Rutter, 1972).

Location	Maximum Ice Elevation (masl)	Approximate Ice Thickness (m)
Park Boundary on SW side of Bow Valley	1554	229
Near Canmore, SW side of Bow Valley	1509	152
Near Canmore, SW side of Bow Valley	1554	229

Eisenhower Junction Advance

Rutter (1972) termed the final ice advance between 25,000 – 21,000 years BP as being the Eisenhower Junction Advance. This advance did not reach the Canmore area and thus has little, if any, significance to sedimentation processes in the Cougar Creek watershed.

2.5.3. Late Pleistocene and Holocene Sedimentation

Paraglacial Processes

An important component of the development of Quaternary sedimentation is the notion of paraglacial processes. Church and Ryder (1972) defined the term as ‘non-glacial processes that are directly conditioned by glaciation’. The ‘paraglacial period’, in which enhanced sediment yields occur, begins during the commencement of deglaciation and follows an exponential decline through time based on the proportion of sediment that is available to be reworked. The timing and magnitude of sediment yield can be influenced by the size of deglaciated catchment basins, with smaller basins having a peak sediment yield early after deglaciation and larger basins having a longer more gradual peak (Harbor and Warburton, 1993). Ballantyne (2002) discussed the occurrence of ‘renewed paraglacial sediment reworking’ by ‘extrinsic effects’ including ‘climate change, extreme climatic events’ and ‘anthropogenic activity’. This renewed sediment release can occur millennia after deglaciation occurs. The importance of the paraglacial period lies in the early fan formation and the fact that fan aggradation rates may not have been constant during the Holocene. This realization is key when using fan volumes to compare with the frequency-magnitude relationship (see Section 6.0).

Kame Terraces

Sediment terraces flank the main valleys of the Canmore area and were interpreted as kame terraces by Rutter (1972). Kame terraces are ‘gently sloping depositional terraces perched on valley sides and are deposited by meltwater streams flowing between glacier margins and the adjacent valley walls’. They are composed primarily of fluvial sands and gravels with some lacustrine sediment resulting from glacial meltwater ponding. Since the retreat of the glaciers, the kame terraces that likely blocked the Cougar Creek drainage, have been eroding and reworked by periodic stream flow and flooding events. As such they provide a contemporary sediment source for Cougar Creek debris floods.

Colluvial and Alluvial Fans

Most of the colluvial[13] and alluvial[14] fan development occurred in the lower Bow Valley between the retreat of trunk valley ice (~12,000 years BP) and the Hypsithermal (~ 6000 years BP), as determined by the stratigraphic location of Mazama tephra (Section 4.4) in the upper sediments of a number of fans (Roed and Waslyk, 1973). Kostaschuk (1980) discussed the two distinct types of colluvial and alluvial fans in the Bow Valley. Colluvial fans built primarily from debris flow deposition, appear to have witnessed higher sediment delivery rates during the Early Holocene prior to 6,600 years BP whereas alluvial fans built primarily by debris flood and flood deposition maintained a more constant rate of sediment delivery

[13] Fans primarily formed by debris flows.

[14] Fans primarily formed by floods or debris floods, the latter are significantly lower gradient than the former.

during the Holocene. The debris-flow fans are characterized by muddy matrix-supported unsorted clasts, while the fluvial fans consist of generally well sorted gravels. Jackson (1987) determined that fans with a slope angle greater than 8% are generally debris flow dominated and those of a lesser angle tend to be fluvial dominated.

Recent studies on active fans in the region include a detailed analysis of the August 1999 debris flow at Five Mile Creek Basin near Banff by de Scally *et al.* (2004). The event was triggered by an intense localized rain event and caused the closure of the Trans-Canada Highway. Most of the fan was considered to be constructed shorty after deglaciation through debris flow dominated paraglacial processes, but had been considered inactive until the 1999 event (de Scally *et al.*, 2004).

Glacial Lacustrine

Kostaschuk and Smith (1983) interpreted the origin of late Quaternary lacustrine and deltaic sediments in the Bow Valley, Alberta. The study found that the site of the present day Vermilion Lakes near Banff, Alberta had gone through three distinct phases from the late Pleistocene to the mid Holocene. Sedimentological evidence in the form of beach gravel and near shore sands (~ 1400 m elevation) indicated that the ice-dammed Glacial Lake Vermilion (10.5 km^2) developed during the retreat of the Canmore glacial advance (Rutter, 1972). When the glacial ice continued retreating to the west, Proglacial Lake Vermilion (15 km^2) formed at the elevation of the present day valley floor (~ 1383 m). Between 10,000 and 8000 years BP, the third stage termed Holocene Lake Vermilion (11 km^2) formed and the Bow River delta prograded into the lake to produce the present Vermilion Lakes.

Evans *et al.* (1999) completed a stratigraphic and sedimentological analysis of glaciolacustrine deposits in the Barrier Lake area of Kananaskis Country, Alberta and concluded that a proglacial lake had been dammed by the Bow Valley Advance. Later during the Canmore Advance.

It is unknown which of the above described lakes flooded tributary valleys but is not considered to be a major source of sediment to present-day fan formation processes. However, their existence provides a convenient base level above which sediments have been deposited. Accumulations of rock slide and debris flow sediments can thus indicate the rate of deposition since at least 8000 years BP.

Tephras in the Study Area

During the Holocene, several volcanic eruptions distributed volcanic ash (tephra) over the region. While there are several known tephras distributed further north in the Canadian Rockies, the two tephras generally found in the Lower Bow Valley are the Mazama tephra (Crater Lake, Oregon) and the Bridge River tephra (Mount Meager, British Columbia) (Osborn *et al.,* 2001). Kostaschuk and Smith (1983) located Mazama and Bridge River tephras within sediments near Banff, Alberta. Mazama tephras generally have a bed thickness of greater than 10 cm.

According to Osborn *et al.* (2001), the Mazama tephra has a radiocarbon age of ca. 6,730 years BP and the Bridge River tephra 2,332 years BP based on varve counts from Hector Lake.

These deposits are stratigraphic markers as the age of eruptions is known and are thus useful when encountered in test trenches to determine fan aggradation rates at the specific location where the tephra is encountered (see Section 5 and 6)

2.5.4. Summary

A review of the late Pleistocene and Holocene history of the study area provides insight into the history and availability of colluvial and alluvial sediment deposition in the study area. It is likely that a period of high sediment recruitment from mobilization of Late Pleistocene sediments was followed by lower rates of fan aggradation as the majority of such sediments were depleted and replaced by modern day erosion processes.

3.0 DEBRIS FLOOD PROCESSES

3.1. Terminology

Steep mountain creeks are typically subject to a spectrum of mass movement processes that range from clear water floods to debris floods to debris flows in order of increasing sediment concentration. There is a continuum between these processes in space and time with floods transitioning into debris floods and eventually debris flows through progressive sediment entrainment. Conversely, dilution of a debris flow through partial sediment deposition and tributary injection of water can lead to a transition towards debris floods and eventually floods.

Debris flows typically require a channel gradient in excess of some 30% for transport over long distances and have volumetric sediment concentrations typically in excess of 50-60%. The distinction between floods, debris floods and debris flows is important, as they differ in flow mechanics and potential consequences.

A debris flood can be defined as: “a very rapid surging flow of water heavily charged with debris in a steep channel” (Hungr *et al.*, 2001). Debris floods typically occur on creeks with channel gradients between 3 and 30%. The term “debris flood” is similar to the term “hyperconcentrated flow”, defined by Pierson (2005) on the basis of sediment concentration as “a type of two-phase, non-Newtonian flow of sediment and water that operates between normal streamflow (water flow) and debris flow (or mudflow)”. Transitions from water flow to debris flood / hyperconcentrated flow and vice versa occur at minimum volumetric sediment concentrations of 3 to 10%. Debris floods (as defined by Hungr) have slightly lower sediment concentrations than hyperconcentrated flows (as defined by Pierson), but this range depends on the overall grain size distribution and the ability to acquire yield strength[15]. In this report, both debris floods and hyperconcentrated flows are termed debris floods.

3.2. Debris Flood Populations

BGC completed a number of investigations on the fan and watershed to determine the nature of the primary fan-formation processes. These included test trenching on the fan and a traverse of the mainstem channel of Cougar Creek from the upper watershed to the fan apex.

3.2.1. Test Trenching

A total of 16 test trenches were dug by use of hydraulic excavators between August 5 and 8, 2013 on Cougar Creek fan down to a depth of approximately 5 m. The test trenches were

[15] The yield strength is the internal resistance of the sediment mixture to shear stress deformation; it is the result of friction between grains and cohesion (Pierson, 2005).

excavated as part of the frequency-magnitude analysis, which is described in more detail in Sections 4.0 and 5.0. Test trench locations are shown on Drawing 2.

Three sides of the test pits were sloped to 2V:1H to allow safe access to the trench and the vertical face that served for logging was stepped at approximately half depth with a 1.5 m wide bench for access and safety reasons. The vertical face was cleaned by shovel and trowel and each unit was logged separately using texture and structure as principal characteristics. Observations were specifically focused on whether the samples were clast-supported (i.e. a majority of the clasts are in contact) or matrix-supported (i.e. individual clasts are rarely in contact). The former is typical for flood and debris flood deposits, while the latter is indicative of mass movement processes such as debris flows or debris floods initiated by landslide dam outbreak floods. Clast imbrication[16], bedding, normal or inverse grading or the absence thereof were also noted and helped in the identification of individual flow units. In addition to the excavated test trenches, one point along the east side of the channel was also logged, where the 2013 debris flood had eroded part of the bank. This location is also shown on Drawing 2.

3.2.2. Channel Traverse

Cougar Creek channel was hiked from approximately 8 km upstream of the fan apex to the apex. During this descent, BGC identified 13 locations at which landslide dams may have formed in the past (Drawing 3). Six of those are at the bottom of gullies or steep tributaries and are likely associated with debris flows. The other seven are likely associated with rock slope failures as evidenced by the sedimentary stratigraphy of the landslide dams. BGC considers it possible that debris flow damming may occur simultaneously in a single heavy storm. However, since rock slope failures are not as clearly associated with heavy storms, we consider it less likely that such failures occurred during the same storm. In absence of known dates of such events, this is speculative. An example of such a landslide dam is shown in Figure 3-1 and Figure 3-2 below. Judging from the location of the dam at the mouth of a steep tributary creek, BGC believes that this landslide dam may have been associated with a particularly large debris flow.

A LiDAR survey was completed soon after the June 2013 event by LiDAR Services International Inc. (LSI) on June 28, 2013. However, that survey only extended to the municipal boundary of the Town of Canmore. McElhanney Consulting Services Ltd. (McElhanney) was therefore retained by the Town to conduct an additional LiDAR survey along the mainstem channel of Cougar Creek that extended to the upper watershed. The extent of this survey is shown on Drawing 3. This second LiDAR survey was completed on August 23, 2013, and provided BGC with invaluable data for this assessment. Drawings 9 and 10 show profiles of Cougar Creek fan and the watershed, respectively.

[16] Clast imbrication is the preferential orientation of individual boulders such that they overlap one another in a consistent fashion like a run of toppled dominoes.

Figure 3-1. Large landslide deposit overlying fluvial sediments approximately 1.1 km upstream of the fan apex. Figure 3-2 shows the detail delineated here as a red box. The height of the landslide deposit above the current channel bed is approximately 25 m. BGC photograph of August 29, 2013, looking west.

Figure 3-2. Fluvial sediments underlying coarse, angular matrix-supported landslide debris at the location of Figure . BGC photograph of August 29, 2013.

3.2.3. Interpretation

From these investigations, BGC has concluded that debris floods on Cougar Creek are triggered by two processes that may interact to some degree:

- Intensive rainfall events (potentially augmented by concurrent snowmelt)
- Landslide dam outbreak floods.

The former process is more likely associated with lower magnitude – low return period events (high frequency), and will result in fluvial-dominated deposition on the fan (i.e. a clast-supported deposit). In contrast, landslide dam outbreak floods are associated with high magnitude – high return period events, and are perhaps more likely to generate a matrix-supported deposit. The former process is more consistent with the 'debris flood' terminology of Hungr *et al.* (2001), while the latter is more consistent with the term 'hyperconcentrated flow' as championed by Pierson (2005). As described in Section 3.1, for simplicity, both terms are referred to as debris floods in this report.

The 2013 debris flood was highly erosive and exposed cut banks (2 to 4 m high) along Cougar Creek for much of its length. These cut banks show pronounced layering of sediments with variable characteristics, and indicate that debris flood and flood events are a common occurrence. A particularly illustrative example is shown in Figure 3-3 below. This approximately 2 m high cut bank shows what appears to be two separate massive and matrix-supported deposits overlying a fluvial deposit that shows sorting, imbrication and is clast-supported. The massive nature of the matrix-supported deposits is consistent with the hypothesis of landslide dam outbreak floods and resulting hyperconcentrated flows, while the underlying fluvial deposit is more suggestive of a flow similar to the June 2013 event. Similar stratigraphic layers were observed in the test trenches (Section 4.4).

However, it was not possible to count the number of floods and debris floods from exposures because cycles of channel bed aggradation and degradation censor the available record.

It should be noted that this process distinction by sedimentary stratigraphy is associated with significant uncertainty. For example, downstream dilution of the events from tributary confluences may lead to a change in the sedimentary characteristics of the event to a degree where a landslide dam outbreak flood may no longer be clearly recognizable as such from its deposits on the medial or distal[17] fan.

[17] On alluvial fans, one can separate three zones of roughly equal distance as measured radially from the fan apex. "Proximal" is used for the one third of the fan sector closest to the fan apex, "medial" is used for the middle fan section and "distal" is used for the fan sector furthest away from the fan apex.

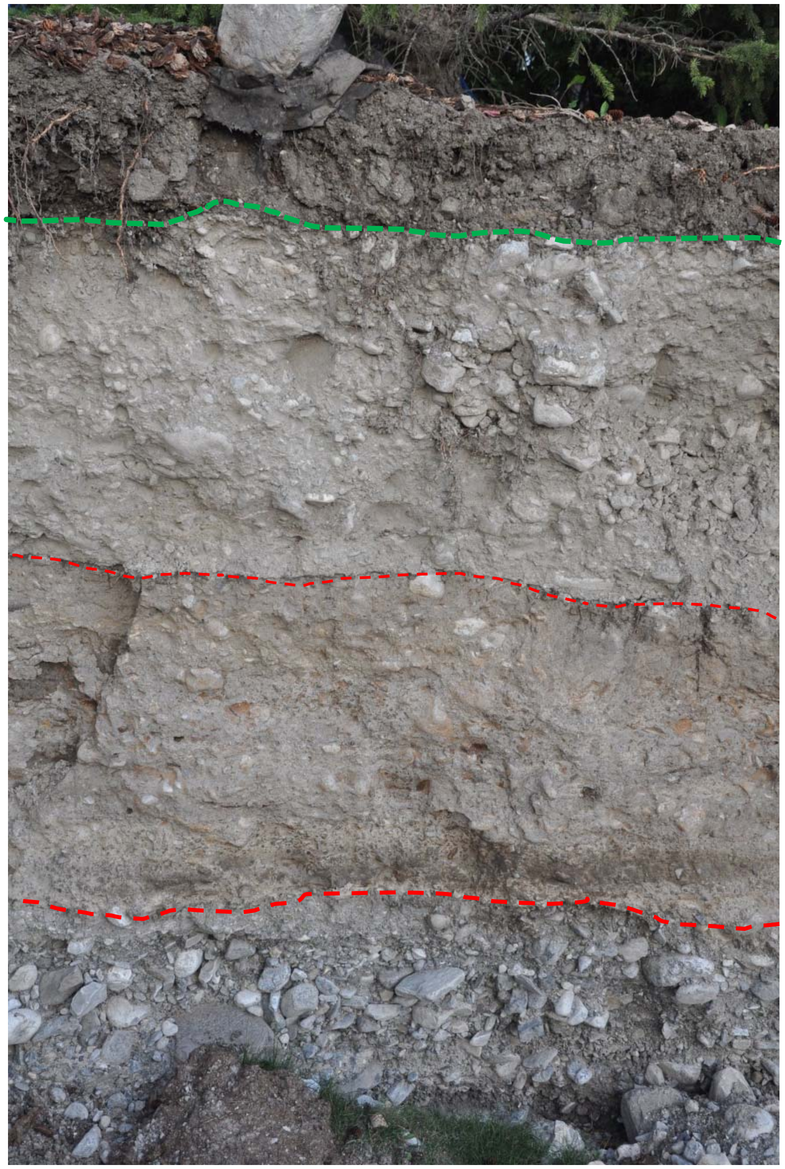

Figure 3-3. Exposed cut bank along the left bank of Cougar Creek between the pedestrian bridge and Elk Run Boulevard. The two dashed red lines delineate a massive matrix-supported hyperconcentrated flow deposits overlying a fluvial deposit. The unit below and above the green dashed line is likely construction fill. BGC photograph of July 23, 2013.

3.3. Grain Size Analysis

Grain size samples were obtained for granulometric analysis to attempt a differentiation of deposits by process. BGC hypothesized that samples with higher fines content in the matrix of the bulk samples are possibly associated with landslide dam outbreak floods. If confirmed, this would need to be reconciled in the construction of frequency-magnitude curves that account for bi-model process types.

The presence of matrix-supported sediments is often used as a distinguishing criterion between debris flow deposits and fluvial deposits (Costa, 1984). However, as noted by Jordan (1994), this interpretation is questionable if matrix and clasts cannot clearly be defined. Jordan found that in the case of debris flows there is only a weak bimodality and thus, little basis for defining matrix and clasts. Jordan used a threshold of < 4 mm grain size to define "matrix". Jordan (1994) noted that the distinction between matrix-supported and clast-supported appears to result from orientation of large clasts in the debris-flow deposit, which can be inferred visually but not through quantitative sampling. Therefore, while the grain size analysis described herein is useful for general inference, it needs to be recognized that by itself it is an insufficient tool to separate deposits by their originating process. Moreover, debris flows and debris floods are transitory phenomena that can change from one rheology to another over short distances depending on influx or loss of water to the slurry as well as the size-dependent entrainment or deposition of sediment.

Thirty-one (31) samples were submitted for grain size analysis. Samples were truncated at 0.08 mm and 50 mm and analysed by a combination of dry sieve, wet sieve and hydrometer by Shelby Engineering Ltd. in Edmonton, AB. The samples were taken from test trenches BGC-TP-2, BGC-TP-6, BGC-TP-9, BGC-TP-13, BGC-TP-18, BGC-TP-19, BGC-TP- 20, BGC-TP-21, BGC-TP-30, BGC-TP-38, BGC-TP-41, BGC-TP-45, BGC-TP-46, BGC-TP-47, and BGC-TP-48, as well as three samples collected from matrix-supported diamictons[18] exposed on the left (east) bank of Cougar Creek from erosion during the June 2013 event. These are interpreted as originating from landslide dam outbreak floods and shown in Figure 3-3. The majority of samples show a fairly distinct grain size distribution that can be attributed to high sediment transport rates and are labeled in red in Figure 3-4. BGC interprets that those samples that show a higher fines content that plot distinctly different from the majority of samples can be attributed largely to landslide dam outbreak floods. Those with even higher fines contents and few or no cobbles are interpreted as flood or overbank deposits (labeled as yellow in Figure 3-4). These are primarily found in the distal fan sectors where deposition prevails and where, during periods of relative quiescence paleosols can develop (labeled as green in Figure 3-4).

Clay contents in the sampled fine fractions range from 3 to 11%. The higher clay fractions may again be associated with entrainment of landslide dam debris that may have pulverized to clay fraction during its descent. Jordan (1994) used a matrix clay content of 4 to 5% to differentiate between coarse-textured and fine-textured debris flows in the Coast Mountains of British Columbia, and Scott *et al.* (1992) classified debris flows as cohesive (> 3 to 5% clay) and non-cohesive (< 3% clay). The former, they noted, resist mixing with water in stream channels and travel longer distances downslope. Such percentages may be somewhat different in the Canadian Rocky Mountains that are dominated by limestones. Jordan (1994) further pointed out that the fine-textured debris flows are more uniform in

[18] Diamicton consists of a wide range of non-sorted to poorly sorted sediment, i.e. sand or larger size particles that are suspended in a mud matrix

thickness and leave more uniform layers of fine debris in the channel after they pass which is typical also for debris floods. Furthermore, none of the observed natural exposures or test trenches showed upward coarsening of the stratigraphy that would be indicative of coarse-grained debris flows.

It should be recognized that debris floods and landslide dam outbreak floods are transient processes in which water dilution or water loss during avulsions can change the rheological and thus sedimentary signature of these flows. This transient nature implies that, while grain size analysis provides some clues as to the origin of the sediments analysed, it is insufficient to conclusively confirm or reject hypotheses as to the exact process type.

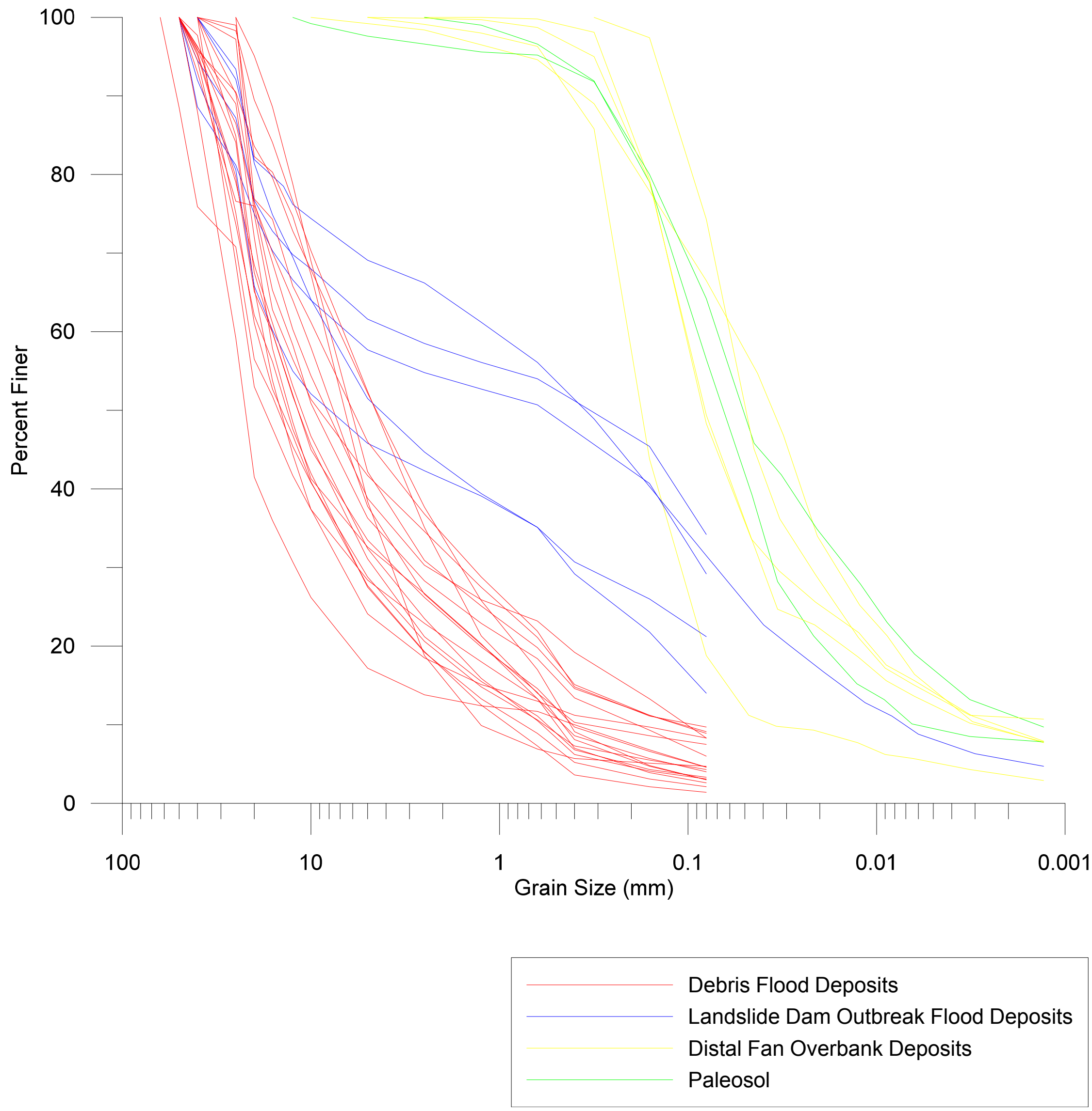

Figure 3-4. **Grain size curve from all samples with interpreted process type. The blue lines include the 'diamictons' interpreted from field observations. Note that some of the red lines here described as debris flood deposits may also include some**

landslide dam outbreak flood deposits which may have diluted during downstream transport.

In summary, the grain size analysis suggests that the majority of sampled deposits are interpreted to having derived from debris floods with a relatively high content of coarse (> 4 mm grain size) materials, but with clay contents up to 11% in their distal portions. It is believed that deposits with higher fines content may be indicative of landslide-dam outbreak floods (hyperconcentrated flows) during which a higher portion of fines from the remnants of the landslide dam is integrated into the resulting flow. This interpretation is complicated by the fact that rock slide dams, particularly those with sources close to the stream channel, may incorporate less fines than a tributary debris flow that also dammed the main channel. Significant variability in the grain size distribution can therefore be expected. Based on these limitations, BGC believes that processes cannot be reliably separated based on grain size analysis only.

3.4. Fan Slope

Further support for landslide dam outbreak floods at Cougar Creek is gained through the observation of an overall convex fan slope. The channel gradient on the upper fan is approximately 3%, increasing to 5.1% between Elk Run Boulevard and Highway 1, and 4.3% between Highway 1 and 1A (see Drawing 6, BGC 2013). Usually, fans have a fairly even slope, or display some concavity where they interfinger with floodplain deposits. In contrast, a convex channel profile may be indicative of mass movement processes (landslide dam outbreak floods) which preferentially deposit the majority of their sediment load in the proximal fan portions where channel confinement is lost and flow depth abruptly decreases.

4.0 FREQUENCY ANALYSIS

4.1. Introduction

Frequency analysis assesses how often hydro-geomorphic[19] events such as debris floods and debris flows occur, on average. Frequency can be expressed either as a return period or an annual probability of occurrence. For example, if five debris floods have occurred within a 100 year period, the average return period is 20 years and the annual probability is the inverse, so 0.05, or a 5% chance that a debris flood may occur in any given year.

Frequency and magnitude (volume and peak discharge) of floods and debris floods are inversely related. The higher the frequency, the lower the debris flood magnitude and vice versa. In short, the rarer an event, the larger it will be. This inverse frequency-magnitude relationship also occurs with other geophysical phenomena such as earthquakes, tsunamis and hurricanes. A frequency analysis alone does not inform on the relationship between magnitudes and frequencies. This relation is the subject of Section 5.0.

The frequency principle is complicated by several factors:

1. A continuum exists between flooding and debris flooding and sometimes even debris flows. Exact differentiation can only be achieved through direct sampling of the sediment-water slurry and subsequent measurement of the water-sediment ratio. Furthermore, it is often difficult to detect when bedload transportation through rolling and saltation[20] of individual particles ends, and mass mobilization of the channel bed begins. As this process hinges on channel slope, as well as grain size distribution and stream power, it may also undergo flux in time and space in the same event.

   Just like debris floods, floods in steep mountain creeks such as Cougar Creek transport large amounts of debris as bedload, which is being differentially deposited. Characteristic flood deposits with normal grading (finer particles on top) may be observed along the fan fringes but are rare on alluvial fans in mountainous environments. Clear differentiation by deposit texture and structure is challenging. With respect to frequency analysis, this implies that mixed (debris flood/flood) populations can be expected in the stratigraphic column and that some judgment needs to be applied to assign the observed deposits to either a debris flood or a hyperconcentrated flow as defined by Pierson (2005).

2. Frequency analysis assumes that the occurrence of debris floods or either origin (heavy rain or landslide dams) is stationary over time and that there is no upward or downward trend in the occurrence of debris floods. While one can still average return

---

[19] Hydro-geomorphic processes are Earth-surface processes whose dominant driver is water, albeit at varying concentrations with respect to sediment.

[20] Saltation is a specific type of particle transport by fluids such as wind or water. It occurs when loose material is removed from a bed and carried by the fluid, before being transported back to the surface.

periods over time series in the past, an observed trend would not allow one to extrapolate the long-term average into the future as such an average may over or underestimate future debris flood frequencies. This is especially important in light of climate change, which increasingly challenges the stationarity assumption (Milly *et al.*, 2008). BGC's initial analyses and a precursory scanning of the pertinent literature (BGC, 2014) demonstrated that the frequency of extreme rainfall and runoff events have been increasing for the last two decades or so. Thus, average frequencies of the past may no longer serve as adequate surrogates for debris-flood frequencies of the future.

3. Frequency analysis assumes that all data stem from the same data population (data homogeneity), which assumes the same debris flood triggering process. At Cougar Creek, this assumption is likely not valid and this limitation should be noted. Debris floods may be generated by the following processes:
    a. intensive rainfall events with or without concurrent snowmelt; and
    b. landslide dam outbreak floods

   These separate processes imply data non-homogeneity which needs to be recognized in the analysis.

4. Frequency analysis assumes data independence. This implies that one climatic event leading to a debris flood cannot influence the occurrence of the next one. While this is likely true for individual debris floods on Cougar Creek, it is possible that larger climatic cycles may create time-dependent clusters of climatic events leading to debris floods. Furthermore, supply-limited tributary debris flows will need to recharge after large events that deplete sediment supply sources. This will create some time dependency in reoccurrence as individual channel will need to recharge. At this stage, such clustering is somewhat speculative and does likely not warrant a different type of statistical analysis.

In the following sub-sections, sources of frequency data are detailed that were applied at Cougar Creek to determine debris-flood event frequencies. These include the following:

- Previous reports
- Newspaper records
- Historical accounts
- Historic air photograph interpretation
- Radiocarbon dating
- Dendrochronology
- Observations of historic landslide dam locations along the mainstem channel of cougar creek.

4.2. Historical Accounts

4.2.1. Previous Reports

BGC reviewed several engineering reports in the forensic review (BGC, 2013), and identified previously reported debris flood and/or flood events on Cougar Creek in 1948, 1956, 1967, 1974, 1980, 1990, 1995, 2003, 2005, and 2012. A summary of the reported comments on these events is included in Appendix A.

4.2.2. Newspaper Records

Newspapers at the Alberta Provincial Archives and the Alberta Legislature Library were searched for articles reporting debris floods and/or floods on Cougar Creek. The available newspapers were:

- The Banff Crag and Canyon (1900 – 2013)
- The Canmore Miner (1975 – 1983)
- The Canmore Leader (1983 – 2013)
- The Calgary Herald (1888 – 2013).

The search focused on the events listed in the reviewed engineering reports listed above. However, a review of precipitation data from the Kananaskis climate station indicated additional years, other than those listed above, that had high 1 to 3-day rainfall occurring in the spring months. These dates include 1952, 1953, 1963, 1969, 1992, 1998, 1999, 2002, 2007, and 2008. In some cases, these unreported years had higher observed rainfall than the years that had reported flood events. Because a complete-as-possible record of events is critical to a frequency analysis, years with high rainfall but yet undocumented flooding were examined.

Appendix B summarizes the information found during the newspaper search. BGC's search focused on flooding on Cougar Creek but also noted flooding on the Bow River as a potential indicator for regional flooding. The newspaper articles mostly confirmed what was written in the reviewed engineering reports (Appendix A,) but did provide additional information. There were also some inconsistencies between the reviewed engineering reports and the newspaper reports. The main findings are summarized below. Appendix B provides a more extensive summary of each reviewed newspaper article.

- The Bow River was reported to have high water levels in 1879, 1897, 1902 (Dawson, 1885), 1918, 1923, 1933, and 1948.
- A Trans-Canada bridge crossing collapsed due to a debris flood on Cougar Creek in 1967. The Calgary Herald reported that an estimated 70,000 to 80,000 cubic feet of sediment was deposited under the bridge. Of note is that this sediment volume was reported as cubic yards in a 1993 report by CH2M HILL.

- The 1974 flood was only reported on the Bow River in the Banff Crag and Canyon. There were no archived local Canmore papers until 1975, and this may be why reports of flooding on Cougar Creek were not found.
- There was only a brief mention of high water levels (presumably on the Bow River) in the reviewed 1980 news reports.
- There was extensive coverage of the 1990 dam break on Cougar Creek in both the local Banff and Canmore papers. Reports also noted that the flooding could have been much worse if temperatures were higher and more snowmelt occurred.
- On June 6, 1995, an estimated 2100 to 2400 m^3 of sediment was hauled out of the channel during a debris flood on Cougar Creek.
- There were no reports of flooding on Cougar Creek in 1999. Heavy snows and rains were reported which was consistent with the high precipitation data from the Kananaskis station.
- The work of backhoes clearing sediment from the culverts prevented washout at the Canadian Pacific Railway (CPR) tracks during a debris flood on Cougar Creek in 2005.
- There were reports of flooding on the Bow River in 2007; however, no flooding on Cougar Creek was mentioned.
- Rain, snow, and cold weather were reported on May 27, 2008. No flooding was reported.

4.2.3. Historical Records

BGC received information from the Town of Canmore regarding previously reported event dates, as well as for the years that had high rainfall, but no reported flood activity. Table 4-1 summarizes this information. BGC also contacted CPR and Alberta Transportation (AT) to obtain additional data on debris floods or flooding. CPR provided the following data which were received from their contractor:

2005	8,780 m^3	2010	5,980 m^3
2006	3,450 m^3	2011	4,550 m^3
2007	4,310 m^3	2012	6,805 m^3
2008	0 m^3	2013	28,586 m^3
2009	6,360 m^3		

While these data are of interest, they do not allow the conclusion that such volumes relate to single debris floods as they dates of arrival of these sediments is unknown and the volumes relate to only the location near the train tracks.

BGC also interviewed a local resident and contractor. A summary of all BGC personal communications is included in Table 4-1.

Table 4-1. Summary of personal communications.

Date of Communication	From	Comments
August 7, 2013	Ms. Straw 94-year old local Canmore resident	Ms. Straw remembered a large flood on Cougar Creek on May 24, 1948. She remembered this date specifically since it was when she first moved to Canmore, and it was the beginning of the summer season.
November 8, 2013	Richard Bremner, P.Eng. President of Bremner Engineering & Construction Ltd. (BEC)	Bremner Engineering has been contracted by the Town of Canmore to clear debris from Cougar Creek for many years. • Mr. Bremner recalled 1990, 1995, 2005, and 2013 as being the worst flood years on Cougar Creek in his memory. During these years, there were roughly 12 of his machines working in the creek to keep the crossings clear. • 2003 and 2012 were not very bad flood years for Cougar Creek. BEC cleans out roughly 5,000 to 8,000 m^3 of sediment between Bow Valley Trail and the CPR every year.
November 4, 2013	Terry Riva Senior Engineering Technician, Engineering Services, Town of Canmore	• Canmore became a village in 1963 and before then, it was a mining community, with most of the community's operations being controlled by the Mine. Flood records were likely lost when the mine closed in 1979. • Very little information exists for any dates before 1969. Damages during this period of time would have most likely been to the Mine on the southwest side of the Bow River • The largest flood on Bow River was in 1974, when the Town declared a natural disaster. Town records improved after 1983; however, much of the flood events were recorded by the province.
November 7, 2013	Bob Kuzminski Director of Disaster Services and Community Preparedness, Town of Canmore	• Cougar Creek flooded in 1974 • In 1990, the constructed dam collapsed on Cougar Creek. Heavy flow occurred but resulted in minimal damage • In 2003, heavy flow occurred with minimal damage. • Damage to CPR culverts occurred in 1995 and 2003. • Expressed the opinion that heavy rainfall is not always indicative of high and potentially destructive flows and that the key to predicting flooding on Cougar Creek is how much snowmelt has occurred prior to heavy rainfall.

4.2.4. Summary

Based on the above review of historical accounts, there were likely debris floods on Cougar Creek in 1948, 1956, 1967, 1974, 1980, 1990, 1995, 2003, 2005, and 2012. Including the most recent debris flood in 2013, there have been reports of 11 events in 66 years, giving a 6-year return period for events on Cougar Creek.

The historical accounts do not provide a clear indication of the scale of each event relative to each other. More damage was reported in newspapers of the floods in the 1990s and 2000s, but this is likely due to increased local Canmore coverage, as well as increased development on the fan. The Town records and personal communications were similarly skewed as there was poor record-keeping prior to the 1980s and most people interviewed could only comment on the more recent events.

The high rainfall years with no reported events are likely accurate and may indicate either a lack of concordant snowmelt, snowfall at higher elevation or lack of antecedent moisture, or a combination thereof. Only 2007 had reports of flooding on the Bow River, with no mention of flooding on Cougar Creek. Flooding on the Bow River at Banff, though fed by mountain creeks upstream of Banff, does not necessarily indicate simultaneous debris floods from mountain creeks downstream of Banff due to local variations in meteorology, climate and hydrology.

Although these accounts do not provide a clear indication of the frequency-magnitude relationship, the information collected does provide anecdotal indication of magnitude, especially when sediment volumes were reported. There were inconsistent reports of sediment volume in 1967 and this issue was addressed during the frequency-magnitude analysis.

4.3. Air Photograph Interpretation

BGC completed an extensive search of the available air photograph record for the Canmore area and obtained digital copies from the following sources:

- The Alberta Air Photo Library
- The National Air Photo Library
- The University of Calgary Library
- The Canmore Museum and Geoscience Centre.

BGC provided a summary memorandum to the Town of Canmore on October 11, 2013 with a complete list of all the collected material. Table 4-2 summarizes the air photographs analyzed for Cougar Creek fan.

Table 4-2. Cougar Creek historical aerial photographs.

Year	Roll	Photo #	Scale	Date
1925 (oblique)	unknown	unknown	Unknown	unknown
1947	A11101	6-8	1:40,000	September 23
1950	AS 167 5101/5102	14, 15 43, 44	1:40,000	September 23
1958	AS 744 5103	54	1:16,000	August 14
1962	AS 830	51-52 112-114	1:32,000	September 18
1972	AS 1185	5, 6 37, 38	1:21,120	July 8
1975	AS 1383 3	80-81	1:12,000	June 1
1978	AS 1927	49, 50 80-82	1:15,000	August 29
1981	unknown	15, 16	unknown	unknown
1984	AS 3085	73, 105	1:20,000	August 22
1987	AS 3660	126, 127	1:20,000	September 17
1991	AS 4238	107, 108	1:10,000	September 17
1997	AS 4824	79, 80	1:15,000	July 19
2008	AS 5450	240, 241	1:30,000	August 18

A preliminary frequency analysis of the historic air photographs was described in the forensic analysis report (BGC, 2013). From the air photo record alone, BGC concluded that debris floods with magnitudes similar as the one observed in June of 2013 may occur, on average, every 30 years. Upon application of additional techniques, including obtaining additional air photographs from 1972, 1978, 1981 and 1987, this preliminary estimate has since been revised. The June 2013 event is now thought to occur with a lower frequency, as detailed in the following sections.

4.3.1. Method

The collected air photos were examined for evidence of debris floods and flooding. Debris floods on mountain creeks typically strip the affected area of vegetation or obliterate it. If such events are large enough, they leave a cover of flood or debris flood deposits which show up as light grey or white on the air photographs. The air photograph chronosequence was also used to map changes in channel flow direction and avulsions, and to examine the channel systems upstream of the fan apex as well as the watershed. The objective was to search for evidence of landslide activity that can convey sediment to the channel system or that has the potential to block the channel and form a landslide dam.

The air photographs were used in conjunction with the record of reported events to estimate a frequency of debris floods from 1925 until present. Ideally, air photographs can be used alone to identify new events occurring in the period between subsequent photos. Although air photograph coverage of the Canmore area is extensive with many years photographed, the extensive development of the fan and channelization of Cougar Creek made it very difficult to determine new activity especially for smaller events. Photos taken just after a known reported event were orthorectified[21] for later measurement of debris area (Section 5.2).

4.3.2. Results

The air photo analysis described in Section 7.0 of BGC (2013) should be referenced for a complete description. The principal results of this analysis were as follows:

- The aerial photograph review indicates that Cougar Creek has been subject to several historical debris floods and floods.
- A suspected date for a major debris flood event may be June 14, 1923 which demarcates the date of the second highest (highest flow on June 21, 2013) flow recorded at the *Bow River at Banff* hydrometric station. A date of 1923 is consistent with an oblique air photograph of the area taken in 1925. The oblique image looks up (west) the Bow River valley, but it is apparent that there are two major active channels on the Cougar Creek fan (Figure 4-1).
- The 1947 air photographs show that Cougar Creek used to occupy a much larger area on the fan than today and consisted of two major flow paths and a minor channel.
- A large debris flood event may have occurred between 1947 and 1950, which is consistent with historical observations.
- Analysis of the 1950 air photographs shows a recent debris avalanche some 2 km upstream of the fan apex, which may have led to a temporary impoundment and a landslide dam outbreak flood (Figure 4-2).
- The major channels visible on the 1947 air photograph were still prominent on the 1958 and 1962 air photographs and there does not appear to have been a major event between 1950 and 1962, or at least one of sufficient magnitude to create a new avulsion.
- The 1967 channelization work is very apparent on the 1972 air photographs. However, evidence of flooding and sedimentation from the 1967 event is not visible.
- On the 1975 air photograph, some widening of the main channel appears to have occurred compared to the 1972 air photographs. This event likely occurred in 1974, as this was a reported flood year (CH2M HILL, 1994).

---

[21] Process to geometrically correct distortion and provide a consistent scale across the aerial photograph.

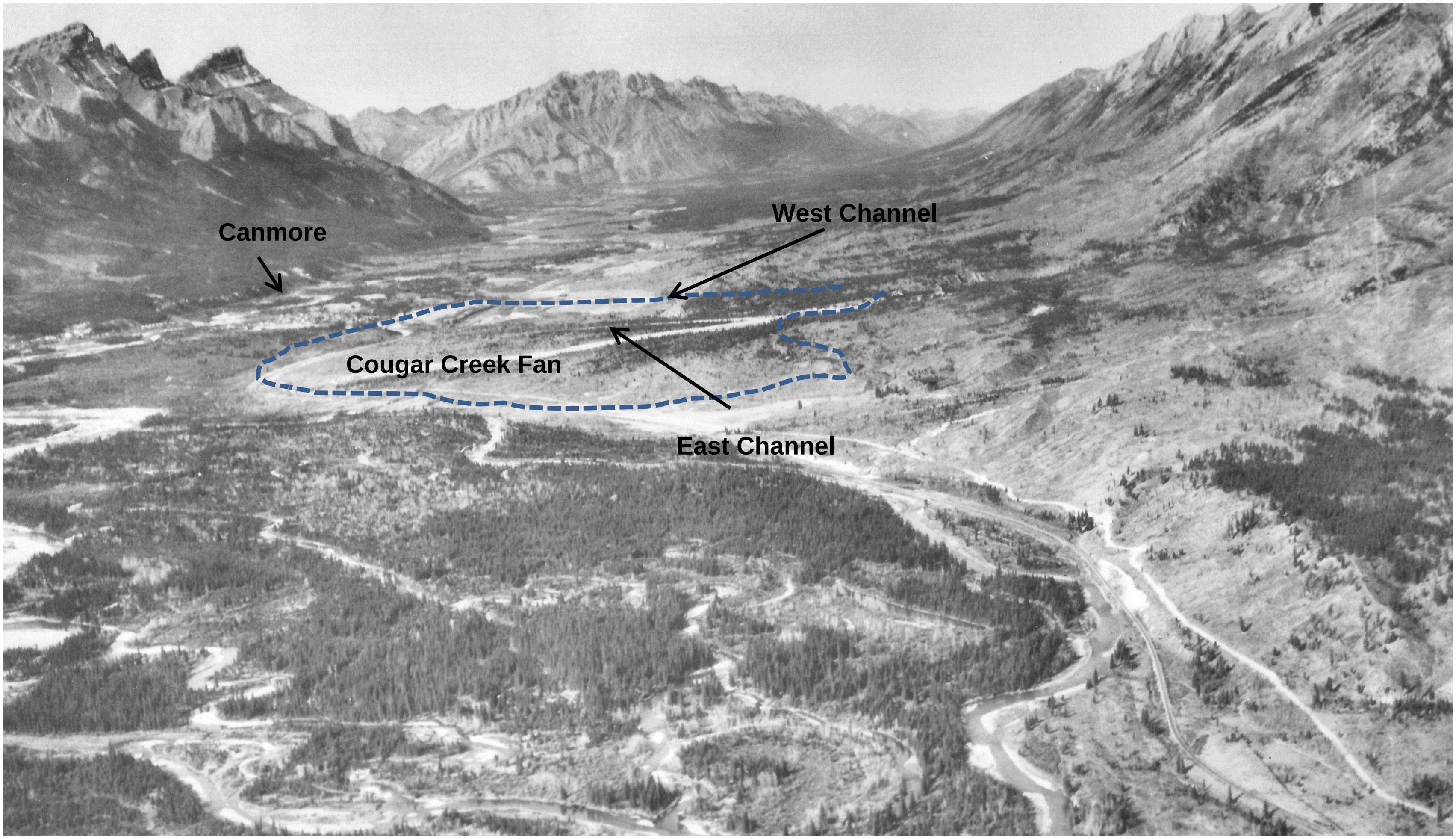

Figure 4-1. 1925 oblique air photograph looking west along the Bow River Valley toward the Cougar Creek fan.

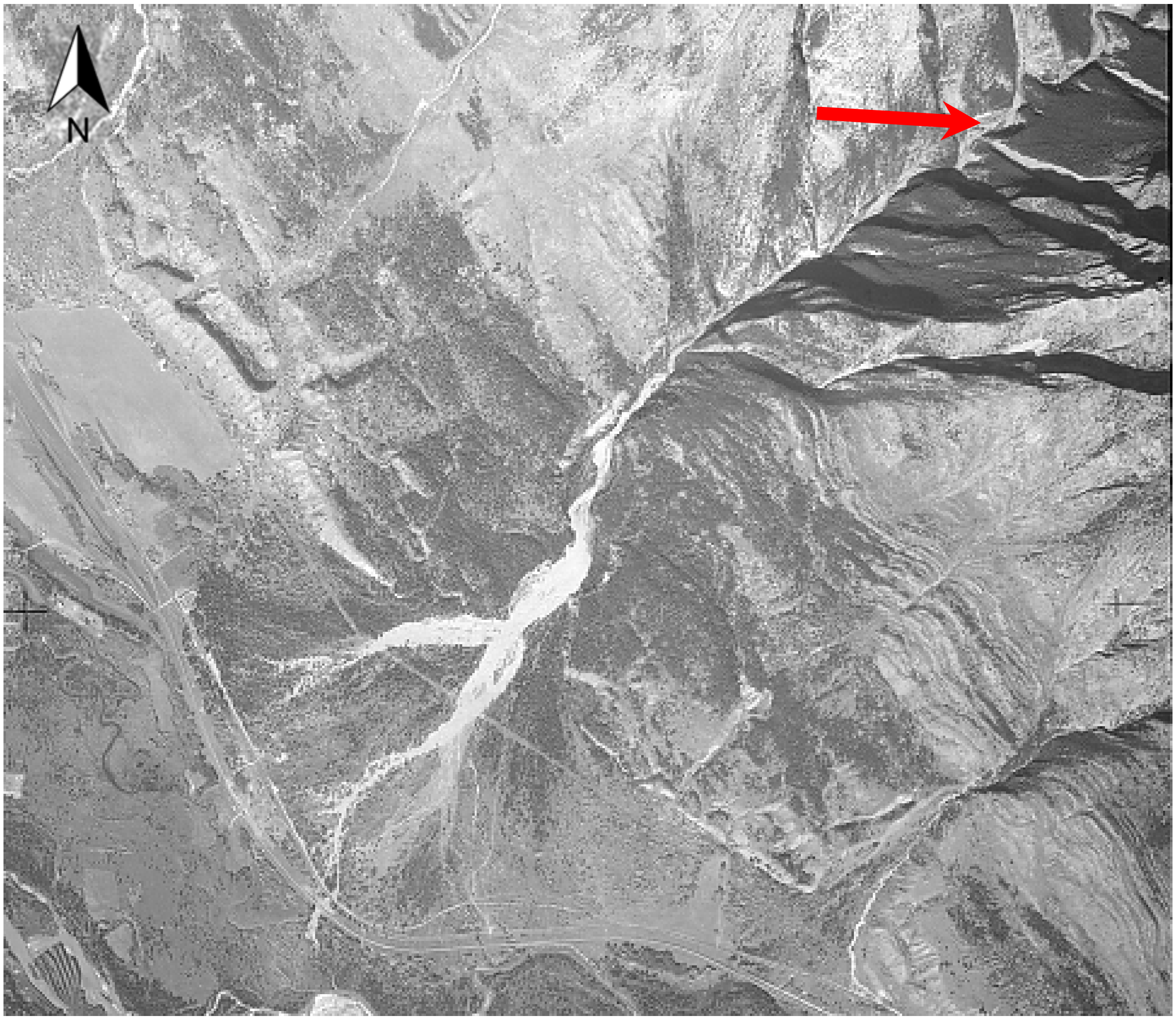

Figure 4-2. 1950 air photograph of the lower reaches of Cougar Creek and the fan. The red arrow indicates a relatively fresh debris avalanche that may have dammed Cougar Creek leading to a landslide dam outbreak flood, as evidenced by fresh (light coloured) deposits apparent on the fan.

- There is no evidence of major flooding between 1975 and 1981.
- By 1984, extensive development of the fan and channelization of the creek had taken place on Cougar Creek fan; however, no signs of a major debris flood event can be discerned on the air photographs.
- There are no signs of a major debris flood having occurred on the fan between 1984 and 1997.
- The 2005 flood, which caused erosion issues on the fan, is hardly visible on this air photograph, demonstrating that events have to be of substantial magnitude to be detected by air photograph analysis.
- The most striking changes on the fan in the past 30 years are residential, commercial and industrial development, which now occupies some 90% of the fan.

4.3.3. Limitations

Small debris flood events (< ~10,000 m^3) cannot be reliably identified from the aerial photographs unless they have led to avulsions from the main channel. The difficulty in observing evidence of debris flood activity was in part due to limitations in photograph scale and quality. However, the ambiguity of new event activity was largely due to the extensive channelization work that occurred after 1967. Channelization was achieved to restrict flooding and debris flooding to the artificial channel and limit the potential for avulsions. The series of air photographs from 1950 to 2008 shows no evidence of extreme debris flood activity as there are no new channel avulsions. These photos are therefore only informative in showing a lack of large events from 1950 to 2012 and provide no evidence for either the frequency or the magnitude of smaller events. Evidence of debris flood and flood activity was also difficult to discern due to development around the banks of the channel and subsequent lack of revegetation.

4.3.4. Summary

In summary, large debris floods possibly occurred in 1923, 1948, 1974 and 2013. Only the event volume of the 2013 debris flood can be reconstructed reliably and thus, it is not possible to combine these three events into one magnitude class. Smaller events (floods or debris floods) did occur during the 1948-2013 period and have been recorded by CH2M HILL (1994) and AMEC (2012), as having occurred in 1956, 1967, 1980, 1990, 2005 and 2012, indicating a return period of approximately 8 years. These smaller events were not apparent in the air photo record.

4.4. Radiocarbon Dating

In contrast to air photographs or historical accounts, radiocarbon dating potentially extends the record of debris flood frequency to include the entire history of fan development, depending on the availability of datable material.

4.4.1. Introduction

Radiocarbon dating involves measuring the amount of the radioisotope ^{14}C preserved in fossil organic materials and using the rate of radioactive decay to calculate the age of a sample. This method requires the deposition and preservation of organic materials within the sedimentary stratigraphy of the fan. The age limit to the application of the method ranges from approximately 45,000 years to several decades. As such, the method is applicable to the time scale of post-glacial fan formation in the Rocky Mountains and Cordillera.

As noted by Chiverrell and Jakob (2013), the deposits that accumulate across the continuum from colluvial to alluvial processes-dominated systems range from:

- Sediment gravity-flow deposits
- Poorly sorted and often matrix-supported angular boulders and gravels

- High energy and often distributary fluvial deposits
- Poorly-sorted clast-supported boulders and gravels
- Lower energy well-sorted sand and silt alluvial deposits.

In large fan complexes such as Cougar Creek, this range can be observed to be spatially variable with a downstream fining tendency, but channel shifts during fan formation challenge this simplified model. Establishing chronological control of alluvial sedimentation through radiocarbon dating can help clarify some of these complexities.

4.4.2. Sampling Methodology

A total of 16 test trenches were dug by use of hydraulic excavators between August 5 and 8, 2013 on Cougar Creek fan down to a depth of approximately 5 m (Drawing 2). The locations and number of excavations were a compromise between access, property ownership and safety, and obtaining a representative trench distribution.

Paleosols[22] were identified as distinct units and sampled for relict organic materials. Radiocarbon measurements from paleosols provide ages that can give minimum (or older than) or younger than relationships with the overlying or underlying units. Furthermore, short-lived plant detritus such as leaves or seeds that are incorporated within a debris-flood unit are thought to be contemporaneous with the depositional event. Therefore, for each sample obtained, the relationship to the overlying and underlying geomorphic unit was noted. The test trench logs are summarized in Appendix C.

The samples were placed in sealable plastic bags and sent to BETA laboratory in Miami for radiometric analysis. Due to the low weight of most samples and the added precision granted by Accelerator Mass Spectrometer (AMS), this method was chosen for the analysis.

Upon receipt of the results from BETA, BGC lumped those events with similar dates and determined their respective volumes by thickness measurements of the dated units and extrapolation of those units across the fan from one date to another.

4.4.3. Results

The radiocarbon ages from samples during the 2013 sampling on Cougar Creek fan are summarized in Appendix D and the location of each test pit along with the dates of samples retrieved from each pit are shown in Drawing 2.

[22] Paleosols are a stratum or soil horizon that formed as a soil in the past and on an alluvial fan is indicative of a period or relative low sedimentary activity for some time.

From the radiometric dating, eight distinct time periods in which major debris flood events occurred were identified as follows (all dates are reported as years before present):

- 570 years
- 760 to 800 years
- 970 years
- 1070 to 1200 years
- 1450 to 1770 years
- 2390 to 2440 years
- 2650 to 2870 years
- 3010 to 3180 years.

4.4.4. Limitations

Radiocarbon dating was used to date the organic samples collected in the test pits. This process of dating is fairly precise and the reported dates are accurate to ± 30 years. The error in determining event dates is less with the dating process itself, but rather with the collection of samples and associating these samples with different events. Organics may not have necessarily been deposited at the same time as sediment deposition. Erosion, root growth, and many other factors can cause organics to be sampled in a unit that does not share the same date. Experience and judgment of the sampler is required to select samples that are representative of the unit in which they are collected. However, these limitations affect the interpretation of event magnitude more than identification of event dates and frequency.

The eight identified time periods are assumed to represent individual debris flood events. It is not possible to state with certainty if the specified period contained a single large event or rather a series of temporally closely spaced events. Furthermore, it cannot be claimed that all large (approximately > 100,000 m^3) debris flood events were documented through test trenching and radiocarbon dating, particularly as few test trenches were excavated on the western fan sector.

Lastly, while radiocarbon dating is classified an absolute dating method, in fact it is a probabilistic approach. Each radiocarbon measurement forms a scatter around the true age of the sample. This imprecision in the radiocarbon measurement (which does not exist for some other absolute dating methods such as dendrochronology), needs to be reconciled in the interpretation of the results. Allowing for measurement error, the likely scatter and calibration range of an individual radiocarbon measurement provides an age range rather than a precise date (Chiverrell and Jakob, 2013). However, this uncertainty is considered to be low compared to the other uncertainties described above.

4.5. Dendrochronology

Depending on the ages of trees along the mainstem channel of a creek, dendrochronology allows evaluation of the frequency of large flood or debris flood events over the past several hundred years. This method is useful in supplementing historical observations and radiocarbon dating.

4.5.1. Introduction

Dendrochronology provides a method whereby debris flood events can be absolutely dated and a frequency of events established. Debris floods can influence regular tree growth in different ways. Trees may be damaged due to impact by large boulders or logs transported by a flood or debris flood. Tree growth may be reduced or increased in years following a debris flood event due to changes in resource (water/nutrients) access. Growth pattern may also change when a tree is tilted and produces denser (and thus darker) reaction wood to regain vertical alignment. Impacts such as these can be observed within the wood. Because trees produce a new layer of growth each year, these events can be accurately dated by studying the tree's growth ring series.

4.5.2. Method

Twenty-one (21) tree disks and 49 tree cores were sampled on August 29 and 30 and September 26, 2013 from coniferous trees along Cougar Creek. The majority of samples were collected from the upper watershed to the fan apex, with only three samples collected from the fan. More fan samples would have been preferred, but were not possible due to the extensive development that has led to felling of many original trees on the fan and older trees located on private property. Disks were cut from trees that were undercut by erosion of the 2013 debris flood and provide a complete cross section of the tree. No live trees were cut. Tree cores were extracted from living trees using a 4 mm increment borer. Coring is a non-destructive sampling technique and is thus preferred to felling the tree by chainsaw.

Retrieved samples were sanded to a high finish using 400 grit sand paper and examined under a Nikon binocular microscope with up to 80x magnification. The dates during which growth anomalies (reaction wood, traumatic resin tissue, suppression wood, etc.) occurred were determined by counting tree rings back from the outermost ring which corresponds to 2013 growth. These dates were then plotted to determine a pattern between samples. The following criteria were used when correlating anomalies between samples and identifying past debris flood or flood events:

- A tolerance of ±1 year was given when matching anomalies to an inferred event date (to account for possible errors in counting due to extremely narrow tree ring sequences).

- Wherever possible, dates were correlated with known event dates or periods of high Bow River discharge which may be (but is not necessarily) indicative of high flows/debris floods on Cougar Creek. Bow River discharge was taken from the Alberta WaterSMART's white paper (2013), which is included in Appendix F.
- Short periods of abrupt incremental tree growth decrease (up to 2 years) without slow release to pre-event ring widths were assumed to be climatically forced and were therefore excluded from the analysis.

Correlated dates were sorted by likelihood of being a debris flood event depending on the number of samples affected. The following categories were defined:

- > 5 samples – Very Likely
- 4 to 5 samples – Likely
- 2 to 3 samples – Possible
- 1 sample – Unlikely.

4.5.3. Results

Based on the above classifications, 24 Very Likely to Likely events occurred between the year 1674 and 2013 based on the dendrochronology analysis. Appendix E summarizes the inferred event dates from the 2013 sampled tree record.

The following growth anomalies were observed in the collected samples:

- Impact scarring
- Periods of sudden growth reduction with slow growth release
- Periods of sudden growth increase
- Dense and thus darker reaction wood
- Possible traumatic resin production.

The period from 1674 to 1844 was discarded in the frequency analysis as there were too few trees sampled that span that time range to provide a continuous record. From 1844 to the present (169 years), a debris flood/large flood frequency of 7 years was determined based on the identification of 24 Very Likely and Likely events. Figure 4-3 shows the number of Very Likely to Likely events by decade and Drawing 4 shows the locations of the trees impacted by these events.

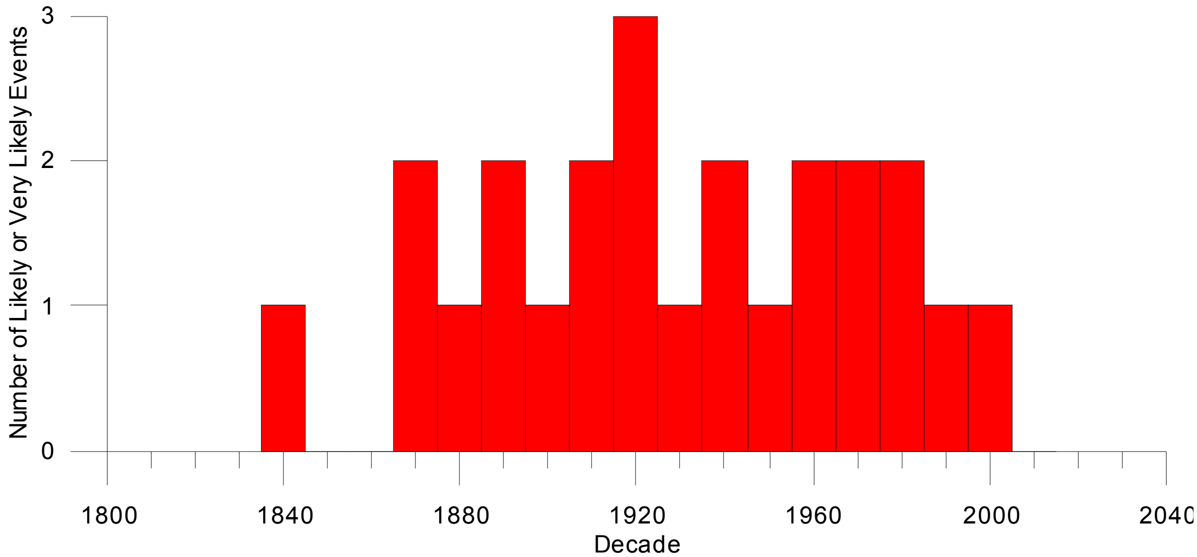

Figure 4-3. Number of very likely to likely events per decade as interpreted from the dendrochronology analysis of 70 tree samples.

In summary, the following two conclusions result from the dendrochronlogic investigation:

- Heavy flooding or debris flooding occurs on a decadal time scale with magnitudes sufficient to affect tree growth along terraces flanking the lower Cougar Creek channel.
- Over the last two centuries, it is very unlikely that an extreme debris flood, such as triggered by a large landslide dam outbreak event, has occurred. This conclusion is reached as such an event would likely have destroyed all vegetation along the low-lying terraces flanking the channel. It is not possible to accurately reconstruct the peak flow required to lead to complete tree mortality along the channel, but from reconstruction of a few representative cross-sections, this peak flow would likely need to be in excess of several hundred cubic metres per second.

4.5.4. Limitations

Dendrochronological analysis does not allow a clear designation of process type and thus the dated events may have been debris floods and floods alike. Not all noted historical events are preserved in the dendrochronologic record as some trees will have been destroyed and obliterated or transported by large debris floods. Over the past 40 years, vegetation along fan reaches has been also been disturbed through channelization, removing records of previous events.

The channel of Cougar Creek upstream of the fan apex undergoes cycles of aggradation and degradation. For example, several years of normal flooding (i.e. with little bedload movement) may scour the main channel, thus deepening it and allowing high flow conveyance. In contrast, a sudden influx of sediment through tributary debris flows, bank erosion, and talus slope undercutting can aggrade the channel bed, leaving little freeboard between the lower paired and terraces and the channel bed.

The level of the channel zone will determine the likelihood of tree damage. For example, a recently aggraded channel section when followed by a high flood event will lead to tree damage even if that flood event was of lesser magnitude than the preceding one. An example of this cyclicity in aggradation and degradation and its hazard potential has been reported in Jakob and Weatherly (2008) at Canyon Creek, Washington County, US.

4.6. Field Observations of Landslide Dams

Cougar Creek channel was hiked from approximately 8 km upstream of the fan apex to the apex. During this descent, BGC identified 8 locations at which landslide dams may have formed in the past (Drawing 3).

Ideally, the landslide dams would have been dated and a chronology of such damming events established that would allow the construction of a frequency-magnitude curve limited to this specific data population. Unfortunately, only one organic sample was extracted from a truncated tributary fan that had two observable debris flow (and/or rock avalanche events). This sample was retrieved from a paleosol formation very rich in organics, underlying a past debris flow and overlying a past rock avalanche (or very large debris flow) in the upper reaches of Cougar Creek Channel (WP-11, Drawing 3). The sample was sent to BETA Analytic for radiometric analysis and was dated at 1140 years BP. Because the sample was collected from a paleosol that likely developed in the period of quiescence between the two events, it can only constrain the relative timeframe of two events (e.g. an event occurring pre 1140 BP and another post 1140 BP), which does not meet the requirements for a frequency-magnitude curve of landslide dam events.

A simple calculation that uses the total number of observed landslide dam locations and assumes that they are representative of all Holocene landslide damming events is possible, but likely results in a minimum, rather than maximum return period estimate. The 8 landslide dams identified by BGC along the mainstem of Cougar Creek results in an average return period of 1,250 years over a 10,000-year period. This figure is likely an overestimate of the return period because:

- Tributary debris flows with mainstem damming potential likely occur at higher frequencies
- Some landslide dams may have been completely eroded or obliterated by talus accumulation and are thus, no longer identifiable.

Therefore, BGC estimates the return period of any landslide dams to be between 100 and 1000 years.

The pertinent question is at what magnitude does an outbreak flood from a landslide dam translate into a potentially hazardous debris flood? The magnitude (peak flow and sediment volume) of a landslide dam outbreak flood hinges on the dam height, the amount of impounded water volume, the breach rate (rate of incision into the landslide dam during overtopping or piping failure), and the amount of attenuation during its decent to the fan apex. These factors are considered as part of numerical modelling of landslide dam outbreak floods, as described in Section 7.0.

4.7. Summary

Historical accounts, air photo interpretation, dendrochronology and radiocarbon dating were applied to decipher the frequency of debris floods on Cougar Creek:

Each of these methods is associated with advantages and pitfalls and each spans a different, but often overlapping, time range. For this study, the highest yielding information from a hazard point of view was obtained from historical accounts and radiocarbon dating with the other two methods providing supplemental information. This information is also used in the debris flood magnitude reconstruction discussed in the next section.

5.0 MAGNITUDE ANALYSIS

5.1. Introduction

The objective of this magnitude analysis is to estimate volumes and/or peak flows for previous debris floods. Such an analysis is central to the hazard assessment because the range of magnitudes is used as input into the numerical modelling (Section 7.0). This, in turn, forms the basis for the quantitative risk assessment. Ultimately, a design magnitude (volume and peak discharge) will need to be selected for the preferred debris-flood mitigation strategy along Cougar Creek with the goal to reduce risk to tolerable levels, as defined by stakeholders.

Determining debris flood magnitudes is difficult and subject to some uncertainty because older deposits can be eroded or reworked and are therefore, often difficult to distinguish unambiguously from one another. Moreover, it is problematic to differentiate between the amount of debris that is introduced to the fan from upstream past the fan apex, and debris that is recruited from bank erosion from the fan reaches.

Rather than relying on a single method to estimate debris flood magnitude, BGC employed a variety of methods, which, in combination, increase the confidence in the chosen frequency-magnitude relationship (Section 6.0) and thus, the design magnitude. The methods are as follows:

- Area measurements of debris deposits from orthorectified air photographs
- Volume estimations from stratigraphic analysis and radiocarbon dating
- Peak flow estimates from dendrochronology
- Volume estimates from empirical rainfall-sediment transport relationships
- Volume estimates from landslide dam outbreak flood modeling (see section 7.0).

None of the above methods is likely to provide a completely reliable magnitude estimate of future debris floods, but a comparison of the methods with the respective limitations and uncertainties will improve the understanding and estimation of a reasonable range of debris flood magnitudes.

5.2. Photogrammetric Area Measurements and Thickness Estimates

5.2.1. Methodology

Air photographs from 1947 to 2013 were purchased from the Alberta and National air photo libraries, as well as the University of Calgary's collection. Subsequently, the air photographs were imported into ArcMap and compared to an online imagery service for orthorectification (Bing Maps). Subsequently, prominent features visible in the stereopair were used as 'control points', which then help reshape the image to be georeferenced. Depending on the image and amount of elevation-caused distortion, between 3 and 12 control points were digitized to obtain a reasonably accurate orthorectified image for relatively flat terrain (fans).

This process allows measurements of debris areas directly from the air photographs which otherwise would be distorted. Air photographs have not been taken on an annual basis, so event areas can only be estimated for periods bracketed by air photographs. Areas were then digitized in a Global Mapper workspace. Deposit thicknesses were estimated from test trenching and natural exposures. Minimum and maximum thicknesses were recorded to allow a range of volume estimates.

5.2.2. Results

The results from the photogrammetric area and thickness measurements are presented in Table 5-1.

Table 5-1. Volume estimates from photogrammetric area measurements and thickness estimates. Note that the volumes correspond to bracketed years between respective photographs.

Aerial Photo Date	V_{min} (m^3)	V_{BE} (m^3)	V_{max} (m^3)
1950	90,000	200,000	300,000
1958	15,000	20,000	29,000
1972	26,000	20,000	85,600
1975	28,000	60,000	92,000
1997	25,000	50,000	84,000
2008	19,000	40,000	62,000
2013	82,000	180,000	273,000

V_{min} is the minimum volume calculated using the minimum estimated sediment thickness
V_{max} is the maximum volume calculated using the maximum estimated sediment thickness
V_{BE} is the best estimate for volume using this method and is the average between V_{min} and V_{max}

5.2.3. Uncertainties

These results appear to be over-estimates in light of the direct observations. For example, the sediment volume of the 2013 event was measured at approximately 90,000 m^3 (see next section) rather than the 180,000 m^3 determined from the indirect methods above.

Several limitations and sources of uncertainties exist with this method, as outlined in the following

- The debris deposition area delineated may be affected by the occurrence of several events in the time period bracketed by chronosequential air photographs. It is rarely possible to differentiate two flows if they have occurred within a short (a few years) time frame because they remain unvegetated for this period.
- Debris floods do not homogenously deposit sediment and the concept of an average deposition thickness is difficult to justify. However, it is not possible to determine reliable differences in erosion and deposition unless two detailed topographic images are available that can be overlain as was done for the 2013 event.

The recognition of these limitations led to an abandonment of this method in determining volumes of historical debris floods.

5.3. 2013 Debris Flood DEM Comparison

5.3.1. Methodology

The volume of sediment transported onto the fan during the 2013 flood was investigated using LiDAR data. A LiDAR survey was completed soon after the 2013 event by LiDAR Services International Inc. (LSI) on June 28, 2013. LSI post-processed the LiDAR data and provided BGC with a 1 m x 1 m post spacing XYZ file, which was then used to generate a digital elevation model (DEM). An earlier LiDAR survey had been completed by McElhanney Consulting Services Ltd. on May 23, 2009 along the Bow River Valley. Those survey data were procured by the Town and BGC generated a second DEM of the Cougar Creek fan. Volumetric changes along the channel were quantified by overlaying the 2009 and 2013 DEMs.

For the DEM comparison, BGC generated 5 m x 5 m grids using the 2009 and 2013 LiDAR data. The grids were then overlaid in ArcGIS and a mask was generated so that the comparison was restricted to the active channel of Cougar Creek. Results of the comparison are shown in Drawing 5. Areas of deposition are delineated by the colour yellow and shades of green, while areas of erosion are shown in orange and red. Deposition is most obvious along the former channel, which was completely infilled during the 2013 event. Up to 8 m of aggradation occurred locally. Erosion occurred along the channel margins and was most prevalent upstream of Elk Run Boulevard and for half the distance between Elk Run Boulevard and Highway 1. Erosion of up to 5 m occurred locally.

5.3.2. Results

Table 5-2 below summarizes the volumetric changes downstream of the bedrock canyon which is defined as the fan area.

Table 5-2. 2009-2013 LiDAR comparison on Cougar Creek.

Reach	Cut (m^3)	Fill (m^3)	Net Change (m^3)
Bedrock Canyon to Elk Run Boulevard	-79,100	67,600	-11,500
Elk Run Boulevard to Highway 1	-48,300	93,100	44,800
Below Highway 1	-9,500	66,800	57,300
Total	**-136,900**	**227,500**	**90,600**

Table 5-2 indicates that approximately 90,000 m^3 of sediment was deposited on the Cougar Creek fan during the 2013 event. Two additional factors require consideration when evaluating this total. The first is that some bedload was likely transported beyond the distal margins of the fan into the side channel of the Bow River which will not have been captured in the LiDAR topography comparison. The second factor is that Cougar Creek experienced a major flood on June 5-6, 2012. Details of the damage caused by that event are provided in BGC's forensic report (2013). More importantly for this evaluation, eight cross-sections were surveyed following the flood and compared to a previous survey in 2006. That analysis indicated a net increase in channel area between the upstream end of development and Highway 1A, indicating that is was mostly an erosional event (AMEC, 2012). However, the survey was limited and did not capture channel changes below Highway 1A where deposition was likely to have occurred. Furthermore, between 19,000 and 27,000 m^3 (best estimate of 23,000 m^3) of sediment were calculated to having been transported onto the fan using the empirical relationship developed in Section 5-6. Therefore, it must be recognized that the 90,000 m^3 calculated from the 2009 and 2013 LiDAR overlay for the 2013 event may be slightly over-estimated.

5.4. Debris Flood Volume Estimates from Fan Trenching

5.4.1. Methodology

Test trenches were selected based on access, lack of underground utilities, land ownership and hazards that could be created by the trenches. Because much of the land on the Cougar Creek fan is privately owned, a regular grid based sampling that would have been preferable was not possible. For applied studies on fans that are already developed (those are the focus of most applied fan studies), such limitation is the rule and is unavoidable. This means that likely only a certain subset of events has been identified during the analysis.

The trench sampling method was described in Section 4.4.2. In addition to sampling organics, the thickness of the dated unit was recorded. In some instances uncertainty prevailed regarding if a specific unit consists of one event or of a series of events that are not clearly separated by changes in texture or structure. In such cases a judgment was made in the field. An example is the 1000 year BP and 1100 year BP events. The corresponding radiocarbon dates for these events are 970, 1070, 1130, and 1140 +/- 30 years BP. Given the relatively small range of dates, these four dates could represent the same event. However, the location of the dates indicated to BGC that they represented two distinct events. It should be recognized though that lumping these two events would not dramatically change the shape of the frequency-magnitude curve.

Once the dates of specific debris flood units had been received from BETA labs, areas were delineated by connecting locations of the noted combined dates by hand. The underlying assumption was that deposition of sediment occurs as individual lobes, which is a pattern observed during past events on air photographs and which was successfully simulated numerically for large events (see Section 7.0). The delineated areas were assumed to be the minimum areas inundated by these past events. This method is imprecise as no evidence exists of the exact shape of the interpreted debris lobes. To account for this uncertainty, the delineated debris lobe estimates were doubled as an estimate for reasonable error and designated as the maximum volumes. The average between the delineated and maximum areas was reported as the best estimate area for each event. Drawings 6 to 8 show the delineated debris flood lobes.

The deposition areas were then measured in Global Mapper. A simple multiplication of these areas with the measured depth of the individual debris-flood units was believed to be too simplistic as the thickness of individual unit was found to vary significantly even over short distances. Accordingly, an approach was chosen that is based on a semi-empirical relation developed by Iverson *et al.* (1998) between the planimetric deposition area (B) and the deposited volume (V) assuming geometric similarity:

$$B = k_B V^{2/3}$$ [Eq. 5-1]

Where k_B is a dimensionless, empirically derived mobility coefficient. For granular debris flows, Iverson *et al.* (1998) proposed a k_B of 20, while for volcanic debris flows a k_B of 200 was determined. Volcanic debris flows inundate larger areas with thinner flow depths than granular debris flows due to the fact that they are more mobile (i.e. typically have lower sediment concentrations and are less likely to have a bouldery flow front that creates frictional resistance and thus slows the flow). In fact, some reported volcanic debris flows that form part of Iverson *et al.* (1998) dataset could have equally been described as debris floods or hyperconcentrated flows. In that sense, they resemble debris floods and thus, a k_B of 200 was adopted for the analysis.

5.4.2. Results

Table 5-3 summarizes the results from the volumetric analysis based on test trenching.

Table 5-3. Summary of radiocarbon-dated debris floods, interpolated areas and calculated fan volumes.

Radiocarbon Date (years BP)	A_{min} (m^2)	A_{BE} (m^2)	A_{max} (m^2)	V_{min} (m^3)	V_{BE} (m^3)	V_{max} (m^3)
570	210,000	315,000	420,000	30,000	60,000	100,000
760-800	180,000	270,000	360,000	30,000	50,000	80,000
970	510,000	765,000	1,020,000	130,000	240,000	360,000
1070-1200	380,000	570,000	760,000	80,000	150,000	230,000
1450-1770	320,000	480,000	640,000	60,000	120,000	180,000
2390-2440	210,000	315,000	420,000	30,000	60,000	100,000
2650-2870	640,000	960,000	1,280,000	180,000	330,000	510,000
3010-3180	310,000	465,000	620,000	60,000	110,000	170,000

Minimum (min) areas calculated from the delineated debris flood lobe areas
Maximum (max) areas produced by doubling the delineated areas to account for error
Best estimate (BE) areas are the average between the minimum and maximum areas

5.4.3. Uncertainties

The following uncertainties are associated with determining debris flood volumes from test trenches:

- The delineation of past events, based on similar dates, may be biased as there is no guarantee that the lumped events are indeed representations of one event rather than multiple events with their own date. This error would result in overestimation of debris flood volumes.
- The delineation in separate avulsion lobes on the fan may not have been conservative enough and it is conceivable that the individual dates would have to be connected as a continuous debris cover rather than individual lobes. This would result in an under-estimation of debris flood volumes. There may be some error cancellation between this argument and the one above.
- The chosen mobility coefficient of k_B = 200 was determined from an analysis of volcanic debris flows and may not be applicable fully to debris floods and thus lead to an over or underestimation of debris flood volumes

While it could be argued that the delineation of discrete events into avulsion lobes is not conservative, this depositional concept is supported by the potential size of landslide dams along the mainstem channel. Debris floods in the watershed can be generated by large rainfall events, potentially supplemented by snowmelt, or a landslide dam. The maximum return period event in Table 5-3 has a best estimate volume of 330,000 m^3. Rainfall events are unlikely to generate a debris flood of this magnitude, as discussed later. Therefore, this event was likely generated by a landslide dam outbreak flood, an interpretation that is supported by the matrix-supported deposits encountered in the test trenches. Debris floods on Cougar Creek are unlikely to have a volumetric sediment concentration that exceeds 30%, as channel gradients are not steep enough to sustain higher concentrations. Assuming a volumetric sediment concentration of 30%, the sediment volume estimate of 330,000 m^3 implies a landslide dam that impounded on the order of 1.2 to 1.5 Mm^3 of water. Higher sediment volume estimates would require a landslide dam of much larger size and the available field evidence does not indicate that landslide dams capable of impounding greater than 1.5 Mm^3 of water have previously occurred in the watershed. While it is possible that evidence of such a large landslide dam has been removed by erosional processes, BGC considers this to be unlikely.

5.5. Peak Flow Estimates from Dendrochronology

Dendrochronological information can, in some instances, be used to reconstruct the peak flow of debris flows or debris floods. The cross-section area is measured that was likely occupied by an event and the velocity from channel geometry is back-calculated, yielding a peak discharge.

Debris flood cross-section area was measured off the LiDAR-generated data for some cross-sections along the channel. Velocity was estimated using the standard Manning's formula:

$$v = \frac{1}{n} R^{2/3} S^{1/2} \quad \text{[Eq. 5-2]}$$

where:

n is Manning's roughness coefficient, which was assumed to range between 0.04 and 0.05 for the relevant channel reaches of Cougar Creek;

R is the hydraulic radius which is the cross section area divided by the wetted perimeter of the channel; and

S is the channel slope.

Twenty (20) cross-sections were drawn on the LiDAR-generated hillshade imagery perpendicular to the channel thalweg from the terraces where individual trees had been sampled (Drawing 4). The channel width and approximate flow depth were measured and compared with the field notes. The biggest source of uncertainty is the channel depth below the terrace surface at the time of past flows. To account for this uncertainty, a range of conceivable depths were used.

As shown in Table 5-4, there is a wide span of possible peak discharges possible for the reconstructed events. Because it is not possible to associate event dates with specific peak discharges, a reconstruction of a peak discharge – frequency curve is not possible. However, an examination of the results demonstrates a clustering of peak flows around 1000 m^3/s and around 200-300 m^3/s. Both of these clusters are likely associated with dam outbreak floods as their peak flow estimates exceed the estimated 100-year return period peak instantaneous flow estimate (Q_{100} = 16 m^3/s) by one to two orders of magnitude. The reconstructed peak flows are also comparable with the results achieved from the landslide dam outbreak modelling, which is discussed in Section 7.0.

Table 5-4. Velocity and peak discharge estimates for key cross-sections along Cougar Creek.

Cross-Section	Dendro Sample ID	V_{min} (m/s)	V_{max} (m/s)	Q_{min} (m^3/s)	Q_{max} (m^3/s)	Q_{mean} (m^3/s)
XS-1	CC-DF-27, CC-DF-28, CC-ES-67	2.6	7.8	50	290	170
XS-2	CC-DF-23, CC-ES-62	2.4	7.2	60	360	210
XS-3a	CC-DF-11, CC-ES-12, CC-DF-13, CC-DF-14, CC-DF-15, CC-DF-16	2.4	7.2	50	310	180
XS-3b	CC-DF-11, CC-ES-12, CC-DF-13, CC-DF-14, CC-DF-15, CC-DF-16	3.8	8.4	220	1210	720
XS-4a	CC-DF-09, CC-DF-10, CC-ES-50, CC-DP-52, CC-ES-53	3.4	10.3	80	470	280
XS-4b	CC-DF-09, CC-DF-10, CC-ES-50, CC-DP-52, CC-ES-53	5.4	10.6	420	1630	1030
XS-5	CC-DF-08	3.6	8.1	280	1560	920
XS-6	CC-DF-06, CC-DF-07	4.4	8.5	390	1520	960
XS-7	CC-DF-05	4.8	10.8	340	1880	1110
XS-8	FC-ES-03, FC-ES-04, CC-ES-01, CC-ES-02	3.0	9.3	100	610	360
XS-9a	FC-ES-01, FC-ES-02	10.5	9.7	1150	1340	1250
XS-9b	FC-ES-01, FC-ES-02	12.2	7.4	3070	2330	2700
XS-10a	-	5.8	9.4	230	550	390
XS-10b	-	5.1	12.7	310	2290	1300
XS-11a	-	2.6	8.5	40	300	170
XS-11b	-	6.3	7.9	520	1290	910
12	-	5.2	11.7	310	1720	1020
13	-	4.5	7.3	570	1400	990
14	-	4.2	6.8	160	400	280
15	-	4.1	6.6	290	700	500

5.6. Volume Estimates from Empirical Rainfall-Sediment Transport Relations

5.6.1. Introduction

Prediction of bedload transport can be important for hazard assessments and engineering applications although knowledge on sediment transport is still limited, particularly from a modelling perspective. Furthermore, few sediment transport studies have been completed for steep (> 5%) mountain creeks, and as noted by Hassan *et al.* (2005), sediment transport in such channels may be quite different from low-gradient channels. Hillslope processes are intimately linked to channel processes with some channels being supply-limited while other being supply-unlimited (Jakob and Bovis, 1996; Rickenmann, 2005). As pointed out by Church and Zimmermann (2007), steep mountain creeks can display a multitude of grain sizes, variable sediment sources, rough and structured stream beds with step and pool morphology. Large boulders (keystones), woody debris and occasional bedrock sections further create a significant variation in channel geometry, flow velocity and roughness, all of which render theoretical or flume-derived sediment transport equations questionable (Gomi and Sidle, 2003). These channel characteristics apply to the upper reaches of Cougar Creek, but changes to a largely braided channel in a more homogenous gravel-fill floodplain for the lower 5 km of the channel upstream of the fan apex.

5.6.2. Swiss Case Study

During August 21-23, 2005, severe flooding occurred in a large area of northern Switzerland with significant morphological changes in stream channels (Jaeggi, 2007). Similar to the June 2013 southeastern Albertan flood, this event was associated with more than 200 mm of rain within three days with corresponding return periods exceeding 100 years. Unlike the flood in southeastern Alberta, there was no snowmelt contribution in the Swiss storm. As many mountain creek hazards have been mitigated by catchment basins, the transported sediment volumes could be determined for many watersheds. A database was subsequently created with 33 debris flows and 39 fluvial sediment transport events, details of which are reported in Rickenmann and Koschni (2010). These authors used a variety of transport movement equations to compare modeled and predicted sediment transport volumes including those by Rickenmann (2001), Rickenmann and McArdell (2007), Hunziker and Jaeggi (1992), Ricking *et al.* (2008), and D'Agostino *et al.* (1996). Rickenmann and Koschni (2010) found reasonable agreements between modelled and measured sediment volumes for channels with less than 5% gradient using the Meyer-Peter and Mueller equations. In contrast, for steeper channels, the observed sediment volumes transported by fluvial processes are over-predicted by bedload equations developed for steep channels.

Rickenmann and Koschni (2010) developed an upper envelope for the entire dataset in the form of:

$$GF = 1.95 V_{re} S^{1.5} \quad \text{[Eq. 5-3]}$$

Where GF is the total sediment volume transported into sediment basins, V_{re} is the effective runoff volume and S is the channel slope.

5.6.3. Application to Cougar Creek

Using Equation 5-3 and the total estimated rainfall volume of the June 2013 event (9.1 Mm^3, ignoring the snowmelt contribution), a sediment volume estimate of 200,000 m^3 is obtained for the Cougar Creek fan. This value is roughly twice the volume calculated from a DEM comparison between the 2009 and 2013 LiDAR imagery. As expected from an envelope relation, a higher-than-observed value is not surprising.

Given the value of the Rickenmann and Koschni (2010) database, BGC analyzed the data further. First, BGC separated the debris flow events from the mostly fluvial transport data. Watersheds with very large areas and correspondingly low gradients (< 0.01) were also deleted from the dataset. These deletions provided a final dataset of 36 cases. Multivariate regression analysis was then applied to the log-transformed dataset to determine sediment volumes based on catchment area, rainfall volume, runoff coefficient, surface runoff and channel gradient. This analysis yielded the two following formulae:

$$logV_S = 0.753logV_R - 0.553,\ \ R^2 = 0.79 \qquad \text{[Eq. 5-4]}$$

$$logV_S = -1.55 + 0.877logV_R + 0.019S,\ \ R^2 = 0.81 \qquad \text{[Eq. 5-5]}$$

Where V_S is the total sediment volume displaced and V_R is the total rainfall. The difference between the two formulae is the inclusion of channel slope S in Equation 5-5. However, since the increase in variance is very small (2%), the effect of slope appears small and only Equation 5-4 was used in the analysis. Neglecting slope would not be appropriate had the entire dataset been used as that also includes debris flows. Therefore, the formula presented above is only appropriate for debris floods with channel gradients from approximately 2 to 24%.

BGC (2014) determined that during the rainfall event of June 19-21, 2013 an additional 12-29% of runoff was generated from snowmelt. Using this range, the rainfall volume, V_R, for the Cougar Creek watershed was estimated to vary from 10.1 to 11.7 Mm^3. Applying these values to Equation 5-3 yields a best-fit sediment volume of 53,000 to 59,000 m^3 for the 2013 event. The confidence intervals and supporting statistics are summarized in Table 5-5.

Table 5-5. Summary statistics for sediment movement for the June 2013 debris flood using the range of snowmelt contribution as determined by BGC, 2014.

	V_S (best fit) (m^3)	Lower σ (m^3)	Upper σ (m^3)	Upper 95% PL (m^3)
V_R (12% SWE)	53,000	42,000	67,000	168,000
V_R (29% SWE)	59,000	47,000	76,000	187,000

p-value is 0.000 and standard error of the estimate is 0.24
σ is the 95% confidence interval
PL is prediction limit

A significant difference is observed between the best fit values (53,000 to 59,000 m^3) and the estimated 90,000 m^3 of sediment that was transported onto the fan of Cougar Creek during the June 2013 debris flood. This discrepancy may be explained by significant sediment injections from tributary debris flows during the 2013 event, some of which may have even dammed Cougar Creek for very short (minutes) periods of time. This hypothesis cannot be proven, but the discrepancy between predicted and observed sediment volume suggests that the 2013 event volume was indeed supplemented with significant tributary debris influx, which is consistent with field evidence. It should also be noted that the 90,000 m^3 estimate is derived from comparison of 2009 and 2013 LiDAR surveys, and that a flood event also occurred in 2012 which may introduce some error in the volume estimate. An alternative explanation of the discrepancy between the best fit value are errors in the estimation of precipitation, estimation of snowmelt, inclusion of different hydroclimatic events (mid-summer rainfalls with no snowmelt as well as runoff events with significant snowmelt and possibly frozen soils).

Assuming that Equation 5-4 provides reasonable estimates of transported sediment volumes during significant rainfall events, it should be possible to determine sediment volumes for a range of return periods. This assessment requires a frequency analysis of rainfall at the Kananaskis meteorological station, located approximately 20 km southeast of Cougar Creek. The underlying assumptions are that rainfall measured at this station is reasonably representative of the distributed precipitation on the Cougar Creek basin, and that climate can be approximated by long term stationarity. Therefore, the results below may be associated with some error. To capture potential error the lower and upper confidence interval was used in the calculations of debris volumes. The upper ranges were used for debris-flood modelling to allow for observed upward trends in extreme precipitation events. The results of this analysis are summarized in Table 5-6 based on 3-day rainfall estimates.

Table 5-6. Rainfall frequency analysis at Kananaskis station and estimated sediment volumes based on an average snowmelt contribution of 21%.

Return Period (years)	Rainfall (mm)	Lσ (mm)	Uσ (mm)	V_s+21% SWE (best fit) (m^3)	V_S+21% SWE (Lσ) (m^3)	V_S+21% SWE (Uσ) (m^3)
20	124	107	158	37,000	30,000	45,000
100	178	142	261	49,000	39,000	61,000
200	205	112	305	54,000	43,000	68,000
750	265	185	464	65,000	51,000	80,000
2500	330	212	640	77,000	59,000	103,000

Lσ and Uσ identify the lower and upper 95% confidence interval, respectively.

For the 2013 rainfall event, which delivered approximately 90,000 m^3 of sediment onto the fan, the 750-year 3-day rainfall return period event (upper confidence interval and an additional 15% snowmelt contribution) is the closest estimate (83,000 m^3) to the observed volume.

Using Table 5-6, a 2500-year return period event could mobilize between (rounded) 60,000 m^3 and 220,000 m^3 of sediment past the fan apex, depending on additional snowmelt and the choice of confidence limits versus prediction limits. Note that this analysis does not account for any landslide damming, nor does it account for any non-stationarity in the rainfall trends. Initial trend analysis conducted by Coia and Nolde (2013) for BGC suggest that, if the observed trend is not an artifact of rain gauge replacement and operation (Whitfield, 2014, in press), the 2013 event had a return period of less than 300 years[23]. Moreover, results are based on three-day rainfall, and longer duration rainfall is possible. Therefore, these results should be interpreted with caution. However, it is interesting to note that the trend-adjusted rainfall return period is close to the estimated return period of the 2013 debris flood (~ 400 years) as detailed in Section 6.0.

The same methodology was then applied to calculating debris flood sediment volumes for all debris flood events that had been noted in previous reports. For the 2005, 2012 and 2013 events, the total rainfall volume was determined from isohyet maps that were supplied to BGC from the River Forecast Section of the Alberta Ministry of Environment and Sustainable Resource Development (AESRD). Then, the ratios between the total storm rainfall volume to the 3-day rainfall recorded at the Kananaskis climate station were computed. These numbers which are the total rainfall volume divided by the measured 3-day rainfall at the Kananaskis station correspond to 38,100, 44,100 and 41,600 for the 2005, 2012 and 2013 events, respectively. The average of these factors (41,250) was then applied to calculate the total rainfall for each of the recorded sedimentation events for which isohyet maps were not available. Results are summarized in Table 5-7.

[23] Note the exact interpretation is that the 2013 rainfall event is expected to occur once in the next 294 years.

Table 5-7. Total sediment volumes from calculated rainfall volumes with addition of a 21% snowmelt contribution.

Year	3-Day Rainfall at Kananaskis (mm)	Estimated Runoff Volume[4] (Mm^3)	Sediment Volume ($L\sigma$) (m^3)	Sediment Volume (Best Fit) (m^3)	Sediment Volume ($U\sigma$) (m^3)
1948	49	2.02	12,800	16,000	19,400
1956	38	1.56	10,400	13,000	16,200
1967	67	2.75	16,400	20,000	24,100
1974	69	2.83	16,800	20,000	24,600
1980	83	3.43	19,700	23,000	28,700
1990	68	2.80	16,600	20,000	24,400
1995	94	3.89	21,400	26,000	31,200
2005	149	5.69	28,000	34,000	42,000
2012	86	3.80	21,000	25,000	31,000
2013	265	11.01	45,000	57,000	72,000

[4] Including snowmelt.

Except from the 2013 event, these data were then used to construct a frequency-magnitude curve of the higher frequency events, as discussed in more detail in Section 6.0. The formulae used apply to total sediment moved from sediment stored in the main channel, but does not explicitly account for multiple sediment inputs from tributary channels. Much of this sediment would also be entrained, especially in the lower reaches of the watershed.

5.7. Summary

A number of techniques were combined to determine the sediment volume of past debris floods. For old (several hundreds to thousands of years) debris floods, magnitude estimates were based primarily on radiometric dating in combination with reconstruction of runout areas and application of empirical formulae relating deposit area and volume. For younger events that were recorded by direct observations, an empirical formula was applied that relates the total runoff volume of a given storm to the sediment moved.

Cross-section measurements along Cougar Creek with pronounced terraces and application of Manning's velocity formula yielded an approximation of possible peak flows of significant events in the past. The latter method, however, is fraught with uncertainty as the floodplain elevation and thus, flow depth at the time of terrace formation, is unknown. Irrespective, two clusters appear between 200 and 300 m^3/s and between 800 and 1000 m^3/s which may be attributed to landslide dam outbreak floods along the mainstem channel of Cougar Creek. The age of these large events has not been reconstructed, but the larger of these events likely pre-dates the oldest trees measured on the lower Cougar Creek terraces as those would likely have been destroyed by a flood of such magnitude.

6.0 FREQUENCY-MAGNITUDE RELATIONS

6.1. Introduction

Frequency-magnitude relations are defined as volumes or peak discharges related to specific return periods (or annual frequencies). This relation forms the root of any hazard assessment because it combines the findings from frequency and magnitude analyses (Sections 4.0 and 5.0) in a logical format suitable for numerical analysis. Any frequency-magnitude calculation that spans time scales of millennia necessarily includes some judgment and assumptions, both of which are subject to uncertainty. However, the analysis described in this section is based on the best data available and is considered appropriate for the scale and level of detail of this assessment. Uncertainty can further be addressed by building in redundancies and freeboard in engineering measures.

In this section, five different debris flood classes of varying return period and magnitude (sediment volume) are defined for subsequent use in quantitative risk analyses of existing and proposed assets on Cougar Creek fan.

This section begins with an explanation of the basic frequency-magnitude model and introduces the two approaches in processing and plotting the debris flood age – volume data pairs. The issue of stationarity in the reconstructed time series of debris floods is then addressed, which if violated could lead to erroneous results.

6.2. Frequency-Magnitude Model

6.2.1. Introduction

Commonly applicable rules as to the time window to be used to construct debris-flood or debris-flow frequencies do not exist, but regulatory guidance and/or legislation worldwide mandate a range from several tens of years up to 10,000-year return periods. For example, in British Columbia, Canada, the current guidance to Ministry of Transportation approving officers is that a 10,000 year return period be considered for all life threatening landslide processes (MoTI, 2009). In contrast, present guidance in Austria calls for examination of return periods of up to 150 years (Huebel, pers. comm.), while in Switzerland return period of up to 300 years are considered, including the assessment of residual risk associated with return periods exceeding 300 years. In Switzerland, hazard maps are then based on a combination between debris flow intensity and the occurrence probability. Rudolf-Miklau *et al.* (2011) provide a convenient overview of the hazard and risk assessment guidelines in various European nations.

Once a reasonable documentation of events with estimated age and volume has been achieved, return periods need to be assigned to individual events that allow extrapolation and interpolation into annual probabilities beyond those extracted from the physical record. Such record extension is necessary to develop quasi-continuous event scenarios that are then integrated into numerical runout modeling and finally the consequence analysis that forms part of the risk assessment.

The probability of occurrence of debris floods during a time interval Δt is low and the probability of two or more simultaneous events is negligible in the same channel (see McClung, 1999 who describes this for snow avalanches). Debris floods on Cougar Creek can thus be approximated as discrete, random and (mostly) independent.

Frequency analyses, including those used for debris flows and debris floods, also rely on the premise of stationarity over time, and that they underlie an ergodic (independence from initial conditions) stochastic process. Both assumptions can be questioned. For one, extrapolation into high return periods that are a multiple of the initial record length increases the uncertainty significantly in absence of information on how climatic or geomorphic watershed conditions may have changed. In the case of Cougar Creek, this led BGC to curtail the upper end of the analysis to a 1000 to 3000 year return period rather than extrapolating to larger return periods.

Source material depletion, vegetation changes, wildfire suppression, changes in the frequency and/or magnitude of hydroclimatic events and the occurrence of cataclysmic events such as large landslides in the watershed can all alter the stationary assumption at different temporal scales. Ergodicity, in turn, demands that the geophysical process (in this case debris floods) can be viewed as an infinite number of equally likely stochastic events. This assumption is challenged since an upward trend in multi-day rainfall has been observed by Shook and Pomeroy (2012).

These considerations point towards the possible fallacies of applying traditional flood frequency assessments to debris-flow and debris-flood frequency analysis. Furthermore:

- One dataset is considered to be continuous (without missing debris-flood events over the time period considered) while the other likely missed particularly smaller debris floods; and
- BGC believes that there are two processes acting in the watershed, one being mostly bedload transport during high discharge events, and one that is associated with significant tributary debris influx to the main channel and/or landslide damming.

Therefore, two statistical techniques were applied to the dataset of reconstituted debris flood volumes, each one suited to the specifics of data continuity and data quality. These methods are the cumulative frequency-magnitude analysis and the General Pareto distribution. Each method contains assumptions and uncertainties, but general agreement across these methods overcomes some of the pitfalls related to data scarcity and data discontinuity and improves confidence in the results.

6.2.2. Cumulative Frequency-Magnitude Analysis (MCF)

Seismology has been the precursor to the use of regional magnitude-cumulative frequency curves (MCF), (Gutenberg and Richter, 1954). An inventory of debris flow volumes of known dates in a given time interval T_i is ranked from largest to smallest. The incremental debris-flow frequency of rank *i* is determined as $1/T_i$ and the MCF then states the cumulative incremental frequencies as:

$$F_i = \sum_{i=1}^{n} f_i \qquad \text{[Eq. 6-1]}$$

Where F_i is the annual debris-flow frequency of an event of greater than volume V_i. The MCF curve is then produced by plotting F_i against V_i. Hungr *et al.* (2007) recommended binning debris-flow volume data into categories to avoid the effects of data censoring, particularly for small flows that have been overridden and covered by subsequent flows or may not show up in the fan's stratigraphy.

The use of MCF assumes that all events are known, and volumes can be combined in reasonable volume classes, or that the dataset is stratified into classes where confidence exists that all such events have been included. The latter is believed to be the case at Cougar Creek where return period classes are believed to span ranges of respective volumes. Furthermore, the selection of different plotting methods (cumulative vs. non-cumulative, linear and logarithmic binning, different bin sizes and choice of trendlines for extrapolations) can bias the results (Brardioni and Church, 2004).

The MCF technique is sensitive to the number of events as adding events will invariably decrease the individual return periods for events smaller than those newly added. For example, five additional hypothetical events were added to the event database to examine the influence of additional events on return period estimates. The reasoning is the high chance that the test trenches on the fan did not intercept all large debris flood events that have occurred in the past 3000 years. Adding these hypothetical events to the dataset decreases the estimated return period of the 2013 event from 440 years to 240 years.

The MCF method was applied to the "small" debris flood datasets and plotted on Figure 6-1. The maximum and minimum estimates were added based on the methodologies described in Section 5. For clarity, only the data points of the best estimate are shown. A logarithmic function was fitted to the minimum, best estimate and maximum estimates, respectively, shown as the parallel curved solid lines. Superimposed are the curved lines derived from the General Pareto Distribution, described in the following section.

6.2.3. Extreme Value Statistics

A secondary fitting analysis was completed for the large events using extreme value analysis (EVA). The objective of EVA is to quantify the stochastic behaviour of a process at very large or very small values, such that estimates can be made of the probability of events that are more extreme than any of those already observed. The extreme value paradigm describes a principle for model extrapolation based on mathematical limits as finite-level approximations (Coles, 2001). As with all statistical models, EVA-generated values are best guesses and should be interpreted as such.

Block maxima approaches such as the Generalized Extreme Value Distribution (GEV) necessitates blocking the existing data into bins with equal length. However, this is not possible with discontinuous data, as is the case for this study. Extreme value theory, on which EVA is based, motivates the Generalized Pareto Distribution (GPD) to describe the behaviour of a process in excess of a high threshold. It is therefore suited to analysis of threshold excesses such as could be postulated for debris-flow or debris-flood processes. Goodness-of-fit is most commonly assessed visually by examining probability and quantile plots. Fit is characterized by straight line approximation of the fitted data. Notable of many GPD applications are the considerable uncertainties that typically accrue when the model is extrapolated to higher levels than those observed.

The GPD analysis was completed in the freely available statistical software "R" using the extRemes package developed by the National Center of Atmospheric Research (http://www.assessment.ucar.edu/toolkit/). The input volumes used for the GPD analysis were the same as for the cumulative frequency analysis. Furthermore, the number of observations per year and the lower volume threshold (in this case for sediment passing the Cougar Creek fan apex) has to be specified. For the observation frequency, BGC used the number of large events for the entire data series (9 events/3100 years or 0.003). As the lower volume threshold, BGC applied a value of 49,000 m^3. This value was chosen as it lies below the minimum estimated debris flood volume (50,000 m^3) that was extracted from the trenching program.

One issue with this method is a statistical detail, namely that the extRemes software uses the maximum likelihood estimation (MLE) to fit the model. However, in small samples (less than about 60 observations), ML estimates can perform poorly. The recommended method is this case would be the method of moments (MOM); see Madsen *et al.* (1997). However, a comparison between a MOM and MLE approach completed by Prof. Nolde, University of British Columbia (2013, pers. comm.) showed very little difference between the two methods, and therefore, no adjustment was made.

Using the GPD fit, debris flood volumes were calculated for a range of return periods from 300 years to 10,000 years and plotted on Figure 6-1 (light blue squares). However, due to the increasing uncertainties at very high return periods and issues of data stationarity, the analyses were stopped at the 3000-year return period threshold.

Given the two very different statistical approaches used, the two mean curves (blue curved line for GPD and black curved line for the cumulative frequency analysis) show that the GPD produces higher debris-flood volumes from approximately 400 year to 2000 year return periods compared to the power-law fits of the MCF. The principal differences lie in the extrapolations to lower and higher return period events. For lower return period events, the GPD curve approaches debris flood volumes that are not credible given observed events while for higher return periods, the GPD asymptotically approaches a finite limit, while the MCF analysis suggests an infinite limit.

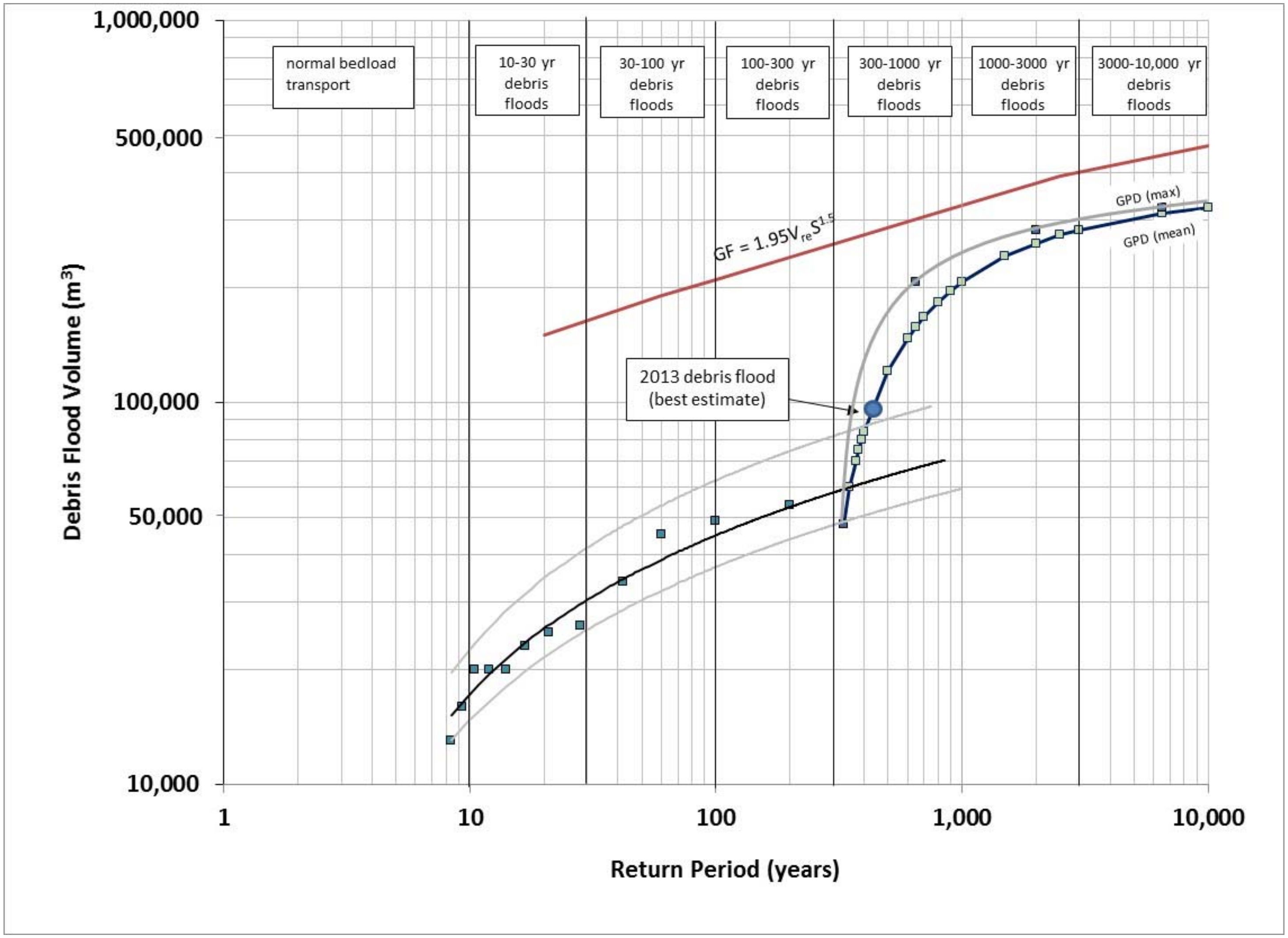

Figure 6-1. **Return period – debris flood volume graph for all reconstructed debris floods including the Rickenmann and Koschni (2010) envelope (thick red line). The curved black and grey lines are based on the MCF analysis, while the curved lines indicates the mean (blue) and maximum (grey) volume estimate of the GPD distribution.**

Following the argument of landslide damming, an infinite limit would necessitate an infinitely large landslide and infinitely large amounts of water impounded upstream of the landslide dam. Extremely large landslide dams in the Cougar Creek watershed are not considered credible for two reasons:

- It appears from Section 2.0 that the size of rock slides or rock avalanches that are able to dam the creek are structurally controlled and thus limit the thickness of bedding planes day lighting and the density of release joints trending perpendicular to the bedding planes.
- BGC did not find evidence of very large landslide deposits during the channel traverse or through detailed inspection of the LiDAR-generated shaded relief imagery along the mainstem channel. Particularly large landslides have proportionally longer persistence in the landscape and thus, should be detected even hundreds or thousands of years after their occurrence (Guthrie and Evans, 2007).

Therefore, the volumes of the 300-1000 year and the 1000 to 3000-year return period classes were determined using the GPD distribution rather than the MCF analysis results.

6.2.4. Application to Cougar Creek

Two separate populations were analyzed as described above. Those populations are designated as “small” and “large” debris floods with a somewhat arbitrary volume separation of around 100,000 m^3 and a corresponding return period of approximately 300 years. This return period approximates the breakpoint of the two data populations, which is believed to be an artifact of the underlying geomorphic processes rather than an artifact of the different sampling techniques.

<u>“Small” Debris Floods</u>

For the MCF-analysed data, that span those debris floods that have been observed and their volumes back-calculated, the data pairs were ranked and the calculated return periods plotted against the respective volume estimates. To close the gap between this dataset and the larger events analysed with the GPD, BGC computed the precipitation amounts for return periods of 60, 100 and 200 years. A power-law function was fitted to the data and the equations from these functions used to determine the volumes corresponding to the return period classes from 1 to 10, 10 to 30, 30 to 100 and 100 to 300 years (Table 6-1).

The outcome of the analysis is sensitive to the choice of trendline fit. A good fit for the “small” debris floods can also be achieved by a logarithmic trendline, which will result in lower sediment volumes for the small (rainfall-triggered) debris flood data population. For this study, a power law fit was favoured because it yields more conservative debris-flood volume estimates.

<u>“Large” Debris Floods</u>

Those events considered to be characterized by abundant tributary sediment influx and/or temporary landslide-damming, were first ranked, plotted in log-log space and a power function fitted to the point distribution as per the "small" debris floods. The principal problem with this approach is that the inclusion of additional events would shift this curve to the left. Because it is unknown how many events were missed during the test trenching campaign, the amount of curve shift to the left is unknown. As discussed in the preceding section, this motivated the use of the GDP. Figure 6-1 shows the GDP curves for the best estimate which corresponds to the mean of the respective return periods. In addition, an upper estimate was plotted (curved grey line in Figure 6-1), which was determined from the GDP estimate of the upper range of the corresponding return period class.

As for the "small" debris floods, and to avoid the illusion of exactness, the lower and upper ranges of the volume estimates as discussed in Section 5.4 were applied. The GPD-derived debris-flood volumes were summarized in continuous return period classes from 300-1000 and 1000-3000 years.

According to Figure 6-1 and irrespective of the 2013 event being classified as a "small" or "large" debris flood, its return period approximates to 400 years.

Table 6-1. Debris flood volume for different return periods.

Return Period (T) (yrs)	Annual Probability (1/T)	Volume Best Estimate (m^3)	Peak Discharge (m^3)	Dominant Hydro-Geomorphological Process
1-10	1-0.1	< 6,000	-	flooding
10-30	01-0.03	30,000	30	flooding/debris floods
30-100	0.03-0.01	40,000	50	flooding/debris floods
100-300	0.01-0.003	60,000	60	debris floods
300-1000	0.003-0.001	*160,000*	*700*	landslide dam outbreak floods
1000-3000	0.001-0.0003	*260,000*	*1000*	landslide dam outbreak floods

Note that the best estimate and peak discharge estimate volumes are based on the mean of the respective return period range. Values in italics are derived from the GPD and assume landslide dam outbreak floods, while all other values are derived from the MCF analysis.

6.2.5. Maximum Credible Debris Flood Volume

Particularly in dam engineering, the notion of the probable maximum precipitation (PMP) or probable maximum flood (PMF) is extensively being used to account for the high loss potential in case of a dam failure. It is also codified in various guidelines. PMPs or PMFs do not have an explicit return period attached, although sometimes the 10,000 year return period is evoked to put these numbers into perspective. To apply this concept to debris floods, BGC used two lines of argument.

The first was to use a published PMP estimate (Verschuren and Wojtiw, 1980) for the study region and apply this value to the Rickenmann and Koschni (2010) upper envelope (Equation 5-3), which is also plotted on Figure 6-1 for comparison. The PMP reported by Verschuren and Wojtiw (1980) for the study area approaches 400 mm for a 3-day rainstorm which corresponds to a runoff volume of 21 Mm^3 including a 25% contribution through snowmelt. Using Equation 5-4, the probable maximum debris flood (PMDF) sediment volume is then estimated to (rounded) 500,000 m^3.

The second approach was to use the maximum volume estimate from the GPD and calculate the debris flood volume corresponding to the 10,000 year return period. This method yields a total volume of (rounded) 300,000 m^3.

BGC estimates that the maximum credible (or probable maximum) debris flood sediment volume on Cougar Creek may lie between approximately 300,000 and 500,000 m^3. This value, as well as the volumes for the different return period classes, is predicated by the assumption of long-term data stationarity which implies no significant changes in the mean and standard deviation of the long-term time series. This assumption is tested in the following sub-section.

6.2.6. Data Stationarity Test

BGC queried the assumption of data stationarity for the 3000 year period that was used in the assessment. A violation of this assumption, i.e. a strong upwards or downward trend, could shed doubt on the validity of the frequency analysis, which assumes stationarity. For this test, BGC determined the fan aggradation rate for each test pit location and normalized by the fan thickness at each location. This normalization accounts for the observed increase in fan thickness towards the proximal (near the apex) fan reaches that is related to the differential debris deposition between the proximal and distal fan portions. Figure 6-2 shows no long-term decline in fan aggradation rates, which implies that the stationarity assumption appears valid. However, climate change is predicted to lead to more extreme rainfall events which may introduce an element of non-stationarity looking forward (see Section 6.2.8.). This possibility ought to be included in debris flood risk management considerations.

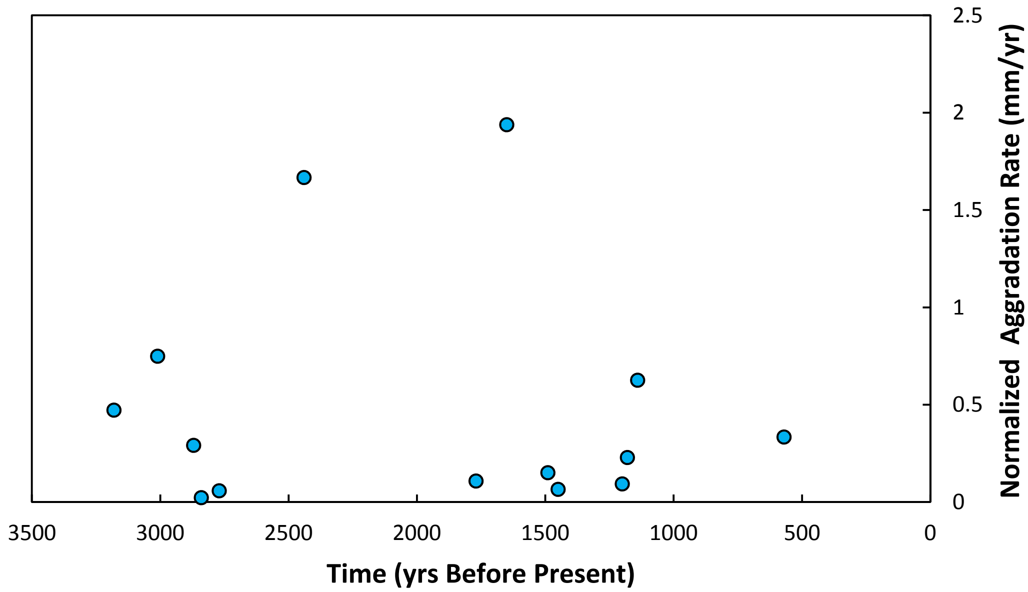

Figure 6-2. Normalized aggradation rates of Cougar Creek fan since approximately 3100 yrs BP.

6.2.7. Frequency-Magnitude Model Test

BGC combined several methods to arrive at a frequency-magnitude model for Cougar Creek, whose results are summarized in Table 6-1 and Figure 6-1. To further test the validity of the bi-model frequency-magnitude model, an independent test was applied.

The choice of the debris-flood volume to be modelled for the respective return periods will strongly influence the model outcome in terms of debris flood intensity (velocity, flow depth and area inundated). Ultimately, since the risk assessment will be based on the hazard intensity maps generated from the model runs, the costs of the mitigation measures will hinge on the chosen volumes. The principal methods used to determine debris flood sediment volume do afford a method to test the reasonableness of the frequency-magnitude relation. The rationale is as follows:

The frequency-magnitude (F-M) relation is based on data obtained back to approximately 3000 years BP. Thus, the volume of the fan overlying a hypothetical 3000 yr BP (V_{3000}) surface would need to approximate the integrated F-M curve, barring some sediment that has been transported into the Bow River. Given that return periods were binned into classes, summing of all debris flow volumes for each return period class should yield approximately the V_{3000}. If the calculated fan volume approximates or is below the best estimate volume sums, this would support the best estimate volumes for numerical modelling.

BGC estimated the fan volume overlying the buried 3000 year BP fan surface using ArcGIS 10.1 Spatial and 3D Analyst. Ten (10) test pits, each with 3 radiocarbon dated depths (minimum, maximum and mean), were used in the analysis. The 2013 LiDAR surface acted as the present day ground surface elevation. The elevations used to create the 3 interpolated surfaces were derived by subtracting the depths at each point from the LiDAR Bare Earth DEM. The fan boundary was assigned elevation values and used as a border for the surface interpolation by extracting the elevations from the LiDAR DEM to the 3D fan boundary. This border constrains the interpolated depth surfaces to meet the present day ground surface outside of the fan boundary. Three triangulated irregular networks (TINs) were generated, one for each surface, assuming the variation in dated fan depths. These TINs were then converted to 5 m resolution raster surfaces using the natural neighbor spatial interpolation method. Volume change surfaces were calculated using the cut fill functionality of ArcGIS. Finally, the 'net gain' attribute of each volume change surface was summed to derive the minimum, mean and maximum fan volumes above the 3000 year BP fan surface. Results are summarized in Table 6-2 together with the sums of all interpolated flood, debris flood and landslide dam outbreak flood events.

Table 6-2. Comparison of fan volumes above the 3000-year fan surface using GIS-based methods and integrated debris flood sediment volumes.

	GIS-based 3000-yr BP Fan Volume Calculations (Mm^3)	**Summed Best Estimate Debris Volumes from Frequency-Magnitude Analysis (Mm^3)**
Minimum Volume Estimate	11.0	11.8
Best Volume Estimate	12.6	10.8
Maximum Volume Estimate	14.5	14.0

The findings presented in Table 6-2 support the best-estimate results from the frequency-magnitude analysis rather than the maximum estimates. Moreover, this analysis offers some insight in the change in rate of fan activity during the early or mid-Holocene. If, in the analysis, the value of 3000 years is replaced with 10,000 years, a total fan volume of 40 Mm^3 to 47 Mm^3 results. This contrasts a calculated total fan volume of 74 Mm^3. Therefore, one can interpret that geomorphic activity on Cougar Creek fan in the time between 10,000 and 3000 years BP may have been double the rates compared to the past 3000 years. Even more drastic declines in fan aggradation rates have been noted on fans west of Banff by Roed and Wasylyk (1973), who describe exposures of Mazama ash some 2.7 m below the distal fan surface of Brewster Creek. Given an approximate age of 6600 years BP for the Mazama ash, this would result in an average fan aggradation rate of 0.4 mm/year. This rate compares to approximately 1.6 mm/year for a distal fan location on Cougar Creek where Bridge River ash (2450 years BP) was found in BGC-TP-18.

6.2.8. Possible Effects of Climate Change

Several limitations to the F-M analysis have been discussed. These are primarily based on the uncertainties related to the chosen analytical techniques as well as time-dependent changes in geomorphic activity as a function of their geological legacy and climate change. In this section, the specific issue of climate change is revisited because mitigation measures proposed for Cougar Creek will be designed to last several decades or longer, and should thus anticipate changes.

It is now scientifically accepted that humans have measurably altered Earth's climate over the past 50 to 60 years (IPCC AR5, 2014). The relevance of climate change with regard to Cougar Creek debris-flood risks is that the predicted warming of the troposphere will very likely[24] increase the intensity of the hydrological cycle in many regions worldwide. Due to more intensive energy exchanges in the vertical air column, as well as the projected intensification of air mass exchange between the low and high latitudes, it is expected that extreme precipitation events will increase in frequency and severity (SREX, 2012; IPCC, 2014). If this were indeed to take place or has already commenced, this could result in several undesirable outcomes with respect to mountain creek hazards:

- The frequency of flooding may increase on small and possibly larger rivers, especially should the timing of extreme storms coincide with the snowmelt season. Over the long term, however, some increases in extreme rainfall may be offset by lesser snowpack thickness due to projected temperature increases.
- The frequency and intensity (volume and peak flow) of debris flows and debris floods may increase for those basins that are sediment supply unlimited. This could lead to higher capital costs in debris flow and debris flood mitigation and in maintaining mitigation structures. Specifically, more frequent hydro-geomorphic processes will require a higher frequency of cleaning out the sediments that accumulate upstream of such structures.
- In sediment supply-limited watersheds in which channel debris is being exhausted by debris flows or debris floods and needs to recharge following an event, an increase in the intensity or frequency of hydroclimatic events would not necessarily lead to an increase in debris flow frequency. However, and depending on changes in vegetation type and density covering adjacent slopes, the sediment recharge rates to the main channel could increase.
- If the design of mitigation measures is based on purely stationary hydroclimatic conditions, they may, in time, be overwhelmed by events that had not been predicted, or by events whose return period has been reduced over time due to observed trends in hydroclimatic extremes.

---

[24] See IPCC (2014) for a definition of "very likely" in the context of that report

In BGC's hydroclimate summary report (BGC, 2014), one section was dedicated to the effects of climate change without claiming to be comprehensive. Conclusions from that report included:

- The frequency and magnitude of extreme, short duration rainfall events at the Kananaskis and Ghost River climate stations appears to be increasing, especially since the early 1990s.
- Peak flow events on Waiparous Creek appear to be increasing in frequency and magnitude.
- These observations are in accordance with recent publications addressing hydro-climatic change in southeastern Alberta.

BGC also retained extreme value statisticians at the University of British Columbia to repeat the frequency analysis carried out by BGC under consideration of a trend in the 3-day rainfall at the Kananaskis station. This analysis suggested that, under the assumption of data non-stationarity, the 750-year return period of the 3-day rainfall at the Kananaskis station would decrease to approximately 300 years. Moreover, the analysis demonstrated that (under the strong assumption of a continuation of the observed linear trend), the 100-year return period 3-day rainfall volume could increase by 10%, a 500-year return period 3-day rainfall event by approximately 30%, and a 1000-year return period 3-day rainfall by over 60%. This analysis cannot predict changes in rainfall intensity. However, increases in rainfall volumes over fixed time periods necessarily will have to be associated with increases in rainfall intensity.

It must be noted that these analyses ignore the unknown forcing mechanism for the observed trend and assume that the trend will continue, both of which are subject to critique. Moreover, the analysis was completed for only one station and would have to be repeated for numerous mountain weather stations in the area to demonstrate that the observed trend is not a legacy of the meteorological station's record or localized effects. In addition, Paul Whitfield (formerly with Environment Canada) notes "The Kananaskis station has been relocated several times and the precipitation measurement system has been changed in addition. The precipitation record from 1939 to present contains several inhomogeneities as a result and any trend analysis that does not properly consider these is likely to be suspect".

While the above analyses are far from a rigorous regional trend analysis, they do point towards trends in maximum 3-day rainfall over their respective observation periods. This has previously been confirmed by the work of Shook and Pomeroy (2012), who identified increasing multiday storm volumes for the Prairie Provinces. The hypothesis of a linear trend in the extreme precipitation can therefore not be discarded and should be acknowledged in risk-based decisions by perhaps allowing extra freeboard in the design of debris-flood mitigation works or including flexible design that allows later design upgrades.

6.3. Summary and Limitations

Debris flood frequency-magnitude relations were developed for Cougar Creek. The data pairs are summarized in Table 6-1 and form the basis for debris flood modelling and subsequent quantitative risk assessment (provided in a separate report).

The analysis relies heavily on the assumption that there are two data populations that can be distinguished based on the hydro-geomorphological processes that cause such events. The intersection between the two regression/GDP best fit lines between a 300 to 400 year return period and associated debris volume of approximately 90,000 m^3 is viewed as a possible division between those two data populations. This interpretation is somewhat simplistic in that it does not account for hybrid events (channel bedload mobilization and short-lived, localized landslide dam outbreak floods) that undoubtedly occur. The 2013 debris flood may serve as an example. In this case, numerous debris flows discharged into Cougar Creek, some of which may have led to temporary short-lived damming of the creek, which may have resulted in a pronounced surging behaviour as observed by some at Elk Run Boulevard (A. Esarte, pers. comm. 2013).

The choice of statistical tools will also strongly influence the outcome. The GDP was used in this study because it avoids the disadvantage of missing data as it is motivated by use of a common detection threshold, which is 50,000 m^3 in the example identified and is insensitive to censored datasets. It also yields the more conservative volume estimates for the time frames considered in this study. Finally, its asymptotic nature suggests a finite debris amount which is realistic given that precipitation and thus runoff amount are subject to meteorological constraints.

7.0 DEBRIS FLOOD MODELLING

7.1. Introduction

Numerical modelling of debris floods is the basis for the delineation of hazard intensity zones, which will serve as input to the quantitative debris flood risk assessment (QFRA). Modelling also helps define the peak discharges associated with the various return period hazard classes, as only sediment volume has been defined to this point. Debris flood modelling is based on the following principal assumptions:

- The frequency-magnitude relation established in the previous section is a reasonable basis to simulate debris floods for return periods from 10 to 3,000 years.
- Bedload entrainment through exceedance of discharge thresholds is the principal process to generate debris floods of return periods up to perhaps 300 years.
- Landslide dam outbreak floods provide hazard scenarios that may correspond to debris floods including and exceeding the 300 to 1000-year return period class. Note that this does not imply that all debris floods corresponding to the return period class will necessarily be landslide dam outbreak floods.
- By varying sediment concentrations, a fluid roughly equivalent to the observed debris floods can be simulated.
- Erosion and re-deposition of debris on the fan cannot be modelled and needs to be assessed by judgment.

The differentiation of debris flood generation by process type requires a staged modeling approach that involves landslide dam outbreak modelling, followed by debris flood routing onto the fan of Cougar Creek.

7.2. Landslide Dam Outbreak Modelling

7.2.1. Introduction

During BGC's channel traverse, 13 potential landslide dam locations were identified along the Cougar Creek mainstem channel (Drawing 3). Landslide dam outbreak scenarios were modelled at location WP-21, the nearest location to the fan apex of Cougar Creek (approximately 1000 m upstream). During field work, BGC estimated that this dam height was between 20 and 25 m high. No organic material was found that would allow an estimate of the dam's age. Figure 7-1 shows an upstream-looking view of this landslide dam location.

This location was chosen for modeling for two reasons. The first is that its proximity to the fan apex results in the least amount of debris flood attenuation. The second is that the estimated landslide dam height was one of the highest measured by BGC along Cougar Creek. Modeling of equal or lesser height landslide dams further upstream would result in lower peak flows at the fan apex and downstream. Thus, the chosen location represents a conservative scenario.

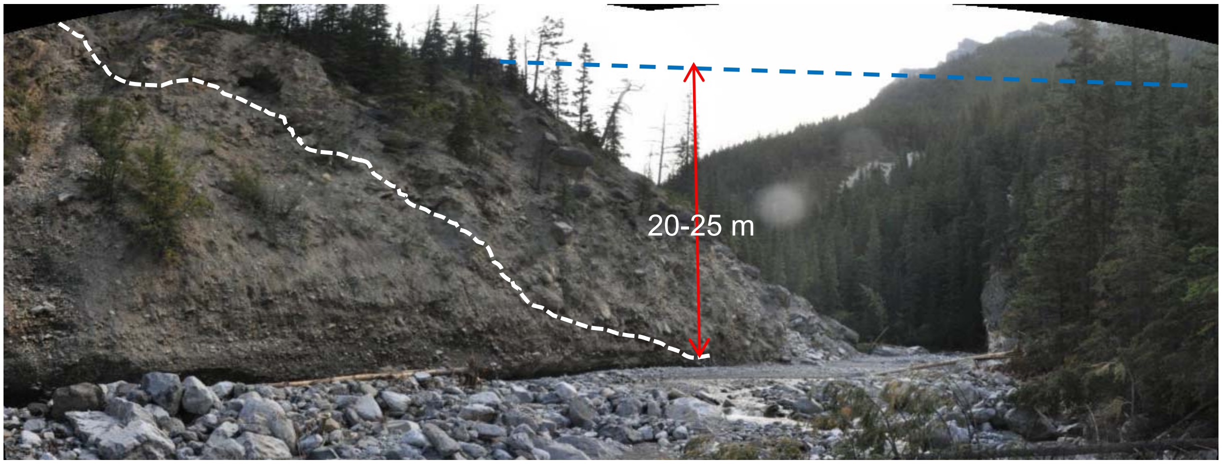

Figure 7-1. Landslide dam location at WP-21 (Drawing 3). The blue line indicates the inferred height of the landslide dam at the time of its occurrence. The white dashed line shows the landslide deposit on the right separated from glacial deposits on the left (underlying). BGC photograph of August 2013, looking upstream along east side of channel.

7.2.2. Landslide Dam Failure Peak Discharge Estimate

The magnitude of landslide dam failures can be expressed as the volume of water and sediment being discharged and its peak discharge. Both factors must be estimated to construct a flow hydrograph that serves as input to route the outbreak flood downstream.

The total outflow volume equals the amount of water that can discharge above the bottom of the landslide dam, which is usually the original ground elevation. For landslide dam failures, peak flow estimates depend on the height of the dam, the erosion rate during overtopping, and the total impounded water volume. Higher dams with high erosion rates will result in the highest peak flows. Erosion rates will depend on the landslide dam's width and internal structure, which in turn depends on the mode of deposition and materials involved.

Based on the 2013 LiDAR data, an artificial landslide dam was simulated that was subsequently allowed to overtop and breach. Two different landslide dams were specified to represent return periods of 300-1000 and 1000-3000 years. Table 6-1 provides the assumed sediment volumes for these hazard classes. Further, BGC assumed that:

- The sediment volume of the debris flood should roughly match the landslide dam volumes, as it is assumed to be fully entrained during the breach;
- Sediment concentrations of debris floods reach up to 30% for return periods exceeding 300 years, which are most likely to be associated with landslide dam failures;
- The breach will reach to the bottom of the original river bed; and
- The failure mode is overtopping rather than piping, as approximately 90% of landslide dams fail by overtopping (Peng and Zhang, 2012).

Based on the assumptions described above, the artificial landslide dam was simulated by adjusting height and landslide dam slopes to approximately equal the debris flood volumes (Table 6-1). The resulting dam heights for the 300-1000 and 1000-3000 year return period classes were 24 m and 30 m, respectively. The last value is approximately 5 m higher than the estimated landslide dam height determined in the field at this location.

The physically-based mathematical model BREACH (Fread, 1991), which is distributed and maintained by NOAA's National Weather Service, was used to model the dam outbreak flood hydrographs. BREACH simulates the physical processes of an overtopping or piping failure using the principles of hydraulics, sediment transport and slope stability. In a typical overtopping breach analysis, BREACH simulates the following processes:

- Flow of fluid over the dam crest initiates erosion of a narrow channel on the downstream dam face
- The channel incises into the dam face and expands laterally through a combination of continuous erosion and episodic bank failures
- After intersecting the upstream dam face, the channel begins to incise vertically and continues to expand laterally.

Inputs to BREACH include the geometry and physical soil properties of the dam and impounded lake, inflow hydrograph (i.e. baseflow), tail water cross sections, roughness co-efficient, and numerical simulation control parameters. Given the landslide dam breach may be triggered by a flood event, for modeling purpose, a 100-year return period flood discharge, approximately 16 m^3/s (AMEC, 2003), was used as the inflow discharge.

The program BREACH outputs a hydrograph and peak discharge, but given the uncertainties related to the assumed dam geometry and soil properties, peak discharge estimates can vary significantly. Therefore, peak discharge was estimated based on empirical equations prior to BREACH modeling. This approach is independent of landslide dam geometry other than its height.

Table 7-1 summarizes peak discharge estimates for the two return period classes calculated with the principal equations developed by various authors for natural landslide dam studies worldwide: Walder and O'Connor (1997), Costa and Schuster (1988) and Costa (1980).

The first of these equations, Walder and O'Connor (1997), derives physically-based peak flow estimates by using impounded water volume, water depth, and vertical erosion rate. An erosion rate 1.5 m/min was chosen by BGC based on the maximum erosion rate among 28 recorded landslide dam failure events documented in O'Connor and Beebee (2009). Peak discharges were also estimated using regression equations developed by Costa and Schuster (1988) and Costa (1988). These equations use impoundment volume and landslide dam height to estimate peak discharge from natural dam failures. As illustrated by Table 7-1, the Walder and O'Connor's equation provided the highest estimate and were subsequently used as reference values for peak flow estimates using the BREACH model.

These peak discharge estimates are consistent with back-calculated discharges using existing terrace heights, as discussed in Section 4.6.

Table 7-1. Landslide breach peak flow estimates.

Return Period (years)	Dam Height (m)	Impounded Water Volume (m^3)	Authors	Peak Discharge (m^3/s)	Peak Discharge (m^3/s) from BREACH
300-1000	24	373,000	Walder and O'Connor (1997)	700	700
			Costa and Schuster (1988)	650	
			Costa's (1988)	470	
1000-3000	30	650,000	Walder and O'Connor (1997)	1000	1000
			Costa and Schuster (1988)	870	
			Costa (1988)	650	

7.2.3. Output Hydrographs

Using the empirical formula of Walder and O'Connor (1997), the peak flow was specified for the two return period scenarios. However, this approach does not specify the shape of the hydrograph, which is an important variable for flood routing. Therefore, the output discharge hydrograph for each return period scenario was calculated in BREACH using the mass conservation equation:

$$Q_i - (Q_b + Q_o) = S_a \frac{\Delta H}{\Delta t} \quad \text{[Eq. 7-1]}$$

where Q_i is reservoir inflow, Q_o is crest overflow, Q_b is breach outflow, ΔH is the change in water surface elevation during the time interval Δt, and S_a is the surface area at elevation H.

Figure 7-2 shows the resulting hydrographs for the 300-1000 and 1000-3000 year return period classes. The corresponding peak discharges determined by BREACH were approximately 700 m^3/s and 1000 m^3/s, respectively, matching the peak discharges estimated with Walder and O'Connor equation (Table 7-1).

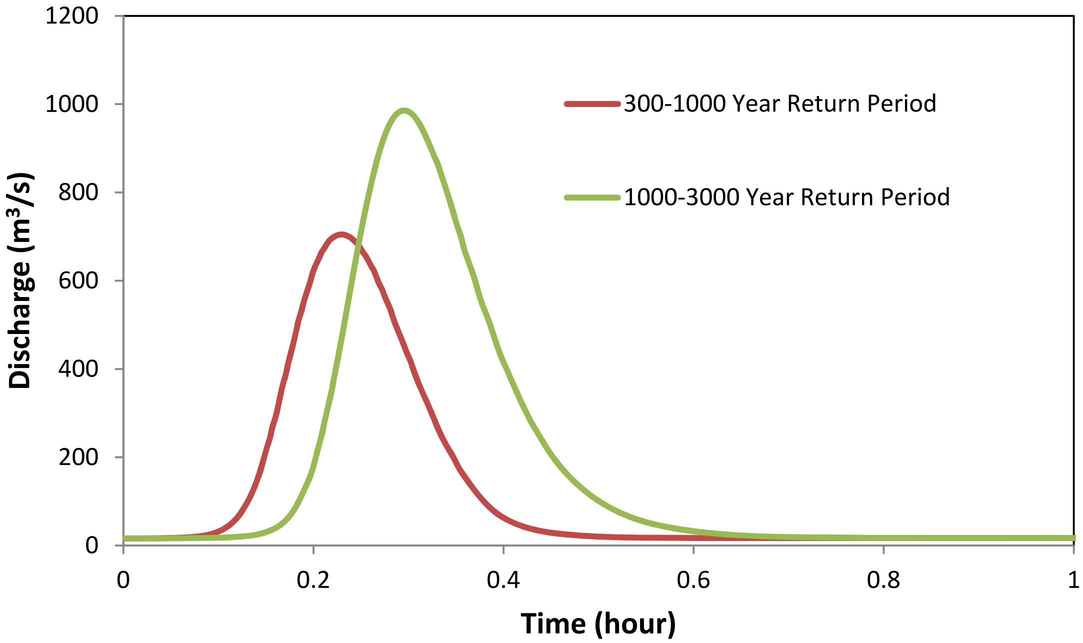

Figure 7-2. Dam outbreak hydrographs from BREACH for 300-1000 and 1000-3000 year return period classes.

7.2.4. Uncertainties

Several sources of uncertainty related to peak discharge estimation remain:

- The geometry of modelled landslide dams (side slope angles and crest width) is unknown and will depend on the type of landslide (for example rock slide versus debris flow). In this study, the landslide volume was varied from 160,000 m^3 to 260,000 m^3 and the landslide geometry was adjusted to match the estimated sediment volumes for each debris flood return period class.
- Sediment entrainment between the landslide dam and the fan apex (1 km distance) was neglected.
- In this assessment, the best estimate of the landslide dam height was based on extrapolating a line from the observed landslide deposit horizontally to the opposite valley side. Depending on the geometry and impact of landslides, the dam slope may vary.
- Both the peak discharge and outflow hydrograph shape may be different in future landslide dam outbreak floods than modelled.
- This assessment used overtopping as the principal failure mechanism for a landslide dam breach. However, other failure mechanisms are conceivable (overtopping vs. piping vs. a combination of both processes as appeared to have been the case in the 1990 dam failure). Because the hydrograph at dam failure determines peak discharge downstream, it affects the outcome of subsequent numerical runout modelling.

7.3. Debris Flood Modelling

7.3.1. Introduction

In order to estimate the flood intensity (maximum flow depth and velocity) and the extent of inundation on the fan, the breach outflow hydrographs were then routed downstream using the commercially available two-dimensional hydraulic model, FLO-2D (2004). FLO-2D is a volume conservation model that conveys a flood within defined channel segments and as overland flow. Flow progression is controlled by topography and flow resistance. The governing equations include the continuity equation and the two dimensional equation of motion (dynamic wave momentum equation). The two dimensional representation of the motion equation is defined using a finite difference grid system, and is solved by computing average flow velocity across a grid element boundary one direction at a time with eight potential flow directions. Pressure, friction, convective and local accelerations components in the momentum equation are retained.

FLO-2D is suited for this type of application as it can model unconfined flows across fan surfaces and simulates flows of varying sediment concentrations. It has been applied numerous times worldwide and is on the U.S. Federal Emergency Management Agency's list of approved hydraulic models.

7.3.2. FLO-2D Modelling

Required inputs to the FLO-2D model are as follows.

The input hydrograph to FLO-2D was provided from the BREACH model and then routed downstream. FLO-2D routes debris floods as a fluid continuum using a quadratic rheological model to simulate flow resistance as a function of sediment concentration. Remobilization of deposits by subsequent surges and the deposition of material cannot be simulated with any accuracy. A yield strength must be exceeded by an applied stress to initiate flow. FLO-2D models the total shear stress, τ, in hyperconcentrated flows and debris flows as a summation of five shear stress components: the cohesive shear stress (τ_c), the Mohr-Coulomb or frictional shear stress (τ_f), the viscous shear stress (τ_v), the turbulent shear stress (τ_t), and the dispersive shear stress (τ_d). Specifics can be found in FLO-2D (2004) and O'Brien and Julien (1988).

For Cougar Creek, typical yield stress and viscosity parameter values were estimated from laboratory experiments on samples of fine-grained mudflows in Colorado and data from China (Table 9, p. 54 in FLO-2D, 2004). Sensitivity analyses showed that simulation results were not overly sensitive to the chosen parameters, particularly for the cases with sediment concentrations less than 30%. Also, when BGC simulated the 2013 debris flood event, the chosen parameters resulted in a good fit with the observed inundation zone, as described later in this section.

Detailed topographic information, which is a key model input, was based on LiDAR data provided by Town of Canmore. In order to reflect the channel capacity prior to the 2013 flood event and expected future conditions, 2009 and 2013 LiDAR data were combined and used for modeling. A digital elevation model (DEM) data was created and then input to FLO-2D's preprocessing program, GDS, to generate a square grid for flow modeling purposes. A 10 m x 10 m grid size was used for the models as it strikes a reasonable balance between the detail needed for risk assessment and computing time. The model was started at the breach location at WP21 with the outflow model boundary set along the downstream Cougar Creek fan boundary, which extends to Bow River.

Flow resistance of the turbulent and dispersive shear stress components are combined in FLO-2D into an equivalent Manning's n-value for the flow. Manning's n was estimated as 0.075 for the entire model domain other than the residential area. For residential areas, Manning's n was estimated as 0.04 to reflect average ground conditions. A Manning's n value of 0.02 was initially assigned to roads, but FLO-2D automatically upward adjusted this value because of high turbulence.

In the residential area, the area reduction factors that reflect the effect of buildings on the flood path were assigned to the models. The footprints of buildings were provided by Town of Canmore. The area reduction factors for individual grids were then calculated with ArcGIS based on the ratio of area of building footprint versus grid area.

While FLO 2D can adequately simulate various discharges and sediment concentrations and the associated inundations, it cannot simulate a sequentially aggrading floodplain. The June 2013 event has amply demonstrated that this aggradation does indeed take place and should therefore be reconciled in the model. BGC achieved this goal by using the 2013 DEM and by adjusting the DEM where the post debris flood excavations had created an artificial channel. This channel was digitally filled to the surrounding grade, while the excavated berms that are clearly visible on the shaded relief image were digitally levelled. This procedure assured that a channel planform was reconstituted that prevailed during the latter parts of the debris flood. While it is not possible to predict during which stages aggradation will occur and to what extent, BGC believes that this procedure creates a more realistic modeling domain than if the human-altered post-flood channel were used as the basis for numerical modeling.

BGC conducted a number of sensitivity model runs to examine the effects of the changed channel planform on the outcome and compared it with the observed debris flood behaviour of the June 2013 event. These sensitivity runs demonstrated that the reconstitution of the 2013 channel planform provided the most realistic results.

7.3.3. Model Runs

Table 7-2 summarizes the specific model runs that were performed and key input parameters including peak discharge and chosen sediment concentration. Model outputs include grid cells showing the velocity, depth, and extent of debris flood scenarios. These outputs are imported into GIS and overlaid on base maps.

Flood scenarios with a return period of less than 10 years were not modeled, as those are very likely to remain in the present channel under consideration of the presently implemented short-term mitigation measures. The model runs shown in Table 7-2 include a simulation of the 2013 debris flood event, assuming a peak discharge of 80 m^3/s at the Elk Run Boulevard culvert (BGC, 2013). This scenario was used to calibrate model parameters (peak flow, sediment concentration, and yield stress and viscosity parameters) to a known event.

The peak outflows for the 300-1000, and 1000-3000 year return period events are based on the landslide dam breach analyses. For the 10-30, 30-100 and 100-300-year return period classes, the landslide dam scenario was not applied as BGC believes that landslide dams are not the primary mechanism for debris floods for those return periods. Peak flows were estimated based on judged multiples of the 100-year return period peak flow (Q_{100}) estimate of 16 m^3/s (AMEC, 2006). In the case of the 10-30 year peak flow, the Q_{100} was multiplied by two while the 30-100 year return period event was multiplied by a factor of 3 and the 100-300 return period by a factor of 4 to account for added sediment transport (Jakob and Jordan, 2001). These multipliers are based on judgment and comparison with previous studies by BGC. However, under a short-term mitigated scenario, even somewhat higher numbers are unlikely to lead to channel avulsions at the Elk Run Boulevard and precision estimates are therefore not warranted. Hydrographs for these lower return period classes were assumed to have a simple triangular shape.

Scenario 3 (Table 7-2) was simulated with two scenarios: one in which the Elk Run Boulevard culvert is assumed to perform to full capacity and one in which it is assumed to be blocked by debris. This culvert has an approximate capacity of 160 m^3/s (CH2M HILL, 1993). This capacity exceeds the assumed peak discharge of the 100-300 year return period class by a factor of 2. However, as was noted during the June 2013 event, the culvert's capacity was heavily jeopardized by sediment accumulations inside the culvert which may have decreased its capacity by more than half. Without the continuous excavation of debris by two excavators on either side of the culvert, it is likely that an avulsion would have occurred. Therefore, it is reasonable to assume a scenario in which the culvert would be blocked. Based on the documented flood events on Cougar Creek, the culverts under Highway 1, Highway 1A and the CPR were always clogged by debris, so those culverts were assumed to be clogged in the model runs as well.

BGC also modelled the 300 to 1000 and 1000 to 3000 return period debris floods trying to force the flow towards the western fan sector, thereby simulating avulsions that may develop due to preferential sediment accumulations or log jams. This was achieved by digitizing a 5 to 10 m high and 200 m long berm in the model on the east side of the creek. The model showed that it was very difficult to force debris flows onto the western fan sector as the upper fan surface is significantly higher at the Elk Run Boulevard than the eastern portion. Because the runout results are similar without and with the berm in place, BGC did not consider it necessary to include such runs in this report. For scenarios 4 and 5 (Table 7-2), additional scenarios for Elk Run Boulevard culvert blockage or performance were not simulated as the estimated peak flows far exceed the culvert capacity and avulsions are expected.

Table 7-2. Simulated scenarios and input parameters.

Return Period (yrs)	Volume Estimate (m^3)	Sediment concentration (%)	Peak* Flow (m^3/s)	Hydro-Geomorphic Processes	ID	Model Runs and Assumptions
< 10	< 6,000	0	-	Flooding		No run
10 to 30	30,000	10	30	Flooding/ Debris flood	1	ERBC performs to capacity
30-100	40,000	20	50	Debris flood	2	ERBC performs to capacity
100 to 300	60,000	20	60	Debris flood/LDOF	3a	ERBC performs to capacity
					3b	ERBC is blocked
300 to 1000	160,000	30	700	LDOF	4	ERBC is blocked
1000 to 3000	260,000	30	1000	LDOF	5	ERBC is blocked
No mitigation[1]	90,000	20	80	Debris flood	6	ERBC performs as it is kept open artificially

LDOF = landslide dam outbreak flood, ERBC = Elk Run Boulevard culvert, [1] represents June 2013 event, * Peak flow as reported here is the total discharge including the sediment in transport.

7.4. Results

Drawing 11 present the results of debris flood modelling. Table 7-3 summarizes key results including a brief description of areas impacted. These descriptions are provided for context but should not be interpreted as an assessment of risk, which will be assessed in BGC's forthcoming risk assessment report.

Two different sets of grid cell values are shown on Drawing 11. For areas with low flow velocity (< 1 m/s), only flow depths are shown. For areas of higher velocity (≥ 1 m/s), a flow "intensity" index is shown, calculated as modelled flow depth multiplied by the square of flow velocity (Jakob *et al.* 2011). This intensity parameter was chosen as it is useful to characterize the destruction potential of modelled flows. Further description of debris-flood intensity parameters and their application to estimate debris-flood risk on Cougar Creek fan will be described in the forthcoming risk assessment.

Table 7-3. Results from numerical debris flood modelling based on the 2013 LiDAR-generated DEM.

Return Period (years)	Scenario	Sediment Volume (m^3)	Results
10-30	1	20,000	• The flow remains within the confines of the channel.
30-100	2	40,000	• The flow stays largely within the confines of the channel to Hwy. 1 • Bank erosion upstream and downstream of Cougar Creek Boulevard to the Hwy. 1 crossing can be expected • Depending on the sequence of sediment deposition during the event, some avulsion could occur towards the western fan sector around the eastern portions of Grizzly Crescent • Inundation of sections of Hwy. 1 and 1A as well as the CPR line is considered very likely • Likely impact and significant introduction of fine-grained sediment of Police Creek
100-300 ERBC at capacity	3a	60,000	• Similar to run 2 but with larger inundation areas and higher likelihood of avulsion near eastern portion of Grizzly Crescent. • Backwater effect from Highway 1 and inundation/erosion of properties on east and west of CC channel • Inundation of Highway 1, Alpine Helicopters, the industrial property south of Lincoln Park Ave, Highway 1A, and the CPR
100-300 ERBC blocked	3b	60,000	• Similar to 3a with less inundation of the area south of Hwy. 1 • Avulsion at the ERBC with flow due south into the Industrial area. • More widespread inundation on the eastern fan sector in the area of Canyon Close and Lady MacDonald Drive • Possibly severe erosion along Lady MacDonald Crescent and Lady MacDonald Drive • Flow depths of up to ~ 3 m and significant deposition in the industrial area • Highway 1A is impacted south of the industrial area
300-1000	4	160,000	• The outcome is similar to a combination of Scenario 3a, b. • Most of the eastern fan sector would be inundated with maximum flow depths of up to 1.6 m and localized flow depth exceeding 3 m. • It is conceivable that 1.2 km of Hwy. 1 and 2.1 km of Hwy. 1A and the CPR be impacted. • At this peak flow, avulsion to the west is possible at Elk Run Blvd. with flows descending Coyote Way area, crossing Kodiak Road and Cougar Creek Drive heading towards the school and Hoodoo Crescent.
1000-3000	5	260,000	• Almost the entire eastern fan sector would be inundated with water and debris and over 50% of the western fan sector. • It is conceivable that 1.5 km of Hwy. 1 and 2.2 km of Hwy. 1A and the CPR be impacted. • Police Creek on the Bow River floodplain are impacted which is likely to lead to a back-water effect and upstream flooding in downtown Canmore • Police station, electrical substation and possibly the firehall would be impacted • Flood flows would extend down Elk Run Blvd to the south and north
2013 event	6	90,000	• No avulsion at ERBC, but backwater effect possible at Highway 1 with properties affected along the southwestern side of Grotto Road and southeastern portions of Grizzly Road • Avulsions possible into the industrial area on the eastern fan sector (parallel to Highway 1) • Inundation of Highway 1, Alpine Helicopters, the industrial area south of Lincoln Park Ave, Highway 1A and CPR • Note that without continuous excavation at the ERBC, avulsion onto the eastern fan sector would have been very likely.

7.5. Uncertainties

Natural landslide dam breaches and subsequent inundation involve complex and dynamic physical processes that are variable in space and time. No two debris floods even with identical volumes are expected to results in the same inundation pattern, avulsions, bank erosion and channel bed aggradation. This is due to the shape of the actual sediment/water hydrograph which in turn hinges on the meteorology of the debris flood triggering storm. A strong double-fronted storm may lead to two distinct rainfall intensity peaks, while a single front storm would lead to a single peak, perhaps amplified or lagged by snowmelt contribution. The hydrograph shape will influence the rates of sediment recruitment and deposition.

Given the impracticality of creating all conceivable hydrograph shapes and modelling these, several simplifying assumptions have to be made. As such, a number of uncertainties exist that influence the model outcome. In this context, it is critical to ensure that model outputs are appropriately used. Model results can be used for the following purposes: (a) determine economic and life loss risk in affected zones and (b) evaluate measures to reduce the risk of debris floods to elements at risk located on Cougar Creek fan. Model results should not be used to determine exactly which buildings are or are not free of hazard since model uncertainty does not allow such decisions. Similarly, velocity estimates are approximations and may vary according to microtopography and various flow obstacles or channelization that may develop during the flow.

In addition to uncertainties associated with model input variables such as debris flood volumes, peak flows, and hydrograph shapes (e.g. those uncertainties described in the preceding sections), model uncertainties include the following:

- The rheological input parameters that affect flow depth and inundation area (somewhat significant)
- The topographic input (little significance after having made channel planform adjustments)
- The detailed effects of buildings and roads on the flow behaviour (possibly significant as their effects will change if obliterated)
- Fan surface erosion (possibly significant, especially if knick points develop)
- Sediment transport and deposition processes (very significant because these will be transient in space and time).

Because the model was calibrated by the 2013 event, BGC is confident that the rheology at least for the lower return period classes (< 300 years) has been reasonably portrayed. For the upper return period classes (> 300 years), the differences in flow behaviour introduced by increasing the sediment concentration to 30% are unlikely to differ fundamentally, particularly in the lower fan reaches but may vary in the upper fan reaches. Here it is conceivable that the leading outbreak flood edge may have higher viscosities and yield strength that what was modeled herein. This uncertainty was accounted for in the development of the composite hazard map that will be produced under separate cover. Given that high precision topography was used for modeling (LiDAR), there is high confidence that topography has been depicted accurately with the planform adjustments that have been made.

The effects of buildings and roads are more difficult to assess. Building footprints were added to the model and flow deflection can be expected. When flow passes through a corridor that is densely developed (e.g. Lady MacDonald Crescent, Drawing 11, run 3b), flow may either destroy buildings or flow velocities in between buildings will increase due to the constriction. In those areas, erosion is more likely due to the higher flow velocities and flow depth, and this potential erosion adds uncertainty that cannot be practically quantified. Deposition of coarse-grained material is also not an output of the FLO-2D model. Sediment transport processes can have a significant impact on flow directions and erosion, as flows are forced around deposited sediments.

It is virtually impossible to accurately forecast the location and extent of erosion and deposition on the fan. However, by conducting multiple models runs with differing sensitivities, confidence has been gained that the scenarios ultimately used for the generation of the hazard map and input to the risk assessment are a reasonably comprehensive representation of possible debris flood outcomes. For example, various sensitivity runs demonstrate a preferred flow path on the eastern fan section from Elk Run Boulevard due south (Drawing 11), which likely follows a previous flow path as seen on the 1947 air photographs. According to the model results, maximum flow depths of around 2 m could be expected along this flow path (see Drawing 11) and potential erosion would be expected to be highest along this flow path.

8.0 CONCLUSIONS

This report assessed debris flood hazards on Cougar Creek fan. Based on a variety of investigative techniques, BGC developed a frequency-magnitude (or return period – volume) curve that served as input to numerical modelling of debris flood runout. Six return period classes were extracted ranging from <10 years to 1000 to 3000 years. Higher return period events were not considered explicitly due to significant uncertainty with their estimation. A probable maximum debris flood of up to 500,000 m^3 in volume was estimated.

The validity of the frequency-magnitude curve was checked by summing all theoretical debris flood events over a 3000-year period and comparing it with a calculated fan volume. The mean and maximum summed debris flood volumes (10.8 Mm^3 and 14.0 Mm^3) closely match the best and maximum fan volume estimates for the above-3000 year BP fan surface (12.6 Mm^3 and 14.5 Mm^3), supporting the general shape of the frequency-magnitude curve.

BGC interprets two different debris flood triggering mechanisms that act over different temporal scales. Debris floods with return periods less than approximately 300 years are likely triggered by heavy rains sometimes associated with snowmelt, while debris floods of at least several hundred year return period may be dominated in discharge and volume by landslide dam outbreak floods. Accordingly, the debris floods with return periods in excess of 300 years were simulated by a combination of a landslide dam break model and a debris flood routing model.

The principal conclusions from the numerical modelling are that:

- Debris floods of return periods up to 30 years will likely remain in the channel of Cougar Creek especially under the assumption of short-term mitigation measures that are currently under way. Such events are unlikely to avulse at Elk Run Boulevard, and unlikely to avulse onto the TransCanada Highway. Due to the low culvert capacity and low channel gradient, avulsions remain a possibility at Highway 1A and the CPR crossing.
- Debris floods of higher return periods and thus, higher volumes and peak flows, are increasingly likely to block the existing culverts, especially those at Highway 1, Highway 1A and CPR crossings.
- For events in excess of a 300-year return period (sediment volumes > 60,000 m^3), fan avulsions are increasingly likely. The most probable avulsion location is the culvert at Elk Run Boulevard. For debris floods with return periods exceeding 300 years, upstream avulsions at the Elk Run Boulevard are very likely and would affect the majority of the eastern fan sections and potentially significant portions of the western fan.
- The presently constructed short-term mitigation measures will reduce channel avulsion potential for flows up to a 30-year return period, and partially reduced avulsion potential for flows up to 300-year return period. For events exceeding the 300-year return period, the presently constructed short-term mitigation measures will

have little effect on reducing the potential of debris flood avulsion, though they are expected to significantly reduce erosion along Cougar Creek channel in its fan reaches.

- Debris floods on Cougar Creek are believed to reach a maximum probable volume of up to 500,000 m^3.
- Portions of the east fan sector would likely have been affected during the 2013 debris flood if not for the efforts by the Town of Canmore to keep the Elk Run Boulevard culvert free of debris.

The results of this report will be used as the basis to assess risk to persons and development on Cougar Creek fan in in a forthcoming risk report. The risk report will then serve as the basis to optimize the design of long-term mitigation measures.

9.0 CLOSURE

This report presents the results of the debris flood hazard assessment completed on Cougar Creek. We trust the information provided will allow the Town of Canmore to proceed with the next steps in the hazard and risk assessment of Cougar Creek. Please do not hesitate to contact us if you have any questions or comments, or if we may be of further assistance.

Thank you for the opportunity to undertake this assessment.

BGC ENGINEERING INC.
per:

ISSUED AS DIGITAL DOCUMENT.
SIGNED HARDCOPY ON FILE WITH
BGC ENGINEERING INC.

Matthias Jakob, Ph.D., P.Geo. (AB/BC)
Senior Geoscientist

Reviewed by:

Hamish Weatherly, M.Sc., P.Geo. (AB/BC)
Senior Hydrologist

Kris Holm, M.Sc., P.Geo. (BC)
Senior Geoscientist

APEGA Permit to Practice: 5366

MJ/HW/KH/jc/cm

REFERENCES

Alberta WaterSMART Water Management Solutions Ltd. (2013) The 2013 great Alberta flood: Actions to mitigate, manage and control future floods, final version. August 2013.

AMEC Earth & Environmental Ltd. (2003) Cougar Creek flood control and maintenance study. Report prepared for the Town of Canmore. January 2003.

AMEC Earth & Environmental Ltd. (2006) Cougar Creek erosion protection Highway 1 to Highway 1A. Report prepared for the Town of Canmore. July 2006.

AMEC Earth & Environmental Ltd. (2012) Cougar Creek 2012 flood damage repairs. Report prepared for the Town of Canmore. August 2012.

Ballantyne CK (2002) Paraglacial geomorphology. *Quaternary Science Reviews* **21**(18–19): 1935-2017.

Beierle BD (1997) Early Holocene climate of southwestern Alberta, Canada, reconstructed from lake sediment cores. M.Sc. Thesis, Department of Geography, The University of Calgary, Calgary, A.B.

Beierle B and Smith DG (1998) Severe drought in the early Holocene (10,000–6800 BP) interpreted from lake sediment cores, southwestern Alberta, Canada. *Palaeogeography, Palaeoclimatology, Palaeoecology* **140**(1–4): 75-83.

Ben DI and Evans DJA (2010) Glaciers and glaciation (Second Ed.), London: Hodder Education.

BGC Engineering Ltd. (2013) Cougar Creek, forensic analysis and short-term debris flood mitigation. Final report prepared for the Town of Canmore. December 2013.

BGC Engineering Ltd. (2014) Hydroclimatic analysis of the June 2013 storm. Final draft report prepared for the Town of Canmore. January 2014.

Bobrowski P and Rutter NW (1992) The Quaternary geologic history of the Canadian Rocky Mountains. *Geographie Physique et Quaternaire* **46**: 5-50.

Brardioni F and Church M (2004) Representing the magnitude-frequency relation: Capilano river basin. *Earth Surface Processes and Landforms* **29**: 115-124.

CH2M HILL Engineering Ltd. (1993) Cougar Creek flood protection study. Final report prepared for the Town of Canmore. March 1993.

CH2M HILL Engineering Ltd. (1994) Cougar Creek flood risk mapping study. Final report prepared for Alberta Environmental Protection, River Engineering Branch. March 1994.

Chiverrell R and Jakob M (2013) Radiocarbon dating: Alluvial fan/debris cone evolution and hazards. Invited chapter to *Dating Methods on Alluvial Fans and Debris Cones.* Springer, Netherlands, p. 265-282.

Church M and Ryder JM (1972) Paraglacial sedimentation, a consideration of fluvial processes conditioned by glaciation. *Geologic Society of America Bulletin* **83**: 3059-3072.

Church M and Zimmermann A (2007) Form and stability of step-pool channels: Research progress. *Water Resources Research* **43**: W03415. DOI: 10.1029/2006WR005037.

Clague JJ (1989) Quaternary geology of the Canadian Cordillera. *In* RJ Fulton (Ed.) Quaternary geology of Canada and Greenland. Geology of Canada, 1. *Geological Survey of Canada*, p. 15–96.

Coia, V. and Nolde, N. 2013. Return level analysis of Kananaskis rainfall. Prepared for BGC Engineering Inc.

Coles S (2001) An introduction to statistical modeling of extreme values. Springer Verlag, London, p. 208.

Costa JE (1984) Physical geomorphology of debris flows. *In* JE Costa and PJ Fleisher (Eds.) Developments and applications of geomorphology. Springer Verlag, Berlin, Heidelberg, p. 268-317.

Costa JE and Schuster RL (1988) The formation and failure of natural dams. *Geological Society of America Bulletin* **100**: 1054-1068.

Cruden DM and Eaton TM (1987) Reconnaissance of rockslide hazards in Kananaskis Country, Alberta. *Canadian Geotechnical Journal* **24**:414-429. DOI: 10.1139/t87-052

Cruden DM and Hu X-Q (1988) Basic friction angles of carbonate rocks from Kananaskis country, Canada. *Bulletin of the International Association of Engineering Geology* **38**(1): 55-59. DOI: 10.1007/BF02590448.

Cruden DM and Hu X-Q (1999) The shapes of some mountain peaks in the Canadian Rockies. *Earth Surface Processes and Landforms* **24**:1-13.

Dawson GM (1885) Preliminary Report on the Physical and Geological Features of That Portion of the Rocky Mountains between Latitudes 490 and 51'30, Canada Geological Survey Annual Report, N.S., Vol. 1, 1885, Montreal, 1886, p. 33B.

D'Agostino V, Cerato M, and Coali R (1996) Il trasporto solido di evento estremi nei torrenti del Trentino Orientale. Schutz des Lebensraumes vor Hochwasser, Muren, Massenbewegungen und Lawinen, Vo. 1. Interpraevent 1996. Tagungsband, Garmisch-Partenkirchen, Germany, p. 377-386.

de Scally F, Mattson E and Rowbotham D (2004) The August 1999 debris flow at Five Mile Creek, Banff National Park, Alberta. *Western Geography* **13/14**: 1-18.

Evans DJA, Salt KE, and Allen CS (1999) Glacitectonized lake sediments, Barrier Lake, Kananaskis country, Canadian Rocky Mountains. *Canadian Journal of Earth Sciences* **36**(3): 395-407.

FLO-2D Software Inc. (2004) FLO-2D User's Manual Version 2004.10, October 2004.

Fread DL (1991) BREACH: An erosion model for earthen dam failures. NWS Report, National Oceanic and Atmospheric Administration, Silver Spring, Maryland.

Gadd B (1995) Handbook of the Canadian Rockies (Second Ed.). Corax Press, Jasper, A.B.

Gomi T and Sidle RC (2003) Bed load transport in managed steep-gradient headwater streams of southeastern Alaska. *Water Resources Research* **39**(12): 1336. DOI: 10.1029./2003WR002440.

Gutenberg B and Richter CF (1954) Seismicity of the Earth. (Second Ed.). Princeton University Press, Princeton, N.J.

Guthrie RH and Evans SG (2007) Work, persistence, and formative events: The geomorphic impact of landslides. *Geomorphology* **88:** 266-275.

Harbor J and Warburton J (1993) Relative rates of glacial and nonglacial erosion in alpine environments. *Arctic and Alpine Research* **25:** 1–7.

Hassan MA, Church M, Lisle TE, Bradinoni F, Benda L, and Grant GE (2005) Sediment transport and channel morphology of small forested streams. *Journal of the American Water Resources Association* **41**: 853-876.

Henderson CM, Richards B, and Johnston B (2009) ICOS 2009 Rocky Mountain field trip. Permophiles: Newsletter of the Subcommission on Permian Stratigraphy, 53(supplement 2).

Hungr O, Evans SG, Bovis MJ, and Hutchinson JN (2001) A review of the classification of landslides in the flow type. *Environmental and Engineering Geoscience* **7**(3): 221-228

Hungr O, McDougall S, Wise M, and Cullen M (2007) Magnitude-frequency relationships of debris flows and debris avalanches in relation to slope relief. *Geomorphology.* DOI: 10.1016/j.geomorph.2007.03.020.

Hunziker RP and Jäggi M (1992) Grain sorting processes. *Journal of Hydraulic Engineering* **128**: 1060-1068.

Intergovernmental Panel on Climate Change (IPCC) (2013) The physical science basis. UNEP.

Iverson RM, Schilling SP, and Vallance JW (1998) Objective delineation of lahar-inundation hazard zones. *GSA Bulletin* **110**(8): 972-984.

Jackson LE Jr. (1980) Glacial history and stratigraphy of the Alberta Portion of the Kananaskis Lakes map area. *Canadian Journal of Earth Sciences* **17**: 459-477

Jackson LE Jr. (1987) Debris flow hazard in the Canadian Rocky Mountains. *Geological Survey of Canada* 86 (11).

Jäggi M (2007) The floods of August 22-23, 2005 in Switzerland: Some facts and challenges. *In* H Habersack, H Piegay, M Rinaldi. (Eds.) Gravel bed rivers 6, from process understanding to river restoration. Elsevier, Amsterdam, p. 587-604.

Jakob M and Bovis MJ (1996) Morphometric and geotechnical controls of debris-flow activity, southern Coast Mountains, British Columbia. *Zeitschrift für Geomorphologie, Supplementband* **104**: 13-26.

Jakob M and Jordan P (2001) Design flood estimates in mountain streams – the need for a geomorphic approach. *Canadian Journal of Civil Engineering* **28**: 425-439.

Jakob M, Stein D, and Ulmi M (2011) Vulnerability of buildings to debris-flow impact. *Natural Hazards*. DOI: 10.1007/s11069-011-0007-2.

Jakob M and Weatherly H (2008) Integrating uncertainty: Canyon Creek hyperconcentrated flows of November 1989 and 1990. *Landslides* **5**(1): 83-95.

Jordan P (1994) Debris flows in the southern Coast Mountains, British Columbia: Dynamic behaviour and physical properties. Unpublished Ph.D. thesis. The University of British Columbia, Vancouver, B.C., p. 258.

Kostaschuk RA (1980) The late Quaternary history of the Bow River near Banff, Alberta. M.Sc. thesis, University of Calgary, Calgary, A.B, p. 90.

Kostaschuk RA and Smith DG (1983) Late Quaternary lacustrine and deltaic sedimentation near Banff, Alberta. *Canadian Journal of Earth Sciences* **20**(12): 1834-1842.

Luckman BH (2000) The little ice age in the Canadian Rockies. *Geomorphology* **32**: 357-384.

McClung D (1999) The encounter probability for mountain slope hazards*. Canadian Geotechnical Journal* **36**(6): 1195-1196.

Menounos B, Osborn G, Clague JJ, and Luckman BH (2009) Latest Pleistocene and Holocene glacier fluctuations in western Canada. *Quaternary Science Reviews* **28**(21): 2049-2074.

Milly PCD, Betancourt J, Falkenmark M, Hirsch RM, Kundzewicz ZW, Lettenmaier DP, and Stouffer RJ (2008) Stationary is dead: Whither water management? *Science* **319**(1): 573-574.

Ministry of Transportation and Infrastructure (MoTI) (2009) Non-referenced bulletin to approving officers: Subdivision preliminary layout review – Natural Hazard Risk.

O'Brien JS and Julien PY (1988) Laboratory analysis of mudflow properties. *Journal of Hydraulic Engineering* **114**: 877-887.

O'Connor JE and Beebee RA (2009) Chapter 8: Floods from natural rock-materials dams. *In* DM Burr, PA Carling and VR Baker (Eds.) Megaflooding on Earth and Mars. Cambridge University Press, p. 128-171.

Osborn G and Gerloff L (1997) Latest Pleistocene and early Holocene fluctuations of glaciers in the Canadian and northern American Rockies. *Quaternary International* **38–39**(0): 7-19.

Osborn G, Robinson BJ, and Luckman BH (2001) Holocene and latest Pleistocene fluctuations of Stutfield Glacier, Canadian Rockies. *Canadian Journal of Earth Sciences* **38**: 1141-1155.

Osborn G, Stockmal G, and Haspel R (2006) Emergence of the Canadian Rockies and adjacent plains: A comparison of physiography between end-of-laramide time and the present day. *Geomorphology* **75**(3–4): 450-477.

Peng M and Zhang LM (2012) Breaching parameters of landslide dams. *Landslide* **9**(1): 13-31.

Pierson TC (2005) Hyperconcentrated flow- transitional process between water flow and debris flow. *In* M Jakob and O Hungr. (Eds.) Debris-flow hazards and related phenomena, Springer-Praxis Publishing, Chichester, U.K., p 159-202.

Price RA (1970) Map 1266A, Geology: Canmore (west half), west of fifth meridian, Alberta. Scale 1:50,000. Geological Survey of Canada.

Reasoner MA, Osborn GD, and Rutter NW (1994) Age of the Crowfoot advance in the Canadian Rocky Mountains: A glacial event coeval with the Younger Dryas oscillation. *Geology* **22**: 439-442.

Recking A, Freey P, Paquier A, Belleudy P and Champagne JY (2008) Feedback between bed load transport and flow resistance in gravel and cobble bed rivers. *Water Resources Research* **44**: WO5412. DOI: 10.1029/2007WR006219.

Rickenmann D (2001) Comparison of bed load transport in torrents and gavel bed streams. *Water Resources Research* **31**: 773-781.

Rickenmann D (2005) Geschiebetransport be steilen Gefällen. *In* Mitteilungen der Versuchsanstalt für Wasserbau, Hydrologie und glaziologie, ETH Zürich, No. 190, p. 107-119.

Rickenmann D and Koschni A (2010) Sediment load due to fluvial transport and debris flows during the 2005 flood events in Switzerland. *Hydrological Processes* **24**: 993-1007.

Rickenmann D and McArdell BW (2007) Continuous measurement of sediment transport in the Erelenbach stream using piezoelectric bedload impact sensors. *Earth Surface Processes and Landforms* **32**: 1362-1378.

Rudolf-Miklau F, Baek R, Skolaut C, and Schmid F (2011) Alpine Mass Movements: Implications for hazard assessment and mapping, Special Edition of Journal of Torrent, Avalanche, Landslide and Rock Fall Engineering No. 166. http://www.alpine-space.eu/fileadmin/media/Running_Projects/AdaptAlp/AdaptAlp_-_Results/Handbook_Hazard_mapping_for_mass_movements.pdf

Roed MA and Waslyk DG (1973) Age of inactive alluvial fans: Bow River Valley, Alberta. *Canadian Journal of Earth Sciences* **10**: 1834-1840.

Rutter NW (1965) Surficial geology of the Banff area, Alberta: Unpublished Ph.D. thesis, The University of Alberta, Edmonton, A.B.

Rutter NW (1966a) Glacial history of the Bow Valley, Alberta. *Canadian Alpine Journal* **49**: 157-153.

Rutter NW (1966b) Multiple glaciations in the Banff area, Alberta. *Bulletin of Canadian Petroleum Geology* **14**: 620-626.

Rutter NW (1972) Geomorphology and multiple glaciations in the area of Banff, Alberta. *Geological Survey of Canada, Bulletin* **206** (55).

Scott DL (1964a) Stratigraphy of the lower Rocky Mountain supergroup in the southern Canadian Rocky Mountains. Ph.D. thesis, The University of British Columbia, Vancouver, B.C., p. 133.

Scott DL (1964b) Pennsylvanian stratigraphy. *Bulletin of Canadian Petroleum Geology* **12**(Flathead Valley Guidebook Issue): 460-493.

Scott KM, Pringle, PT and Wallance, JW (1992) Sedimentology, behaviour, and hazards of debris flows at Mount Rainier, Washington. United States Geological Survey, Open-file Report 90-285, p. 106.

SREX (2011) Intergovernmental panel on climate change 2011. Managing the risks of extreme events and disasters to advance climate change adaptation (SREX). UNEP, p. 594.

Verschuren JP and Wojtiw L (1980) Estimate of the maximum probable precipitation for Alberta. The University of Alberta, p. 321.

Walder JS and O'Connor JE (1997) Methods for predicting peak discharge of floods caused by failure of natural and constructed earthen dams. *Water Resources Research* **33**(10): 2337-2348.

Whitfield PH. In press. Fitness for purpose assessment of climate station data: 3053600 Kananaskis, Alberta. Atmosphere-Ocean.

APPENDIX A
ENGINEERING REPORTS REVIEW

Table A-1. Past debris flood and/or flood events on Cougar Creek reported in the reviewed engineering reports.

Year	Reported Event Date	Source	Comments
1948		CH2M HILL, 1993[1]	"Historical evidence indicated characteristic flash floods occur approximately every 8 to 10 years".
1956		CH2M HILL, 1993	"Historical evidence indicated characteristic flash floods occur approximately every 8 to 10 years".
1967		CH2M HILL, 1993	"Large flood washed out bridge abutments; reports of 70,000 to 80,000 yd^3 (53,500 m^3 to 61,200 m^3) of sediment pushed through 40-ft (12.2-m) span". "Channelization of the creek completed following flood". "Historical evidence indicated characteristic flash floods occur approximately every 8 to 10 years".
1974		CH2M HILL, 1993	"Historical evidence indicated characteristic flash floods occur approximately every 8 to 10 years".
1980		CH2M HILL, 1993	"Some gravel reported in culverts".
1990	May 25	CH2M HILL, 1993	"Cougar Creek dam failed".
	May 25	Alberta Environment, 1991[2,3]	Cougar Creek flows were high prior to the dam failure. The peak flow in the hour before the failure was estimated at 13 m^3/s. This peak flow was the result of rainfall and coincident snowmelt. Rainfall totals of 22 mm and 30 mm were recorded on May 24 and 25, 1990 at Banff. In addition, snowpillow data indicate that rapid snowmelt was occurring at higher elevations (> 2000 m). The dam contained approximately 35,000 m^3 of water at the time of failure. Based on gravel terraces observed during the site visit, the estimated sediment volume was 15% (or 5,250 m^3) of the water storage capacity of 35,000 m^3. Failure attributed to instability of the downstream slope induced by erosion of the core material (i.e. a piping failure). The dam failure caused major erosion downstream and the culverts under Highway 1, Highway 1A and the CP Rail tracks were either partly or completely filled with sediment, resulting in a partial washout of the CP Rail tracks.
	May 25	AMEC, 2003[4]	Reported "6,000 m^3 (of sediment) hauled upstream of CPR; 10,000 m^3 dozed up on banks upstream of Highway 1A".
1995	Late May, Late June	CH2M HILL, 1995[5]	"Significant volumes of material were transported in each of two rainfall/runoff events, the first of which took place in May, and the second in July 1995". Reported "major flows in the creek in late May following unusually heavy rains. As well as direct rainfall runoff, the storms caused more rapid snowmelt in the upper bowl where Cougar Creek originates. The result was a more concentrated runoff combination which produced higher than usual flows in the creek. Subsequent heavy rains in late July also resulted in flows and sediment transport in the creek".
	June, July	AMEC, 2003	Reported sedimentation as "5000 at CPR; 5000 to 6000 m^3 pushed up on slopes upstream of Highway 1A; 3000 m^3 pushed up on slopes upstream of Highway 1".
2003	May	AMEC, 2006[6]	"During the spring runoff period of May 2003, erosion damage occurred to the east and west banks of Cougar Creek in the reach between Highway 1 and Highway 1A. Subsequent to the damage, the Town of Canmore completed emergency repairs to the eroded channel banks, which consisted of reshaping and compaction of the banks".
2005	June	AMEC, 2007[7]	"During the June 2005 flood, large volumes of sediment were transported from the upstream channel reaches downstream to the CPR Mainline and Highway 1A crossings. Bank erosion occurred between Highway 1 and Elk Run Boulevard, and some of the erosion protection works completed just prior to the flood event at the Highway 1A crossing were washed out".
2012	June 5-6	AMEC, 2012[8]	"Based on the cross sections collected after the 2012 flood event, there has been a net increase in channel area of more than 25,000 m^3 since the sections were last surveyed in 2006. Approximately 9000 m^3 of sediment was removed from the area between the Highway 1A and CP Rail crossings during and following the June 2012 event".

1 CH2M HILL Engineering Ltd. (1993) Cougar Creek Flood Protection Study. Final report prepared for the Town of Canmore. March 1993.
2 Alberta Environment, Dam Safety Branch (1991) Report on the Cougar Creek Dam failure. February 1991.
3 Comments on 1990 dam failure taken from BGC (2013a).
4 AMEC Earth & Environmental Ltd. (2003) Cougar Creek Flood Control and Maintenance Study. Report prepared for the Town of Canmore. January 2003.
5 CH2M HILL Engineering Ltd. (1995) Annual Monitoring Report No. 1. Report prepared for the Town of Canmore. October 1995.
6 AMEC Earth & Environmental Ltd. (2006) Cougar Creek Erosion Protection Highway 1 to Highway 1A. Report prepared for the Town of Canmore. July 2006.
7 AMEC Earth & Environmental Ltd. (2007) Sediment Transport and Flood Hydrology in Cougar Creek. Report prepared for the Town of Canmore. May 2007.
8 AMEC Earth & Environmental Ltd. (2012) Cougar Creek 2012 Flood Damage Repairs. Report prepared for the Town of Canmore. August 2012.

APPENDIX B
NEWSPAPER REVIEW

Table B-1. Reported debris floods, flooding and extreme precipitation in the reviewed newspapers.

Article Date	Newspaper	Comments[1]
June 11, 1948	The Banff Crag and Canyon	High water levels on the Bow River due to "the late spring runoff from the mountains coming all at once". June 1918, June 1923 (record high), May 1933 were other years with recorded high water levels "Government records show that on June 15, 1918 the gauge read 11.43 feet; June 10, 1923, 11.93; May 31, 1933, 10.74 and June 9, 1948, 11.17 feet. On the same dates above the volume of water flowing down the Bow river was recorded at the bridge meter as follows: 1918, 12,155 cubic feet per second; 1923, 14,100; 1933, 9,490 and 1948, 10,780. The 1948 water levels were still below the 1918 and 1923 levels. Highways were closed due to washouts.
May 31, 1967	The Calgary Herald	Trans-Canada Highway closed due to bridge collapse at Cougar Creek. "Rampaging waters from Cougar Canyon… carried an estimated 70,000 to 80,000 cubic feet of gravel under the unnamed bridge… before washing it out". [Note: this sediment volume was reported as cubic yards in the CH2M HILL 1993 report].
June 26, 1974	The Banff Crag and Canyon	"The Bow River (at Canmore) is high, muddy and swift running". "Residents have commented that they have never before seen the river so high". "The snows high up in the mountains have not been melting that quickly and many lakes are still not open". Erosion along the banks of the Bow River.
July 3, 1974	The Banff Crag and Canyon	Bow River at Canmore was six feet above its normal level. "The reasons for the high water this year are numerous. Heavy winter snowfall, coupled with a cool spring allowing little early runoff, and then subsequent warm weather".
June 4, 1980	The Banff Crag and Canyon	"The Ashk Corporation has been forced to shut down work on water and sewer lines because of high water".
May 30, 1990	The Banff Crag and Canyon	"Crews worked over the weekend to repair the rail line, the footings for which were washed away when the Cougar Creek dam broke".
May 31, 1990	The Canmore Leader	"At press time the river flow was topping 210 cubic meters per second (cms) of flow. Infiltration flooding is expected to begin within 24 hours of a flow rate of 214 cms". "Our problem is that it's been raining from the top of the mountains down, we've got 9,000 feet". Dam collapse at Cougar Creek on May 25 "sending a… wall of water down the already swollen watercourse." "Water also washed out the approach to a bridge on the Ghost River on the Richards Road about 15 km north of the 1A highway". "There was also minor flooding on the east side of Exshaw when the Dura Creek overflowed its banks and a number of culverts washed out".
June 7, 1990	The Canmore Leader	Weather system shifted giving "a reprieve (to the flooding) just at the last minute"."The danger now lies in a sudden melt of snow in the back country. If it perks up and gets up to 22 to 24 degrees it could start moving very quickly".
June 6, 1995	The Canmore Leader	"A CP Rail crew was hard at work (June 1) clearing out debris that had been washed into the culvert guiding Cougar Creek under the railway tracks". "A late spring combined with several days of warm weather have torrents of water threatening to spill over the top of the creek."
June 13, 1995	The Canmore Leader	On June 6th the Bremner Engineering crew "removed 300 truckloads of gravel, with each truck holding approximately seven or eight cubic metres of debris, said company president Richard Bremner." "By the time it started raining Tuesday, 12 men were working near the east exit from Canmore off the 1A highway with five excavators, two bulldozers, two rubber tired loaders and eight gravel trucks".
July 7, 1999	The Banff Crag and Canyon	Heavy rain and snowfall in the Bow Valley region. No mention of flooding on Cougar Creek.
June 22, 2005	The Canmore Leader	Long list of closures in Bow Valley region due to "mud and rockslides". "High water dislodged portions of bank and trees were seen falling into (Cougar Creek) between the Trans-Canada Highway and Bow Valley Trail on Friday evening". "Four backhoes were dedicated to keeping culverts clar throughout the night, successfully preventing a washout over the tracks, as two additional backhoes worked further upstream".
June 6, 2007	The Canmore Leader	High river flow advisory warning.
June 13, 2007	The Canmore Leader	Reports of flooding of Bow River due to heavy rains and rapid snow melt. No mention of flooding on Cougar Creek.
May 27, 2008	The Banff Crag and Canyon	Reports of rain, snow and cold temperatures (-20ºC night time low).

[1] In some cases comments are taken directly from the sourced newspaper.

APPENDIX C
TEST TRENCH LOGS

Test Pit #	Date Completed	Method	UTM Coordinates, NAD83		Elevation[1] (masl)[2]	Max Depth[3] (mbgs)[4]
			Northing	Easting		
BGC-TP-2	06-Aug-13	Excavator	5660985	617425	1391	4
BGC-TP-6	06-Aug-13	Excavator	5660752	617244	1364	3.9
BGC-TP-15	06-Aug-13	Excavator	5659561	617540	1300	4.15
BGC-TP-18	06-Aug-13	Excavator	5659499	617005	1305	5.1
BGC-TP-19	06-Aug-13	Excavator	5659594	616877	1312	4.3
BGC-TP-45	07-Aug-13	Excavator	5660503	617074	1351	4.5
EastBank	07-Aug-13	Excavator	5660522	617110	1352	2.3
BGC-TP-38	07-Aug-13	Excavator	5661150	616322	1325	4
BGC-TP-41	07-Aug-13	Excavator	5660591	616744	1344	4.5
BGC-TP-46	07-Aug-13	Excavator	5660429	616938	1346	4.3
BGC-TP-47	07-Aug-13	Excavator	5660177	616799	1333	4.35
BGC-TP-48	07-Aug-13	Excavator	5660229	616728	1333	4.6
BGC-TP-9	07-Aug-13	Excavator	5660173	617597	1330	4
BGC-TP-20	07-Aug-13	Excavator	5659595	616724	1306	4.35
BGC-TP-30	07-Aug-13	Excavator	5659985	616372	1313	4.65
BGC-TP-13	08-Aug-13	Excavator	5659555	617837	1301	3.5
BGC-TP-21	08-Aug-13	Excavator	5659923	616586	1318	4.7

Sample Legend[5]	
◆ (red)	Sediment
◆ (green)	Organic
◆ (yellow)	Other

Notes:

1. Elevations were taken from Google Earth and are approximate
2. masl – meters above sea level
3. Hole depths were not recorded for BGC-TP-2, BGC-TP-41, BGC-TP-48 or EastBank
4. mbgs – meters below ground surface
5. Sample locations indicated on test trench photos are approximate and may not represent the actual location samples. Not all samples are shown in the photos.

TEST PIT # BGC-TP-2

Date:	06 August, 2013
Location:	5660985 N 617425 E
Datum:	UTM NAD 83
Elevation:	1391 masl (taken from Google Earth, approximate)
Equipment:	Excavator
Logged by:	Matthias Jakob, Stephanie Bale, Brent MacDonald
Total Depth:	4.0 m (not recorded, approximate)

Depth From (mbgs)	Depth To (mbgs)	Lithologic Description
0.0	0.6	UNIT 1: DEBRIS FLOOD Matrix supported to clast supported, subangular to subrounded sand gravels, June 2013 event, organic ridge, moist, Dmax=50cm, slightly imbricated, silt veneer around clasts
0.6	2.1	UNIT 2: DEBRIS FLOOD Unsorted, primarily clast supported, sandy gravels with boulders, non-imbricated, no gradation, Dmax=60cm, gravel sample taken at bottom of Unit 2
2.1	2.7	UNIT 3: FLOOD Clast to matrix supported, sandy gravel, Dmax=20cm, no imbrication, no gradation, subangular, moist
2.7	2.8	UNIT 4: DEBRIS FLOOD Clast supported, sharp contact with top and bottom, silt veneer on clasts, could be first surge of Unit 5
2.8	3.8	UNIT 5: DEBRIS FLOOD Clast to matric supported, sandy gravel, Dmax=40cm, no imbrication, no gradation, subangular, moist, dense, clasts need to be chiseled off by shovel impact
3.8	4.0	UNIT 6: FLOOD 10 cm thick laminated coarse sand, leading abruptly into clast supported loose gravel with imbrication

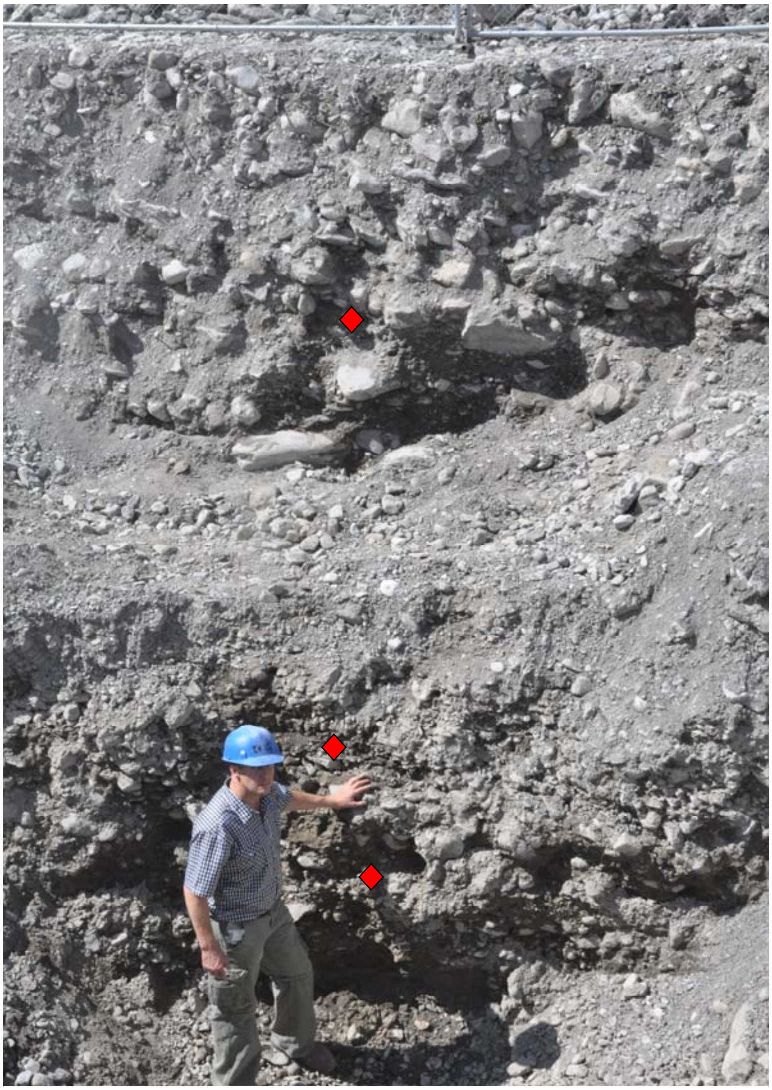

Sample	Depth (mbgs)
◆ BGC-TP-2 Unit 2	2.0
◆ BGC-TP-2 Unit 3	2.4
◆ BGC-TP-2 Unit 5	3.3

TEST PIT # BGC-TP-6

Date:	06 August, 2013
Location:	5660752 N 617244 E
Datum:	UTM NAD 83
Elevation:	1364 masl (taken from Google Earth, approximate)
Equipment:	Excavator
Logged by:	Matthias Jakob, Stephanie Bale, Brent MacDonald
Total Depth:	3.9 m

Depth From (mbgs)	Depth To (mbgs)	Lithologic Description
0.0	1.0	UNIT 1: PLACED FILL Fill material, matrix supported/clast supported, subangular to angular clasts, poorly sorted, Dmax=70cm
1.0	1.2	UNIT 2: DEBRIS FLOOD Clast supported in upper 10 cm and matrix supported in bottom, signs of inverse grading, laminated sand bed, organic (root) material, no inbrication, Dmax=15cm
1.2	1.9	UNIT 3: DEBRIS FLOOD Reverse gradation clast to matrix supported, coarse sand to cobble, alternating stratification (cyclical pattern of coarsening, coarse sands to pebble size), Dmax=14cm, subangular to subrounded clasts
1.9	2.8	UNIT 4: DEBRIS FLOOD Upward coarsening from clast supported (2.6-2.8 m) grading into massive matrix supported sandy gravels, subrounded throughout, slight imbrication of clast supported subunits, no organics, Dmax=20cm
2.8	3.2	UNIT 5: DEBRIS FLOOD Same as Unit 4, Dmax=30cm
3.2	3.9	UNIT 6: DEBRIS FLOOD Same as Unit 4, Dmax=20cm, not getting to clast supported subunit

Sample	Depth (mbgs)
◆ BGC-TP-6 Unit 3	1.55

TEST PIT # BGC-TP-15

Date: 06 August, 2013
Location: 5659561 N 617540 E
Datum: UTM NAD 83
Elevation: 1300 masl (taken from Google Earth, approximate)
Equipment: Excavator
Logged by: Matthias Jakob, Stephanie Bale, Brent MacDonald
Total Depth: 3.15 m

Depth From (mbgs)	Depth To (mbgs)	Lithologic Description	Date
0	1	UNIT 1: FILL Matrix supported sandy gravel with cobbles, subrounded with some well rounded, Dmax=15cm, likely fill material	106.6 ± 0.3 pMC
1	1.1	UNIT 2: PALEOSOL Organic rich paleosol in fine sandy matrix, sharp transition in paleosol and overlying unit	760 ± 30 BP
1.1	1.6	UNIT 3: SAND Fine to medium sand, light ochre coloured	
1.6	1.65	UNIT 4: PALEOSOL Gradational transition to overlying unit	2840 ± 30 BP
1.65	1.9	UNIT 5: SAND Fine to medium sand with some pea gravel lenses	-
1.9	2.7	UNIT 6: DEBRIS FLOOD Mostly clast supported loose sandy gravels and cobbles, Dmax=15cm	-
2.7	3	UNIT 7: SAND Fine to medium silty sand, dense	-
3	3.05	UNIT 8: PALEOSOL Discontinuous, wavy, weakly developed	3010 ± 30 BP
3.05	3.25	UNIT 9: SAND Fine to medium silty sand, moist	-
3.25	4.15	UNIT 10 Massive, unsorted, sandy gravel, Dmax=25cm, clast supported, no imbrication	-

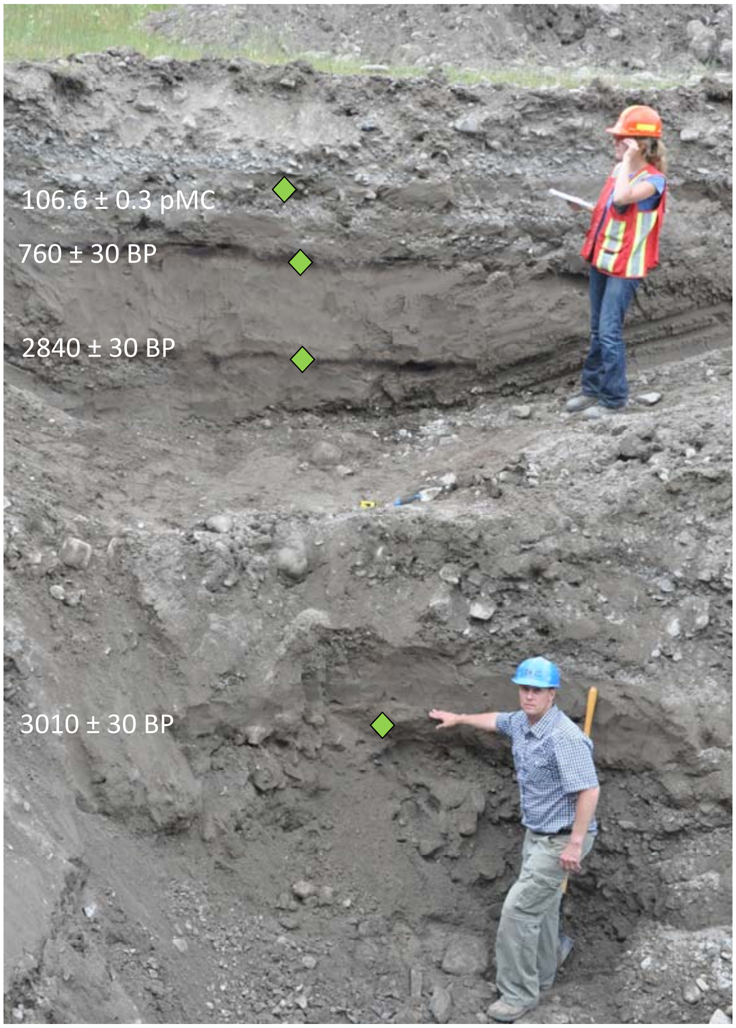

Sample	Depth (mbgs)	Date
◆ BGC-TP-15 Unit 1	1.0	106.6 ± 0.3 pMC
◆ BGC-TP-15 Unit 2	1.1	760 ± 30 BP
◆ BGC-TP-15 Unit 4	1.6	2840 ± 30 BP
◆ BGC-TP-15 Unit 8	3.0	3010 ± 30 BP

TEST PIT # BGC-TP-18

Date: 06 August, 2013
Location: 5659499 N 617005 E
Datum: UTM NAD 83
Elevation: 1305 masl (taken from Google Earth, approximate)
Equipment: Excavator
Logged by: Matthias Jakob, Stephanie Bale, Brent MacDonald
Total Depth: 5.1 m

Depth From (mbgs)	Depth To (mbgs)	Lithologic Description	Date
0	0.35	UNIT 1: DEBRIS FLOOD Varying thickness 25-40 cm, June 2013 event	-
0.35	2.5	UNIT 2 Unsorted subangular to angular clast, Dmax=20cm, imbrication, gog quartzite (main ranges, carried down from Lake Louise, angular), clast and matrix supported (predominantly clast), fine to medium grained sand matrix, two lenses Upper lens: predominantly clast supported pea pebble size, subangular to subrounded, weak stratification Lower lens: pea size to Dmax=10cm, weak stratification	-
2.5	3.55	UNIT 3: SAND Massive weakly stratified fine to medium sand, moist, 1-3 cm discontinuous pea gravel lenses	-
3.55	3.57	UNIT 4: TEPHRA Ash under laid with thin paleosol layer	2390 ± 30 BP
3.57	4	UNIT 5: SAND Massive unstratified fine medium sand, moist	-
4	4.1	UNIT 6: PALEOSOL Better oxidation	2440 ± 30 BP
4.1	4.8	UNIT 7: SAND Medium size sand with interbedded gravel lenses of up to 20 cm thickness	-
4.8	4.9	UNIT 8: PALEOSOL Well developed paleosol	2870 ± 30 BP
4.9	5.1	UNIT 9: SAND Massive unstratified sands	-

Sample	Depth (mbgs)	Date
◆ BGC-TP-18 Surface	0.0	-
◆ BGC-TP-18 Unit 4	3.6	2390 ± 30 BP
◆ BGC-TP-18 Unit 6	4.1	2440 ± 30 BP
◆ BGC-TP-18 Unit 8	4.85	2870 ± 30 BP

TEST PIT # BGC-TP-19

Date:	06 August, 2013
Location:	5659594 N 616877 E
Datum:	UTM NAD 83
Elevation:	1312 masl (taken from Google Earth, approximate)
Equipment:	Excavator
Logged by:	Matthias Jakob, Stephanie Bale, Brent MacDonald
Total Depth:	4.3 m

Depth From (mbgs)	Depth To (mbgs)	Lithologic Description	Date
0	0.45	UNIT 1: FILL Possibly fill	-
0.45	0.9	UNIT 2: SAND Massive weakly stratified sands with numerous modern rootlets from poplar trees	-
0.9	1.6	UNIT 3: DEBRIS FLOOD Clast to matrix supported (mostly clast), subrounded to subangular sandy gravel, loose with modern rootlets, moist, Dmax=20cm	100.5 ± 0.3 pMC
1.6	2.9	UNIT 4: DEBRIS FLOOD[1] Massive gravel with sand layer, thin paleosol layer at 1.9 m	800 ± 30 BP
2.9	3.1	UNIT 5: SAND Massive unstatified sand with modern rootlets, weak bedding	-
3.1	3.3	UNIT 6: FLUVIAL[2] Clast supported and loose gravel, Dmax=10cm, fluvial gravel, silty sand at bottom, peat inclusion	1140 ± 30 BP
3.3	4.3	UNIT 7: DEBRIS FLOOD Silty sandy gravel, unsorted, unstratified subangular, Dmax=30cm, dense	-

[1] Classified as distal sand overbank deposit in grain size analysis
[2] Classified as debris flood deposit in grain size analysis

Sample	Depth (mbgs)	Date
◆ BGC-TP-19 Unit 3	1.5	100.5 ± 0.3 pMC
◆ BGC-TP-19 Unit 4	1.9	800 ± 30 BP
◆ BGC-TP-19 Unit 4	1.9	-
◆ BGC-TP-19 Unit 5	3.0	-
◆ BGC-TP-19 Unit 6	3.2	-
◆ BGC-TP-19 Unit 6	3.2	1140 ± 30 BP

TEST PIT # BGC-TP-45

Date: 07 August, 2013
Location: 5660503 N 617074 E
Datum: UTM NAD 83
Elevation: 1351 masl (taken from Google Earth, approximate)
Equipment: Excavator
Logged by: Matthias Jakob, Stephanie Bale, Brent MacDonald
Total Depth: 4.5 m

Depth From (mbgs)	Depth To (mbgs)	Lithologic Description
0	0.8	UNIT 1: FILL
0.8	2.2	UNIT 2: DEBRIS FLOOD Flood deposit to debris flood, clast supported (predominantly), Dmax=50cm, asphalt slab (slightly imbricated), sunangular to subrounded, predominantly unsorted, slight imbrication, some infill with medium coarse sand matrix, some woody/rooty material, moist down low
2.2	3	UNIT 3: FLOOD DEPOSIT Clast suppported, sandy gravels, subrounded subangular, Dmax=20cm, slight imbrication, loose, interbedded sand lenses
3	3.7	UNIT 4: DEBRIS FLOOD Subrounded to subangular, upward coarsening, dense matrix supported debris flood, Dmax=40cm, unsorted, silt veneers on individual clasts, interbedded gravel lenses with downstream inclination at fan gradient
3.7	4.5	UNIT 5: DEBRIS FLOOD High apparent cohesion, massive unstratified matrix supported debris flood deposit, Dmax=40cm, subangular to angular

Sample	Depth (mbgs)
◆ BGC-TP-45 Unit 2	1.5
◆ BGC-TP-45 Unit 5	3.1

East Bank - Erosion Exposed

Date: 07 August, 2013
Location: 5660522 N 617110 E
Datum: UTM NAD 83
Elevation: 1352 masl (taken from Google Earth, approximate)
Equipment: Excavator
Logged by: Matthias Jakob, Stephanie Bale, Brent MacDonald
Total Depth: 2.3 m (not recorded, approximate)

Depth From (mbgs)	Depth To (mbgs)	Lithologic Description
0	0.3	UNIT 1: TOPSOIL
0.3	0.45	UNIT 2 Matrix supported fine grain [FILL]
0.45	1.25	UNIT 3 Massive matrix supported [FILL]
1.25	1.7	UNIT 4 Organic rich matrix supported, subangular to subrounded
1.7	2	UNIT 5 Matrix supported, subrounded, organic rich
2	2.3	UNIT 6: DEBRIS FLOOD Dmax=60cm (Note: not sure if this is naturally deposited or fill material

TEST PIT # BGC-TP-41

Date: 07 August, 2013
Location: 5660591 N 616744 E
Datum: UTM NAD 83
Elevation: 1344 masl (taken from Google Earth, approximate)
Equipment: Excavator
Logged by: Matthias Jakob, Stephanie Bale, Brent MacDonald
Total Depth: 4.5 m (not recorded, approximate)

Depth From (mbgs)	Depth To (mbgs)	Lithologic Description	Date
0	0.18	UNIT 1: TOPSOIL	-
0.18	0.6	UNIT 2: SAND Silty sand	-
0.6	0.9	UNIT 3 Upward fining, clast supported gravel, Dmax=10cm to pea size gravel	-
0.9	2.7	UNIT 4: DEBRIS FLOOD Matrix supported to clast supported, sandy gravel, unsorted, Dmax=20cm, gravel lenses of variable size, debris flood with flood stages	-
2.7	2.9	UNIT 5: PALEOSOL Ochre to reddish colour from 2.75-2.80 m, diffused boundary to top and bottom in fine sands, 2.90-2.95: sharp contact to black organic layer [Seen in west trench face only]	970 ± 30 BP
2.9	3.55	UNIT 6: DEBRIS FLOOD Same as Unit 4, Dmax=20cm, with flood stages	-
3.55	3.79	UNIT 7: PALEOSOL Fine sands, black to dark brown organic horizon at 3.70-3.72 m [Seen in both east and west trench faces]	1200 ± 30 BP
3.79	4.22	UNIT 8: DEBRIS FLOOD Same as Unit 4	-
4.22	4.42	UNIT 9: PALEOSOL Organic layer at 4.30 m, discontinuous dark brown to black in fine silty sands [Seen in west trench face only]	1450 ± 30 BP
4.42	4.5	UNIT 10: DEBRIS FLOOD Same as Unit 4	-

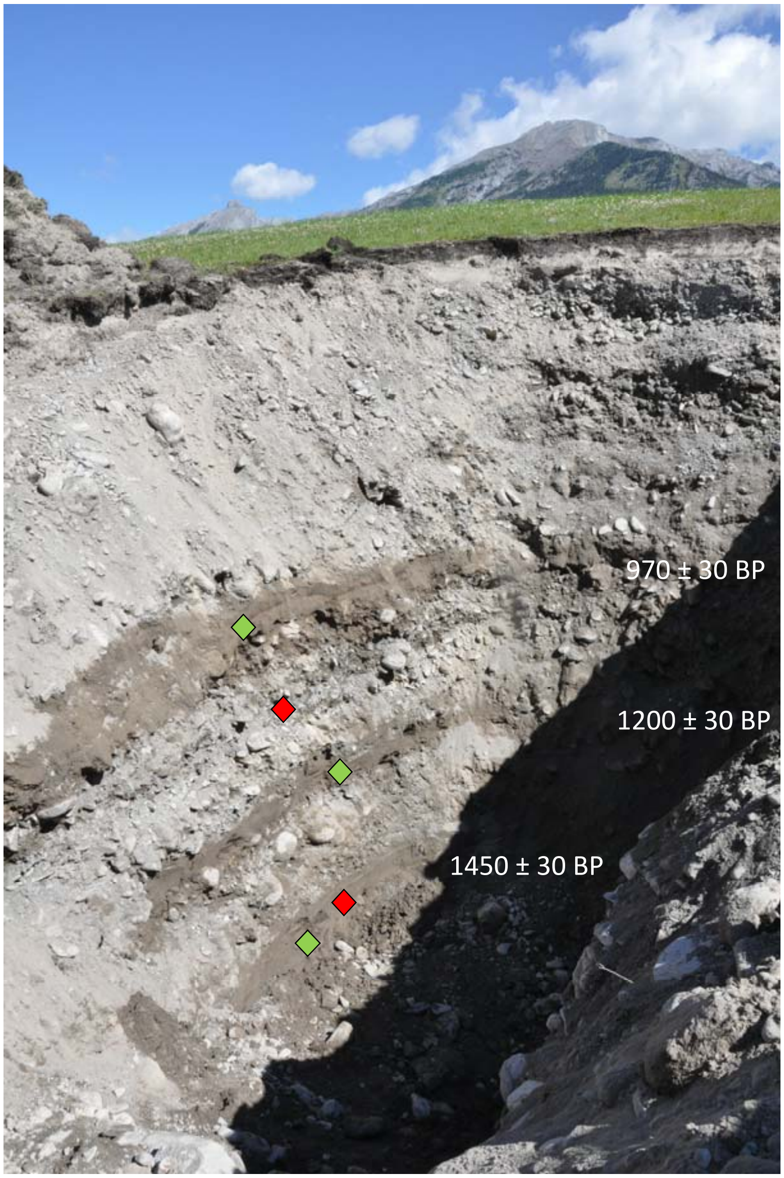

Sample	Depth (mbgs)	Date
◆ BGC-TP-41 Unit 5	2.8	970 ± 30 BP
◆ BGC-TP-41 Unit 6	3.20	-
◆ BGC-TP-41 Unit 7	3.65	1200 ± 30 BP
◆ BGC-TP-41 Unit 9	4.3	-
◆ BGC-TP-41 Unit 9	4.3	1450 ± 30 BP

TEST PIT # BGC-TP-46

Date: 07 August, 2013
Location: 5660429 N 616938 E
Datum: UTM NAD 83
Elevation: 1346 masl (taken from Google Earth, approximate)
Equipment: Excavator
Logged by: Matthias Jakob, Stephanie Bale, Brent MacDonald
Total Depth: 4.3 m

Depth From (mbgs)	Depth To (mbgs)	Lithologic Description
0	1.3	UNIT 1: DEBRIS FLOOD June 2013 event, matrix supported debris flood, poorly graded, concrete slabs from pathway, Dmax=50cm
1.3	2.8	UNIT 2: DEBRIS FLOOD Matrix supported, sandy gravels, subangular to subrounded
2.8	2.9	UNIT 3: FLOOD Clast supported gravel, sunrounded to subangular, Dmax=10cm
2.9	4.3	UNIT 4: DEBRIS FLOOD Same as Unit 2, Dmax=50cm

	Sample	Depth (mbgs)
◆	BGC-TP-46 Unit 1	0.65
◆	BGC-TP-46 Unit 4	3.6

TEST PIT # BGC-TP-47

Date: 07 August, 2013
Location: 5660177 N 616799 E
Datum: UTM NAD 83
Elevation: 1333 masl (taken from Google Earth, approximate)
Equipment: Excavator
Logged by: Matthias Jakob, Stephanie Bale, Brent MacDonald
Total Depth: 4.35 m

Depth From (mbgs)	Depth To (mbgs)	Lithologic Description
0	1.6	UNIT 1: DEBRIS FLOOD Dmax=40cm, June 2013 event, matrix supported, fine to medium sand matrix, no imbrication
1.6	2.3	UNIT 2: FLOOD Clast supported, flood event, pea to gravel size clast, Dmax=10cm
2.3	3.9	UNIT 3: DEBRIS FLOOD Matrix supported, fine to medium sands, massive with slight imbrication at bottom of deposit (flow in south west direction)), Dmax=50cm
3.9	4.35	UNIT 4: FLOOD Developing paleosol at top of unit, evidence of clast supported fluvial deposits beneath, Dmax=15cm, poorly developed pea to gravel sized lenses, some slight imbrication

Sample	Depth (mbgs)
◆ BGC-TP-47 Unit 1	0.8
◆ BGC-TP-47 Unit 3	3.1
◆ BGC-TP-47 Unit 4	3.95

TEST PIT # BGC-TP-48

Date:	07 August, 2013
Location:	5660229 N 616728 E
Datum:	UTM NAD 83
Elevation:	1333 masl (taken from Google Earth, approximate)
Equipment:	Excavator
Logged by:	Matthias Jakob, Stephanie Bale, Brent MacDonald
Total Depth:	4.6 m (not recorded, approximate)

Depth From (mbgs)	Depth To (mbgs)	Lithologic Description	Date
0	1.1	UNIT 1: DEBRIS FLOOD June 2013 debris flood deposit, massive matrix supported, Dmax=40cm, subangular to subrounded, medium to coarse sand matrix (may be reintroduced material when backfilled)	-
1.1	2	UNIT 2: DEBRIS FLOOD Modern rootlets present, top of unit is pre 2013 flood surface, predominantly massive, some indication of slight imbrication, fine to medium sand matrix, Dmax=30cm	-
2	2.3	UNIT 3: PALEOSOL Silty sandy, inconsistent organic deposits, weakly developed horizons	1130 ± 30 BP
2.3	4.3	UNIT 4: DEBRIS FLOOD Matrix supported, subangular to subrounded, Dmax=40cm, gravel lenses, no imbrication	-
4.3	4.4	UNIT 5: PALEOSOL Fine sand with slight oxidation and organic matter	1770 ± 30 BP
4.4	4.6	UNIT 6: DEBRIS FLOOD	-

Sample	Depth (mbgs)	Date
◆ BGC-TP-48 Unit 1	0.5	-
◆ BGC-TP-48 Unit 3	2.15	-
◆ BGC-TP-48 Unit 3	2.15	1130 ± 30 BP
◆ BGC-TP-48 Unit 5	4.35	1770 ± 30 BP

TEST PIT # BGC-TP-9

Date:	07 August, 2013
Location:	5660173 N 617597 E
Datum:	UTM NAD 83
Elevation:	1330 masl (taken from Google Earth, approximate)
Equipment:	Excavator
Logged by:	Matthias Jakob, Stephanie Bale, Brent MacDonald
Total Depth:	4.0 m

Depth From (mbgs)	Depth To (mbgs)	Lithologic Description
0	1	UNIT 1: FILL Disturbed backfill material, lots of rootlets
1	1.3	UNIT 2: FLOOD Clast supported matrix, coarse sands to gravels, Dmax=15cm, may just be lens, subangular to subrounded
1.3	2.1	UNIT 3: DEBRIS FLOOD Massive, no imbrication, matrix supported medium to coarse grained sands, Dmax=30cm, finer sands approaching bottom
2.1	3.1	UNIT 4: FLOOD Loose, clast supported pockets within a predominantly matrix supported unit, Dmax=30cm, pea to gravel size, matrix is medium grained sand, subrounded
3.1	4	UNIT 5: DEBRIS FLOOD Dmax=40cm, matrix supported medium course sand matrix

Sample	Depth (mbgs)
◆ BGC-TP-9 Unit 3	1.7

TEST PIT # BGC-TP-20

Date: 07 August, 2013
Location: 5659595 N 616724 E
Datum: UTM NAD 83
Elevation: 1306 masl (taken from Google Earth, approximate)
Equipment: Excavator
Logged by: Matthias Jakob, Stephanie Bale, Brent MacDonald
Total Depth: 4.35 m

Depth From (mbgs)	Depth To (mbgs)	Lithologic Description	Date
0	0.4	UNIT 1 Overbank deposit, sitly sand	-
0.4	1	UNIT 2: FLUVIAL Clast supported, Dmax=15cm, subangular, subrounded, rounded	-
1	1.65	UNIT 3: DEBRIS FLOOD Dmax=30cm, massive, matrix supported, medium to coarse sand matrix, rootlets	-
1.65	2.25	UNIT 4: DEBRIS FLOOD Same as Unit 3	-
2.25	2.65	UNIT 5: FLUVIAL Cleaner than Unit 2, coarser grained sands, clast supported, imbricated, Dmax=30cm	-
2.65	3.15	UNIT 6: DEBRIS FLOOD Matrix supported debris flow deposit, subangular to subrounded, Dmax=30cm	-
3.15	3.35	UNIT 7: PALEOSOL Peat lenses, contorted, continuous	1070 ± 30 BP
3.35	4.35	UNIT 8: DEBRIS FLOOD matrix supported debris flood deposit, Dmax=225cm, loose to compact, subrounded	-

Sample	Depth (mbgs)	Date
◆ BGC-TP-20 Unit 7	3.25	1070 ± 30 BP
◆ BGC-TP-20 8	3.85	-

TEST PIT # BGC-TP-30

Date: 07 August, 2013
Location: 5659985 N 616372 E
Datum: UTM NAD 83
Elevation: 1313 masl (taken from Google Earth, approximate)
Equipment: Excavator
Logged by: Matthias Jakob, Stephanie Bale, Brent MacDonald
Total Depth: 4.65 m

Depth From (mbgs)	Depth To (mbgs)	Lithologic Description	Date
0	0.4	UNIT 1: DEBRIS FLOOD 2013 flood, matrix supported, medium to coarse sands, Dmax=30cm, gravel lenses (5 cm thick), cleaner	-
0.4	0.5	UNIT 2: SOIL Rootlets, silty sandy soil with some pebble to gravel clasts, dark brown	-
0.5	0.8	UNIT 3: DEBRIS FLOOD Variable matrix, silty sandy in upper portion, medium coarse in lower, rootlets, Dmax=15cm	-
0.8	1.3	UNIT 4: DEBRIS FLOOD Medium sand matrix, Dmax=30cm, massive	-
1.3	1.8	UNIT 5: DEBRIS FLOOD Massive matrix supported, medium to coarse sands, fine sands at transition, Dmax=40cm	-
1.8	3.7	UNIT 6: DEBRIS FLOOD Transitional debris flood, loose sandy gravel with some boulders, matrix to clast supported, majority clast supported, distal debris flood deposit	1570 ± 30 BP
3.7	3.95	UNIT 7 Fine sand flood/ overbank deposit	-
3.95	4.15	UNIT 8 Fluvial gravel, Dmax=25cm	-
4.15	4.45	UNIT 9 Fluvial sands	1650 ± 30 BP
4.45	4.65	UNIT 10: DEBRIS FLOOD	-

Sample	Depth (mbgs)	Date
◆ BGC-TP-30 Unit 1	0.2	-
◆ BGC-TP-30 Unit 6	2.6	1570 ± 30 BP
◆ BGC-TP-30 Unit 9	4.3	-
◆ BGC-TP-30 Unit 9	4.15	1650 ± 30 BP

TEST PIT # BGC-TP-13

Date:	08 August, 2013
Location:	5659555 N 617837 E
Datum:	UTM NAD 83
Elevation:	1301 masl (taken from Google Earth, approximate)
Equipment:	Excavator
Logged by:	Matthias Jakob, Stephanie Bale, Brent MacDonald
Total Depth:	3.5 m

Depth From (mbgs)	Depth To (mbgs)	Lithologic Description	Date
0	0.4	UNIT 1 Soil overbank deposit, silty sandy matrix, modern rootlets present	-
0.4	0.45	UNIT 2: PALEOSOL Poorly developed paleosol of 5 cm thickness, slightly wavy contact with underlying unit	2650 ± 30 BP
0.45	1	UNIT 3 Silty sandy matrix with medium grained sand lenses up to cm thick and 10-20 cm in length	-
1	1.05	UNIT 4: PALEOSOL Weakly developed paleosol 3-5 cm thick, modern rootlets, wavy contact with underlying unit more wavy than Unit 2 contact	-
1.05	1.3	UNIT 5 Same medium grained lenses as Unit 2, wavy sand lenses	3180 ± 30 BP
1.3	1.5	UNIT 6 Predominantly sand and gravel with traces of silty sandy lenses, Dmax=5cm	-
1.5	1.55	UNIT 7: PALEOSOL Same as Unit 2	-
1.55	1.6	UNIT 8	-
1.6	2.5	UNIT 9: FLUVIAL Clast supported, sandy gravels, Dmax=10cm	-
2.5	3.5	UNIT 10: FLUVIAL Clast supported, fluvial gravel, less coarse than Unit 9, mild imbrication	-

Sample	Depth (mbgs)	Date
◆ BGC-TP-13 Unit 2	0.4	2650 ± 30 BP
◆ BGC-TP-13 Unit 5	1.15	3180 ± 30 BP
◆ BGC-TP-13 Unit 10	3.0	-

TEST PIT # BGC-TP-21

Date: 08 August, 2013
Location: 5659923 N 616586 E
Datum: UTM NAD 83
Elevation: 1318 masl (taken from Google Earth, approximate)
Equipment: Excavator
Logged by: Matthias Jakob, Stephanie Bale, Brent MacDonald
Total Depth: 4.7 m

Depth From (mbgs)	Depth To (mbgs)	Lithologic Description	Date
0	0.45	UNIT 1: FILL	-
0.45	0.75	UNIT 2 Silty sandy overflow material (could be fill from pipeline), varying thickness from 20-60 cm	-
0.75	0.85	UNIT 3: PALEOSOL Silty sandy paleosol, lots of rootlets present, wavy contact	830 ± 30 BP
0.85	2	UNIT 4: DEBRIS FLOOD Debris flood and transitional debris flood zone, variable matrix, medium sand to granular matrix, Dmax=20cm	-
2	2.3	UNIT 5: PALEOSOL Weakly developed paleosol or oxidized overflow	1180 ± 30 BP
2.3	4	UNIT 6: DEBRIS FLOOD/ FLOOD Sandy gravels, interbedded units of matrix supported debris flood deposits and clast supported flood deposits, individual events cannot be distinguished, Dmax=20cm, abundant organics, weakly oxidized paleosol between fluvial gravels (weakly developed), east and west pit wall are different	1490 ± 30 BP 2770 ± 30 BP
4	4.7	UNIT 7: DEBRIS FLOOD Matrix supported debris flood deposit, subangular rocks, no imbrication, Dmax=10-15cm	-

Sample	Depth (mbgs)	Date
◆ BGC-TP-21 Unit 2	0.6	-
◆ BGC-TP-21 Unit 3	0.8	830 ± 30 BP
◆ BGC-TP-21 Unit 4	1.75	-
◆ BGC-TP-21 Unit 5	2.05	1180 ± 30 BP
◆ BGC-TP-21 Unit 6	2.7	1490 ± 30 BP
◆ BGC-TP-21 Unit 6	3.8	2770 ± 30 BP

TEST PIT # BGC-TP-38

Date:	07 August, 2013
Location:	5661150 N 616322 E
Datum:	UTM NAD 83
Elevation:	1325 masl (taken from Google Earth, approximate)
Equipment:	Excavator
Logged by:	Matthias Jakob, Stephanie Bale, Brent MacDonald
Total Depth:	4.0 m

Depth From (mbgs)	Depth To (mbgs)	Lithologic Description	Date
0	0.4	UNIT 1: FILL Most likely fill material	-
0.4	0.95	UNIT 2: DEBRIS FLOOD Matrix supported, subangular to subrounded, unsorted, no imbrication, well defined peat layer at bottom, fine to medium sand matrix, Dmax=20cm	0 ± 30 BP
0.95	1.6	UNIT 3: DEBRIS FLOOD Normally graded, clast to matrix supported with pea to gravel sized weakly developed lenses (1.7 m long/ 15 cm wide), more unconsolidated at top and more cemented at bottom, Dmax=20cm	-
1.6	3	UNIT 4: DEBRIS FLOOD Generally unsorted with gravel sized lenses (poorly developed 40 cm across by 4 cm thick), Dmax=19cm, subangular to subrounded, matrix supported	-
3	3.2	UNIT 5: FLOOD Clast supported subrounded gravel, slight imbrication, loose, Dmax=15cm	-
3.2	3.75	DEBRIS FLOOD Same as Unit 4	-
3.75	3.8	UNIT 6: PALEOSOL Organic rich silty sands overplayed by fine sands, dark brown to black, overlying reddish ochre coloured silty sands	570 ± 30 BP
3.8	4	UNIT 7: DEBRIS FLOOD Same as Unit 4	-

Sample	Depth (mbgs)	Date
◆ BGC-TP-38 Unit 2	0.7	-
◆ BGC-TP-38 Unit 2	0.95	0 ± 30 BP
◆ BGC-TP-38 Unit 3	1.3	-
◆ BGC-TP-38 Unit 6	3.8	570 ± 30 BP

APPENDIX D
RADIOCARBON DATES

Table D-1. Radiocarbon ages obtained on Cougar Creek fan.

Trench ID	Depth[1] (m)	Dated Materials	Context[2]	Conventional radiocarbon age ^{14}C yr BP[3]	2-sigma calibrated age (Cal yr BP)	Lab No.
BGC-TP-13 Unit 2	0.4	Charred material	Paleosol	2650 (+/- 30 BP)	Cal BC 840 to 790 (Cal BP 2780 to 2740)	356799
BGC-TP-13 Unit 5	1.15	Charred material	Paleosol	3180 (+/- 30 BP)	Cal BC 1500 to 1410 (Cal BP 3450 to 3360)	356791
BGC-TP-15 Unit 1	1.0	Wood	Fill	106.6 (+/- 0.3 pMC[4])		356805
BGC-TP-15 Unit 2	1.1	Charred material	Paleosol	760 (+/- 30 BP)	Cal AD 1220 to 1280 (Cal BP 730 to 670)	356808
BGC-TP-15 Unit 3	1.6	Charred material	Distal Fan Overbank Deposit	2840 (+/- 30 BP)	Cal BC 1110 to 1100 (Cal BP 3060 to 3050)/Cal BC 1080 to 1060 (Cal BP 3030 to 3010)/Cal BC 1060 to 920 (Cal BP 3000 to 2870)	356806
BGC-TP-15 Unit 8	3.0	Charred material	Paleosol	3010 (+/- 30 BP)	Cal BC 1380 to 1340 (Cal BP 3330 to 3280)/Cal BC 1320 to 1190 (Cal BP 3270 to 3140)/Cal BC 1180 to 1160 (Cal BP 3130 to 3110)/Cal BC 1140 to 1130 (Cal BP 3090 to 3080)	356809
BGC-TP-18 Unit 4	3.6	Charred material	Tephra	2390 (+/- 30 BP)	Cal BC 700 to 700 (Cal BP 2650 to 2650)/Cal BC 540 to 530 (Cal BP 2490 to 2480)/Cal BC 520 to 400 (Cal BP 2470 to 2350)	356800
BGC-TP-18 Unit 6	4.1	Charred material	Paleosol	2440 (+/- 30 BP)	Cal BC 750 to 680 (Cal BP 2700 to 2630)/Cal BC 670 to 610 (Cal BP 2620 to 2560)/Cal BC 600 to 400 (Cal BP 2550 to 2360)	356807
BGC-TP-18 Unit 8	4.85	Charred material	Paleosol	2870 (+/- 30 BP)	Cal BC 1130 to 970 (Cal BP 3080 to 2920)/Cal BC 960 to 940 (Cal BP 2910 to 2890)	356801
BGC-TP-19 Unit 3	1.5	Plant Material	Debris Flood Deposit	100.5 (+/- 0.3 pMC)		356803
BGC-TP-19 Unit 4	1.9	Wood	Distal Fan Overbank Deposit	800 (+/- 30 BP)	Cal AD 1190 to 1200 (Cal BP 760 to 750)/Cal AD 1210 to 1270 (Cal BP 740 to 680)	356804
BGC-TP-19 Unit 6	3.2	Organic sediment	Debris Flood Deposit	1140 (+/- 30 BP)	Cal AD 780 to 790 (Cal BP 1170 to 1160)/Cal AD 810 to 850 (Cal BP 1140 to 1100)/Cal AD 850 to 980 (Cal BP 1100 to 970)	356802
BGC-TP-20 Unit 7-B	3.25	Charred material	Paleosol	1070 (+/- 30 BP)	Cal AD 900 to 920 (Cal BP 1060 to 1030)/Cal AD 940 to 1020 (Cal BP 1010 to 930)	356792
BGC-TP-21 Unit 3	0.8	Charred material	Paleosol	830 (+/- 30 BP)	Cal AD 1160 to 1260 (Cal BP 790 to 690)	356790
BGC-TP-21 Unit 5 Organics	2.05	Organic sediment	Paleosol	180 (+/- 30 BP)	Cal AD 1650 to 1690 (Cal BP 300 to 260)/Cal AD 1730 to 1810 (Cal BP 220 to 140)/Cal AD 1840 to 1840 (Cal BP 110 to 110)/Cal AD 1850 to 1860 (Cal BP 100 to 90)/Cal AD 1860 to 1870 (Cal BP 90 to 80)/Cal AD 1920 to post 1950 (Cal BP 30 to post 1950)	356786
BGC-TP-21 Unit 5 Tree Stump East Face	2.05	Wood	Paleosol	1180 (+/- 30 BP)	Cal AD 770 to 900 (Cal BP 1180 to 1050)/Cal AD 920 to 940 (Cal BP 1030 to 1010)	356784
BGC-TP-21 Unit 6 East Face Paleosol	3.8	Organic sediment	Landslide Dam Outbreak Flood Deposit	2770 (+/- 30 BP)	Cal BC 1000 to 840 (Cal BP 2950 to 2780)	356783
BGC-TP-21 Unit 6 East Face Sand Deposit	2.7	Organic sediment	Debris Flood Deposit	1490	Cal AD 540 to 640 (Cal BP 1410 to 1310)	356785

Trench ID	Depth[1] (m)	Dated Materials	Context[2]	Conventional radiocarbon age ^{14}C yr BP[3]	2-sigma calibrated age (Cal yr BP)	Lab No.
				(+/- 30 BP)		
BGC-TP-30 Unit 6	2.6	Plant Material	Debris Flood Deposit	1570 (+/- 30 BP)	Cal AD 420 to 560 (Cal BP 1530 to 1390)	356797
BGC-TP-30 Unit 9	4.15	Charred material	Distal Fan Overbank Deposit	1650 (+/- 30 BP)	Cal AD 340 to 430 (Cal BP 1610 to 1520)	356787
BGC-TP-38 Unit 2	0.95	Plant Material	Landslide Dam Outbreak Flood Deposit	0 (+/- 30 BP)		356796
BGC-TP-38 Unit 6	3.8	Charred material	Paleosol	570 (+/- 30 BP)	Cal AD 1300 to 1360 (Cal BP 640 to 590)/Cal AD 1380 to 1420 (Cal BP 570 to 530)	356782
BGC-TP-41 Unit 5	2.8	Charred material	Paleosol	970 (+/- 30 BP)	Cal AD 1020 to 1160 (Cal BP 930 to 800)	356798
BGC-TP-41 Unit 7	3.65	Charred material	Paleosol	1200 (+/- 30 BP)	Cal AD 720 to 740 (Cal BP 1230 to 1210)/Cal AD 770 to 890 (Cal BP 1180 to 1060)	356795
BGC-TP-41 Unit 9	4.3	Charred material	Paleosol	1450 (+/- 30 BP)	Cal AD 560 to 650 (Cal BP 1390 to 1300)	356789
BGC-TP-48 Unit 3	2.15	Charred material	Paleosol	1130 (+/- 30 BP)	Cal AD 830 to 840 (Cal BP 1120 to 1110)/Cal AD 870 to 990 (Cal BP 1080 to 960)	356793
BGC-TP-48 Unit 5	4.35	Organic sediment	Paleosol	1770 (+/- 30 BP)	Cal AD 180 to 190 (Cal BP 1770 to 1760)/Cal AD 210 to 340 (Cal BP 1740 to 1610)	356794

[1] Depth below ground surface
[2] Context based on grain size analysis and field classifications
[3] BP = Before Present (1950)
[4] pMC = Percent Modern Carbon

APPENDIX E
DENDROCHRONOLOGY

Table E-1. Record of inferred debris flood/large flood dates on Cougar Creek determined by correlating growth anomalies in 70 sampled trees.

Inferred Event Date	Number of Samples	Likelihood*	Known events from other sources
1674	2	Possible	
1694	2	Possible	
1793	2	Possible	
1804	3	Possible	
1811	3	Possible	
1819	2	Possible	
1830	3	Possible	
1833	2	Possible	
1840	3	Possible	
1844	5	Likely	
1851	2	Possible	
1857	3	Possible	
1861	3	Possible	
1868	3	Possible	
1871	3	Possible	
1876	5	Likely	
1879	4	Likely	High Bow River discharge at Calgary (Alberta WaterSMART)[1]
1884	8	Very Likely	
1886	2	Possible	
1891	4	Likely	
1894	4	Likely	
1897	1	Unlikely	High Bow River discharge at Calgary (Alberta WaterSMART)
1902	2	Possible	High Bow River discharge at Calgary (Alberta WaterSMART)
1905	6	Very Likely	
1911	4	Likely	
1915	2	Possible	High Bow River discharge at Calgary (Alberta WaterSMART)
1918	6	Very Likely	
1921	4	Likely	

Inferred Event Date	Number of Samples	Likelihood*	Known events from other sources
1923	7	Very Likely	High Bow River discharge at Calgary (Alberta WaterSMART)
1929	6	Very Likely	High Bow River discharge at Calgary (Alberta WaterSMART)
1932	1	Unlikely	High Bow River discharge at Calgary (Alberta WaterSMART)
1935	5	Likely	
1941	2	Possible	
1944	4	Likely	
1948	5	Likely	Reported flood (CH2M Hill) [2]
1950	3	Possible	
1956	4	Likely	Reported flood (CH2M Hill)
1959	3	Possible	
1963	5	Likely	
1967	7	Very Likely	Reported flood (CH2M Hill)
1970	4	Likely	
1974	5	Likely	Reported flood (CH2M Hill)
1980	4	LIkely	Reported flood (CH2M Hill)
1984	6	Very Likely	
1988	3	Possible	
1990			Reported flood (CH2M Hill)
1995	2	Possible	
1997	4	Likely	
2000	10	Very Likely	
2003	3	Possible	
2005	2	Possible	Reported flood (AMEC, 2007) [3]
2012	1	Unlikely	Reported flood (AMEC, 2012) [4]

* Likelihood of sample representing a flood or debris flood event.

[1] Alberta WaterSMART Solutions Ltd. (2013) The 2013 Great Alberta Flood: Actions to Mitigate, Manage and Control Future Floods.

[2] CH2M HILL Engineering Ltd. (1994) Cougar Creek Flood Risk Mapping Study. Final report prepared for Alberta Environmental Protection, River Engineering Branch. March 1994.

[3] AMEC Earth & Environmental Ltd. (2007) Sediment Transport and Flood Hydrology in Cougar Creek. Report prepared for the Town of Canmore. May 2007.

[4] AMEC Earth & Environmental Ltd. (2012) Cougar Creek 2012 Flood Damage Repairs. Report prepared for the Town of Canmore. August 2012.

APPENDIX F
BOW RIVER DISCHARGE AT CALGARY

(From "The 2013 Great Alberta Flood: Actions to Mitigate, Manage and Control Future Floods" prepared by Alberta Water SMART Water Management Solutions Ltd. August 2013.)

Figure 2: Maximum Water Discharge in the Bow River at Calgary between 1879 – 2013

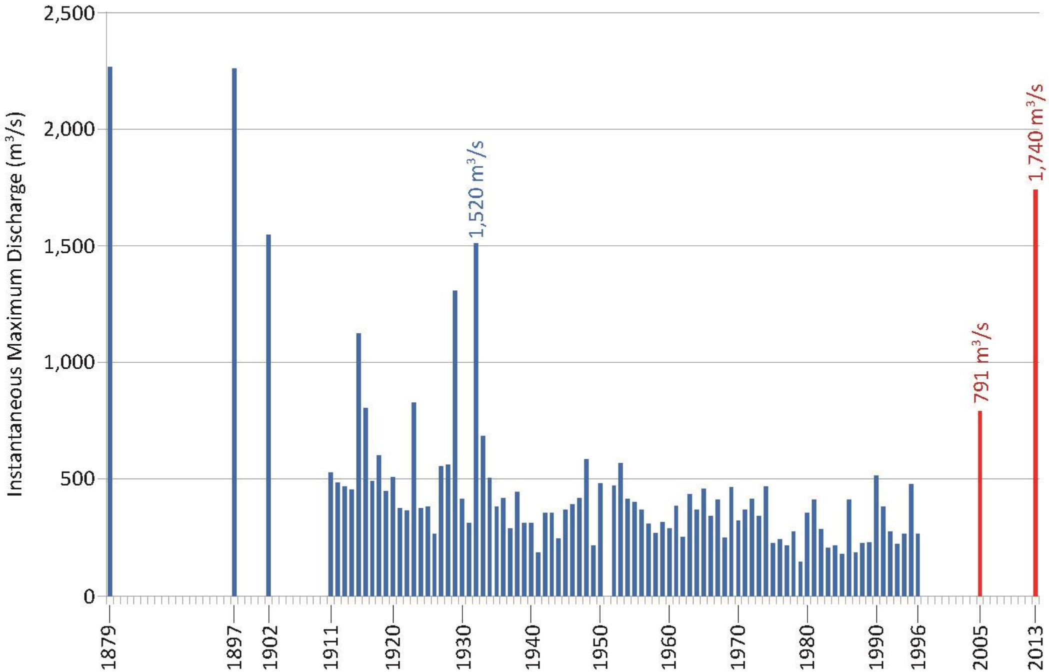

Source: Modified from Neill, C.R. and Watt, W.E., 2001. Report on Six Case Studies of Flood Frequency Analysis. Prepared for Alberta Transportation and Civil Engineering Division Civil Projects. April 2001. Figure 5.1 p44

DRAWINGS

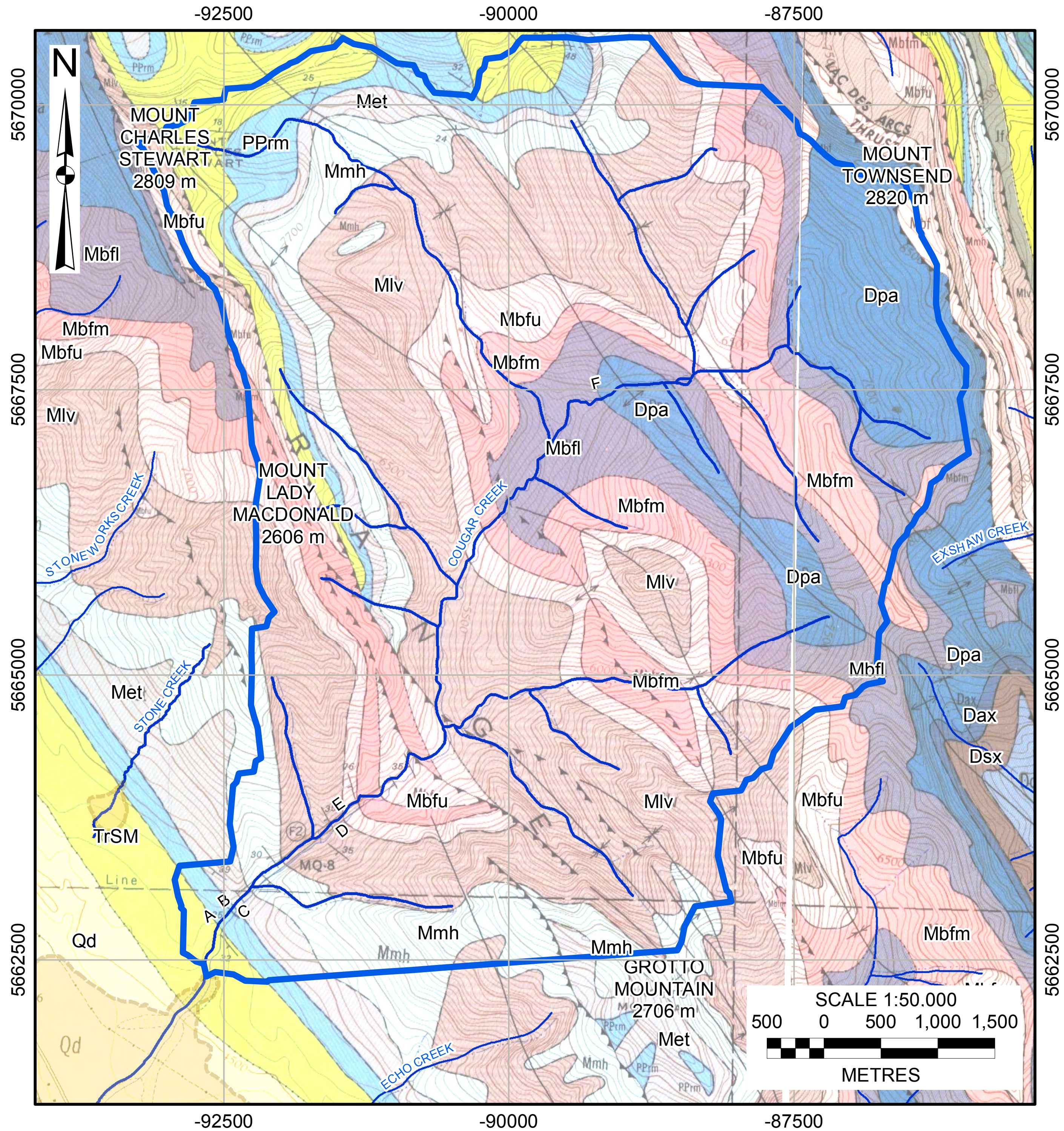

50 m CONTOUR INTERVAL (GEOBASE)

LEGEND

- GEOLOGICAL BOUNDARY (APPROXIMATE, ASSUMED)
- GEOLOGICAL BOUNDARY (ASSUMED PROJECTION UNDER COVER OF YOUNGER DEPOSITS)
- BEDDING, TOPS KNOWN (INCLINED, VERTICAL, OVERTURNED)
- BEDDING, TOPS UNKNOWN (INCLINED, VERTICAL)
- FORM LINES (OCCUR IN STRUCTURE SECTIONS ONLY)
- FAULT, GENETIC TYPE UNKNOWN (APPROXIMATE, ASSUMED)
- FAULT (ASSUMED PROJECTION UNDER COVER OF YOUNGER DEPOSITS)
- THRUST FAULT (TEETH ON UPTHRUST SIDE; DEFINED, APPROXIMATE, ASSUMED)
- THRUST FAULT (ASSUMED PROJECTION UNDER COVER OF YOUNGER DEPOSITS)
- ANTICLINE (TRACE OF AXIAL PLANE, DEFINED, APPROXIMATE)
- SYNCLINE (TRACE OF AXIAL PLANE, DEFINED, APPROXIMATE)
- ANTICLINE, SYNCLINE (OVERTURNED)
- F1 FOSSIL LOCALITY
- MQ-8 STRATIGRAPHIC SECTION, LOCUS OF MEASUREMENT (NUMBERS REFER TO INTERNAL CATALOGUING SYSTEM)
- COUGAR CREEK WATERSHED
- FAN BOUNDARY

Dax	**ALEXO FORMATION**: THINLY BEDDED SILTY DOLOMITE, DOLOMITIC SANDSTONE, LIGHT GREY DOLOMITE, AND BRECCIA
Dpa	**PALLISER FORMATION**: THICKLY BEDDED AND MASSIVE, MOTTLED DOLOMITIC LIMESTONE; GREY DENSE LIMESTONE; GREYISH BROWN DOLOMITE
Dsx	**SOUTHESK FORMATION**: MASSIVE TO THICKLY BEDDED, LIGHT TO MEDIUM GREY; FINELY TO COARSELY CRYSTALLINE DOLOMITE; GREYISH BROWN FINELY TO COARSELY CRYSTALLINE DOLOMITE
Mlv	**LIVINGSTONE FORMATION**: LIGHT GREY SKELETAL CALCARENITE AND CALCARENITIC LIMESTONE; CHERTY LIMESTONE; DOLOMITE
Mbfl	**EXSHAW AND BANFF FORMATIONS**: LOWER PART: DARK GREY AND BROWNISH GREY SHALE AND CALCAREOUS SHALE; BROWN ARGILLACEOUS SILTSTONE; ARGILLACEOUS AND CHERTY LIMESTONE
Mbfm	**EXSHAW AND BANFF FORMATIONS**: MIDDLE PART: LIGHT TO DARK GREY SKELETAL CALCARENITE, CALCARENITIC LIMESTONE, AND ARGILLACEOUS AND DOLOMITIC LIMESTONE
Mbfu	**EXSHAW AND BANFF FORMATIONS**: UPPER PART: DARK GREY, CHERTY ARGILLACEOUS AND DOLOMITIC LIMESTONE AND CALCARENITIC LIMESTONE, AND BROWNISH GREY ARGILLACEOUS DOLOMITE
Met	**ETHERINGTON FORMATION**: LIGHT GREY LIMESTONE, CHERTY LIMESTONE AND CALCARENITIC LIMESTONE; DOLOMITE; CHERTY DOLOMITE; GREEN AND RED SHALE; SILTSTONE; BRECCIA
Mmh	**MOUNT HEAD FORMATION**
Mmhu	**MOUNT HEAD FORMATION**: UPPER PART, DENSE DARK GREY AND BLACK LIMESTONE, ARGILLACEOUS LIMESTONE, AND DOLOMITE, SILTY DOLOMITE
PPrm	**ROCKY MOUNTAIN GROUP**: LIGHT GREY QUARTZ SANDSTONE, DOLOMITIC SANDSTONE, SILTY DOLOMITE; CHERT
Qd	TILL, ALLUVIUM, COLLUVIUM; GRAVEL, SAND, SILT
TrSM	**SULPHUR MOUNTAIN FORMATION**: DARK GREY AND BROWN, THIN-BEDDED SILTSTONE, SILTY MUDSTONE, SHALE, AND DOLOMITIC SILTSTONE

3TM

REV.	DATE	REVISION NOTES	DRAWN	CHECK	APPR.

SCALE:	1:50,000
DATE:	MAR 2014
DRAWN:	ST
DESIGNED:	SB
CHECKED:	MJ
APPROVED:	HW

PROFESSIONAL SEAL:

BGC ENGINEERING INC.
AN APPLIED EARTH SCIENCES COMPANY

CLIENT: TOWN OF CANMORE

PROJECT: COUGAR CREEK DEBRIS FLOOD HAZARD ASSESSMENT

TITLE: BEDROCK GEOLOGY OF COUGAR CREEK WATERSHED

PROJECT No.:	DWG No.:	REV.:
1261001	01	

DWG TO BE READ WITH BGC REPORT TITLED "COUGAR CREEK DEBRIS FLOOD HAZARD ASSESSMENT" DATED MARCH 2014

X:\Projects\1261001\Workspace\20131101_Report_Cougar_Creek_Debris_Flood_Hazard_Assessment\01_Bedrock_Geology_of_Cougar_Creek_Watershed.mxd Date: Thursday, March 06, 2014 Time: 10:43 AM

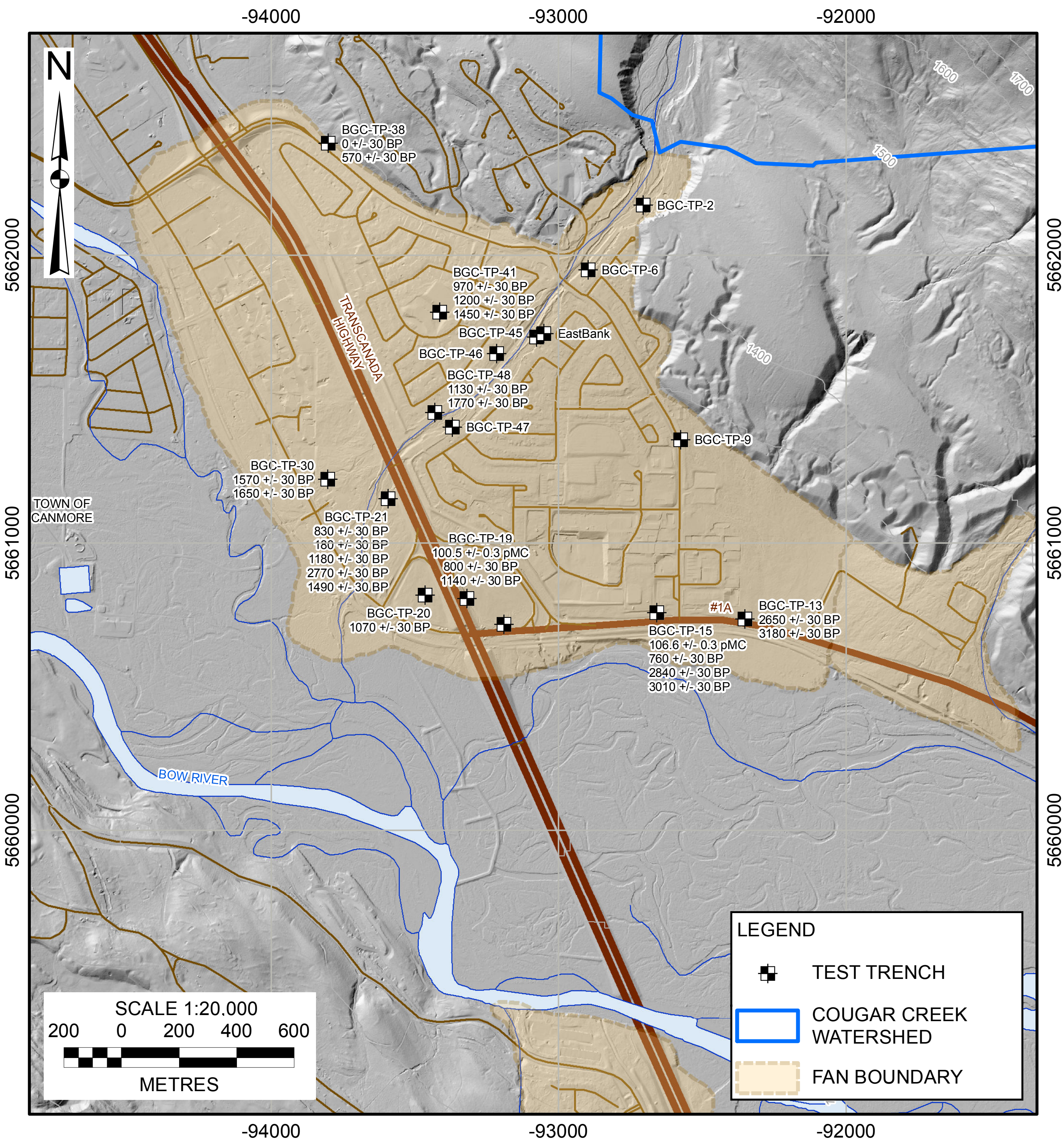

3TM

X:\Projects\1261001\Workspace\20131101_Report_Cougar_Creek_Debris_Flood_Hazard_Assessment\02_Test_Trench_Locations_Showing_Radiocarbon_Ages_of_Collected_Samples.mxd Date: Thursday, March 06, 2014 Time: 10:48 AM

SCALE:	1:20,000	DESIGNED:	SB
DATE:	MAR 2014	CHECKED:	MJ
DRAWN:	JS	APPROVED:	HW

BGC ENGINEERING INC.
AN APPLIED EARTH SCIENCES COMPANY

PROJECT:
COUGAR CREEK DEBRIS FLOOD HAZARD ASSESSMENT

TITLE:
TEST TRENCH LOCATIONS SHOWING RADIOCARBON AGES OF COLLECTED SAMPLES

CLIENT:
TOWN OF CANMORE

PROJECT No.:	DWG No.:	REV.:
1261001	02	

DWG TO BE READ WITH BGC MEMO TITLED "COUGAR CREEK DEBRIS FLOOD HAZARD ASSESSMENT" DATED MARCH 2014

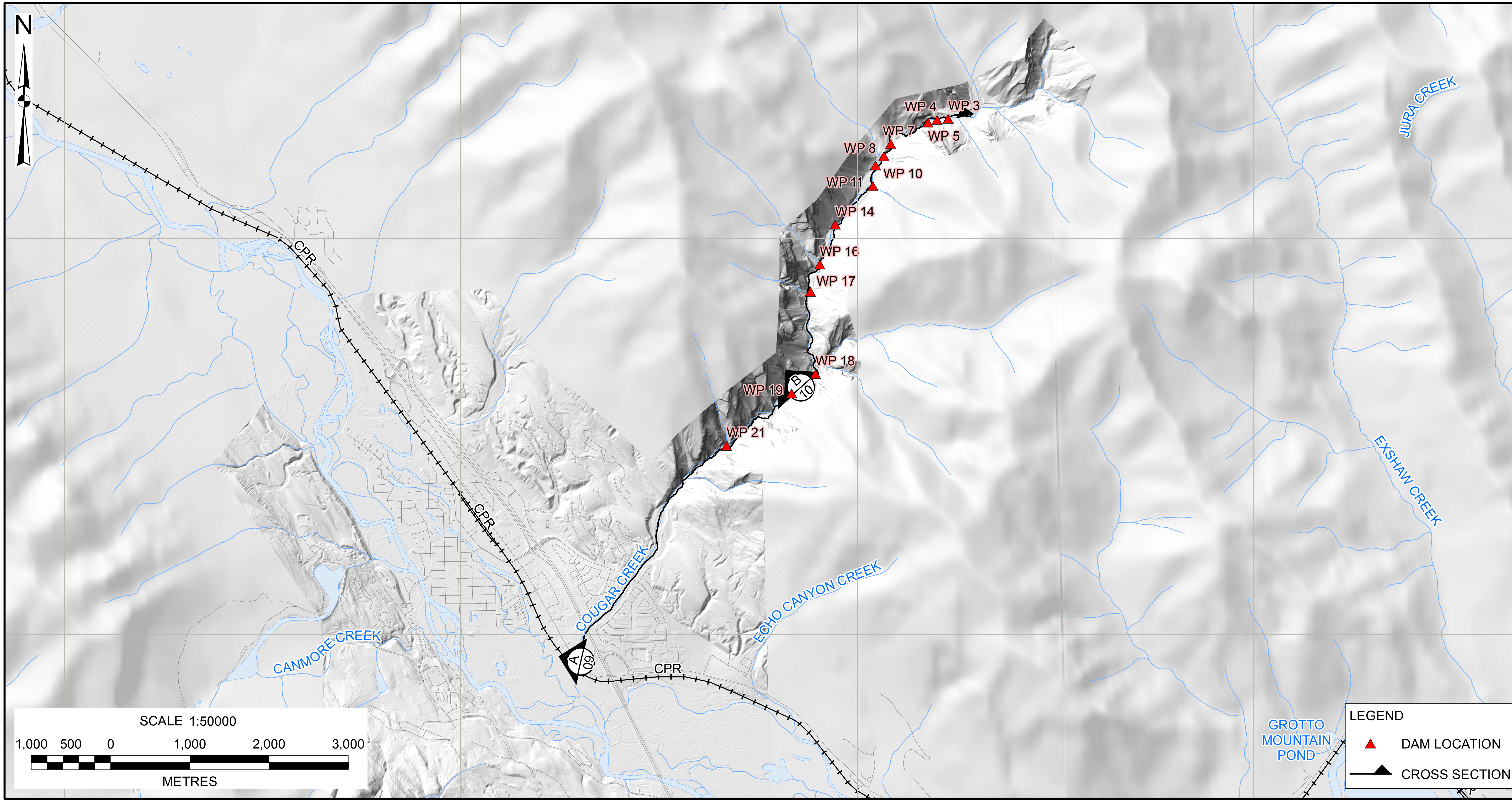

X:\Projects\1261\001\Workspace\20131101_Report_Cougar_Creek_Debris_Flood_Hazard_Assessment\03_Historic_Landslide_Dam_Locations.mxd Date: Thursday, March 06, 2014 Time: 10:50 AM

REV.	DATE	REVISION NOTES	DRAWN	CHECK	APPR.

SCALE:	AS SHOWN
DATE:	MAR 2014
DRAWN:	LL, MIB-C
DESIGNED:	MJ
CHECKED:	HW
APPROVED:	MJ

PROFESSIONAL SEAL:

BGC ENGINEERING INC.
AN APPLIED EARTH SCIENCES COMPANY

CLIENT:
TOWN OF CANMORE

PROJECT:
COUGAR CREEK DEBRIS FLOOD HAZARD ASSESSMENT

TITLE:
HISTORIC LANDSLIDE DAM LOCATIONS

PROJECT No.:	DWG No.:	REV.:
1261001	03	

DWG TO BE READ WITH BGC REPORT TITLED "COUGAR CREEK DEBRIS FLOOD HAZARD ASSESSMENT" DATED MARCH 2014

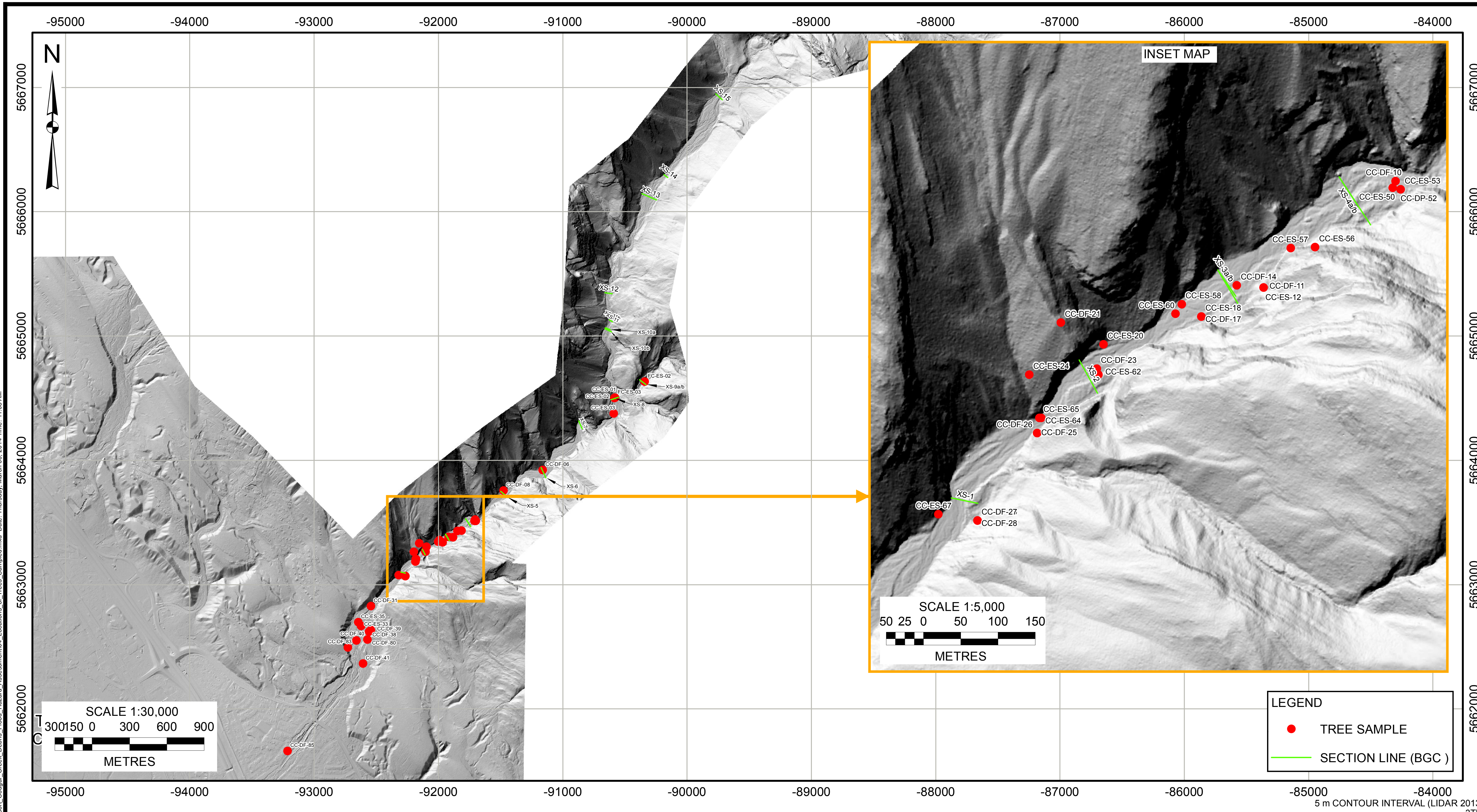

5 m CONTOUR INTERVAL (LIDAR 2013)
3TM

X:\Projects\1261001\Workspace\20131101_Report_Cougar_Creek_Debris_Flood_Hazard_Assessment\04_Locations_of_Trees_Sampled.mxd Date: Thursday, March 06, 2014 Time: 11:08 AM

REV.	DATE	REVISION NOTES	DRAWN	CHECK	APPR.

SCALE:	1:30,000
DATE:	MAR 2014
DRAWN:	JS
DESIGNED:	SB
CHECKED:	MJ
APPROVED:	HW

PROFESSIONAL SEAL:

BGC ENGINEERING INC.
AN APPLIED EARTH SCIENCES COMPANY

CLIENT:
TOWN OF CANMORE

PROJECT:
COUGAR CREEK DEBRIS FLOOD HAZARD ASSESSMENT

TITLE:
LOCATION OF TREES SAMPLED ALONG COUGAR CREEK

PROJECT No.:	DWG No.:	REV.:
1261001	04	

DWG TO BE READ WITH BGC REPORT TITLED "COUGAR CREEK DEBRIS FLOOD HAZARD ASSESSMENT" DATED MARCH 2014

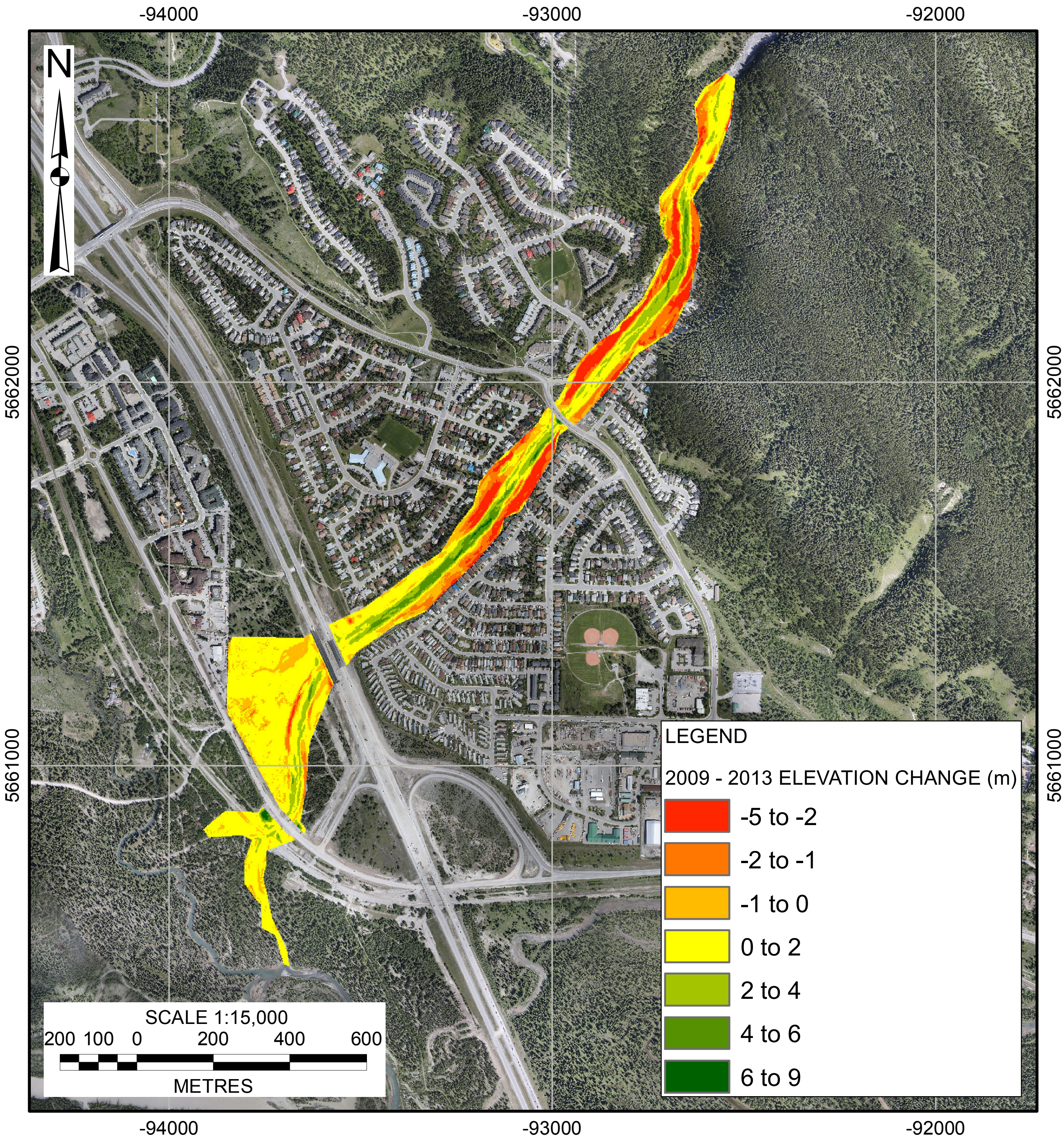

3TM

SCALE:	1:15,000	DESIGNED:	HW
DATE:	MAR 2014	CHECKED:	MJ
DRAWN:	JS	APPROVED:	HW

BGC ENGINEERING INC.
AN APPLIED EARTH SCIENCES COMPANY

PROJECT:
COUGAR CREEK DEBRIS FLOOD HAZARD ASSESSMENT

TITLE:
COMPARISON OF 2009 AND 2013 LIDAR DATA
FOR COUGAR CREEK CHANNEL

CLIENT:
TOWN OF CANMORE

PROJECT No.:	DWG No.:	REV.:
1261001	05	

DWG TO BE READ WITH BGC REPORT TITLED "COUGAR CREEK DEBRIS FLOOD HAZARD ASSESSMENT" DATED MARCH 2014

X:\Projects\1261\001\Workspace\20131101_Report_Cougar_Creek_Debris_Flood_Hazard_Assessment\05_Lidar_Comparison.mxd Date: Thursday, March 06, 2014 Time: 11:14 AM

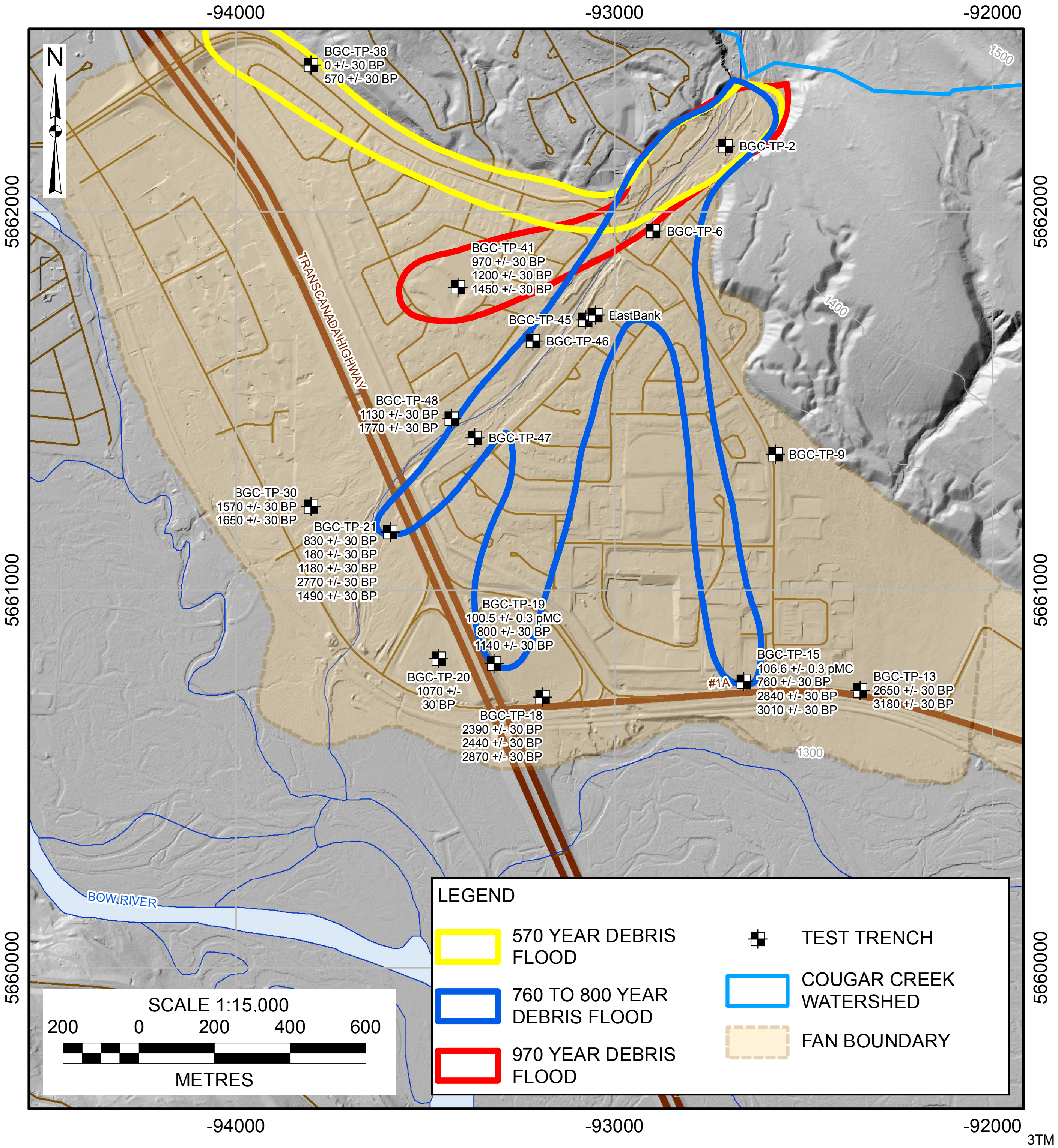

X:\Projects\1261001\Workspace\20131101_Report_Cougar_Creek_Debris_Flood_Hazard_Assessment\06_Interpreted_Debris_Flood_Lobes_570_to_970_Years_BP.mxd Date: Thursday, March 06, 2014 Time: 11:23 AM

SCALE:	1:15,000	DESIGNED:	HW
DATE:	MAR 2014	CHECKED:	MJ
DRAWN:	IL/JS	APPROVED:	HW

BGC ENGINEERING INC.
AN APPLIED EARTH SCIENCES COMPANY

PROJECT: COUGAR CREEK DEBRIS FLOOD HAZARD ASSESSMENT

TITLE: INTERPRETED DEBRIS FLOOD LOBES 570 TO 970 YEARS BP

CLIENT: TOWN OF CANMORE

PROJECT No.:	DWG No.:	REV.:
1261001	06	

DWG TO BE READ WITH BGC REPORT TITLED "COUGAR CREEK DEBRIS FLOOD HAZARD ASSESSMENT" DATED MARCH 2014

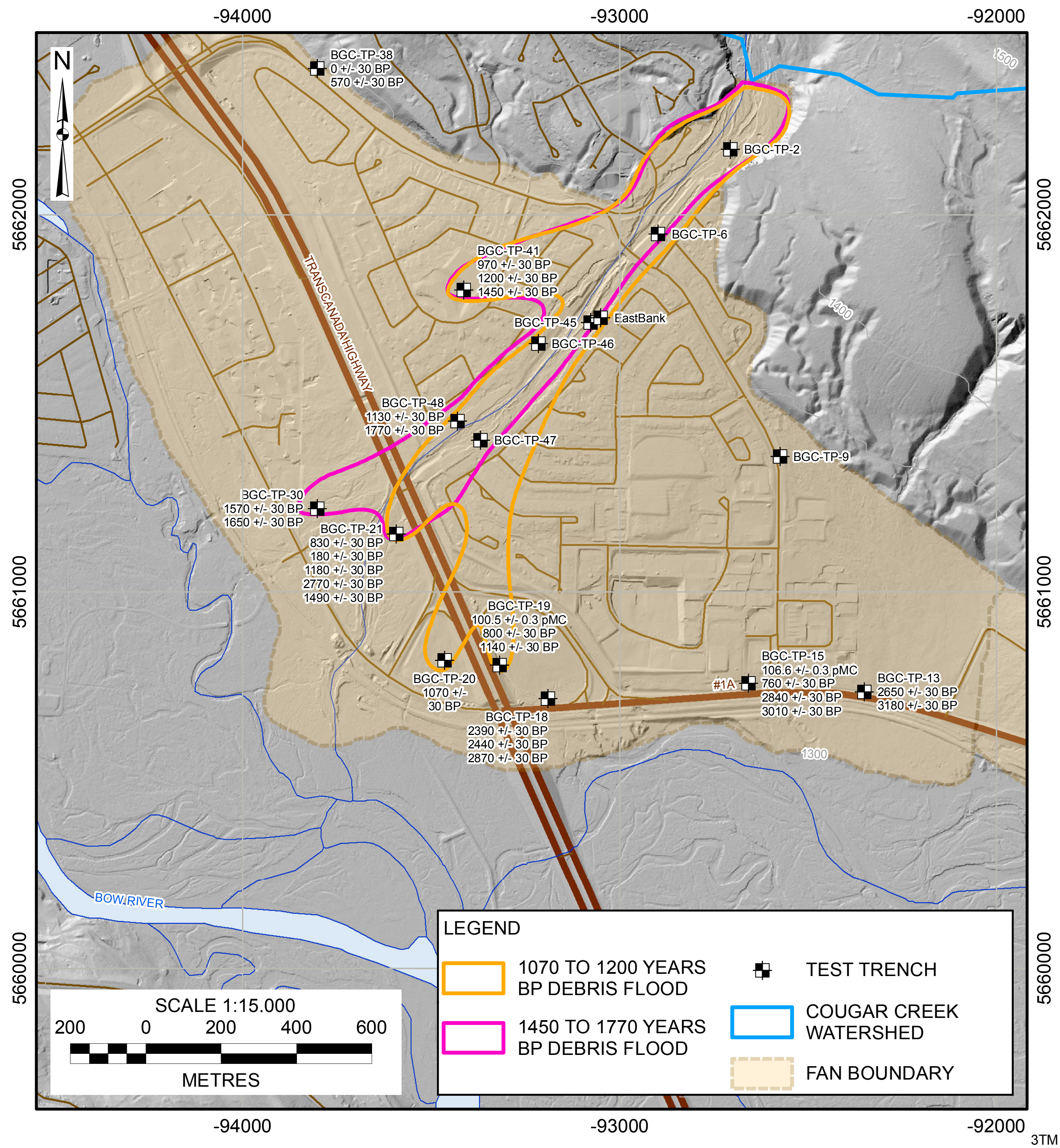

SCALE:	1:15,000	DESIGNED:	HW
DATE:	MAR 2014	CHECKED:	MJ
DRAWN:	IL/JS	APPROVED:	HW

BGC ENGINEERING INC.
AN APPLIED EARTH SCIENCES COMPANY

PROJECT:
COUGAR CREEK DEBRIS FLOOD HAZARD ASSESSMENT

TITLE:
INTERPRETED DEBRIS FLOOD LOBES 1070 TO 1770 YEARS BP

CLIENT:
TOWN OF CANMORE

PROJECT No.:	DWG No.:	REV.:
1261001	07	

DWG TO BE READ WITH BGC REPORT TITLED "COUGAR CREEK DEBRIS FLOOD HAZARD ASSESSMENT" DATED MARCH 2014

X:\Projects\1261001\Workspace\20131101_Report_Cougar_Creek_Debris_Flood_Hazard_Assessment\07_Interpreted_Debris_Flood_Lobes_1070_to_1770_Years_BP.mxd Date: Thursday, March 06, 2014 Time: 11:31 AM

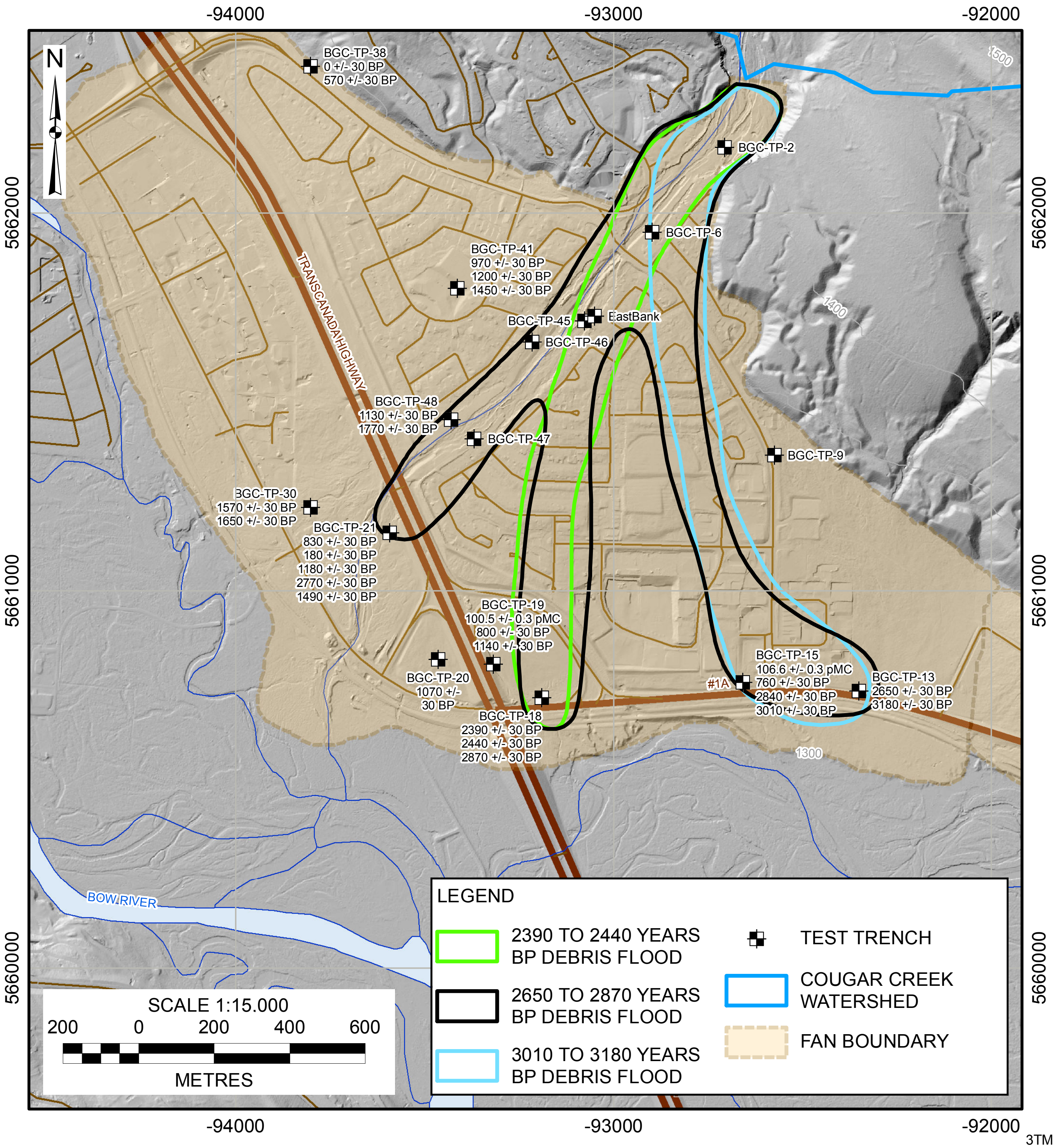

AS A MUTUAL PROTECTION TO OUR CLIENT, THE PUBLIC, AND OURSELVES, ALL REPORTS AND DRAWINGS ARE SUBMITTED FOR THE CONFIDENTIAL INFORMATION OF OUR CLIENT FOR A SPECIFIC PROJECT. AUTHORIZATION FOR ANY USE AND/OR PUBLICATION OF THIS REPORT OR ANY DATA, STATEMENTS, CONCLUSIONS OR ABSTRACTS FROM OR REGARDING OUR REPORTS AND DRAWINGS, THROUGH ANY FORM OF PRINT OR ELECTRONIC MEDIA, INCLUDING WITHOUT LIMITATION, POSTING OR REPRODUCTION OF SAME ON ANY WEBSITE, IS RESERVED PENDING BGC'S WRITTEN APPROVAL. IF THIS REPORT IS ISSUED IN AN ELECTRONIC FORMAT, AN ORIGINAL PAPER COPY IS ON FILE AT BGC ENGINEERING INC. AND THAT COPY IS THE PRIMARY REFERENCE WITH PRECEDENCE OVER ANY ELECTRONIC COPY OF THE DOCUMENT, OR ANY EXTRACTS FROM OUR DOCUMENTS PUBLISHED BY OTHERS.

SCALE:	1:15,000	DESIGNED:	HW
DATE:	MAR 2014	CHECKED:	MJ
DRAWN:	IL/JS	APPROVED:	HW

BGC ENGINEERING INC.
AN APPLIED EARTH SCIENCES COMPANY

PROJECT: COUGAR CREEK DEBRIS FLOOD HAZARD ASSESSMENT

TITLE: INTERPRETED DEBRIS FLOOD LOBES 2390 TO 3180 YEARS BP

CLIENT: TOWN OF CANMORE

PROJECT No.:	DWG No.:	REV.:
1261001	08	

X:\Projects\1261001\Workspace\20131101_Report_Cougar_Creek_Debris_Flood_Hazard_Assessment\08_Interpreted_Debris_Flood_Lobes_2390_to_3180_Years_BP.mxd Date: Thursday, March 06, 2014 Time: 11:46 AM

DWG TO BE READ WITH BGC REPORT TITLED "COUGAR CREEK DEBRIS FLOOD HAZARD ASSESSMENT" DATED MARCH 2014

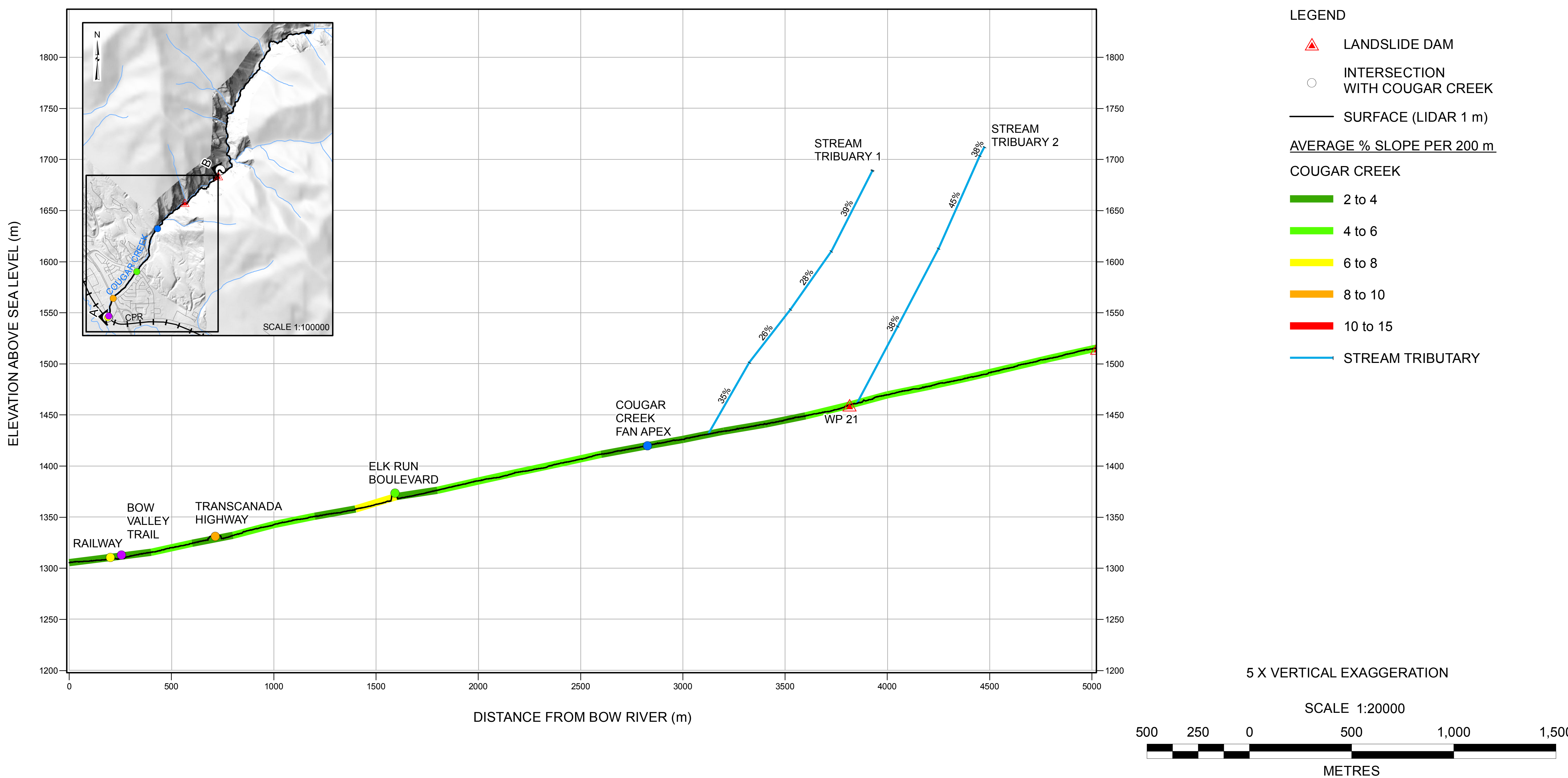

X:\Projects\1261\001\Workspace\20131101_Report_Cougar_Creek_Debris_Flood_Hazard_Assessment\09_Cougar_Creek_Profile_A.mxd Date: Thursday, March 06, 2014 Time: 11:53 AM

REV.	DATE	REVISION NOTES	DRAWN	CHECK	APPR.

SCALE: AS SHOWN
DATE: MAR 2014
DRAWN: LL, MIB-C
DESIGNED: MJ
CHECKED: HW
APPROVED: MJ

PROFESSIONAL SEAL:

BGC ENGINEERING INC.
AN APPLIED EARTH SCIENCES COMPANY

CLIENT: TOWN OF CANMORE

PROJECT: COUGAR CREEK DEBRIS FLOOD HAZARD ASSESSMENT

TITLE: COUGAR CREEK PROFILE A

PROJECT No.: 1261001
DWG No.: 09
REV.:

DWG TO BE READ WITH BGC REPORT TITLED "COUGAR CREEK DEBRIS FLOOD HAZARD ASSESSMENT" DATED MARCH 2014

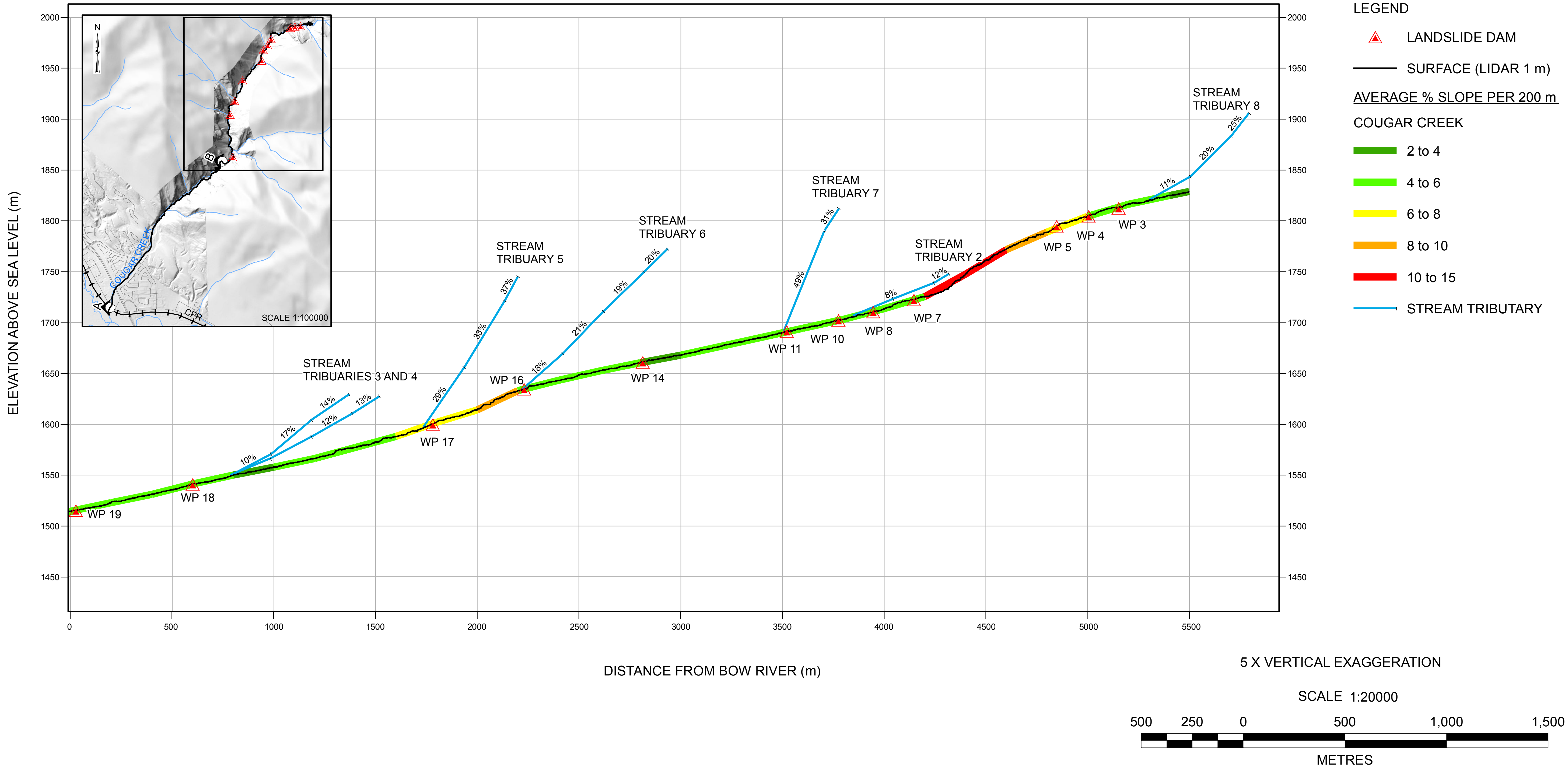

AS A MUTUAL PROTECTION TO OUR CLIENT, THE PUBLIC, AND OURSELVES, ALL REPORTS AND DRAWINGS ARE SUBMITTED FOR THE CONFIDENTIAL INFORMATION OF OUR CLIENT FOR A SPECIFIC PROJECT. AUTHORIZATION FOR ANY USE AND/OR PUBLICATION OF THIS REPORT OR ANY DATA, STATEMENTS, CONCLUSIONS OR ABSTRACTS FROM OR REGARDING OUR REPORTS AND DRAWINGS, THROUGH ANY FORM OF PRINT OR ELECTRONIC MEDIA, INCLUDING WITHOUT LIMITATION, POSTING OR REPRODUCTION OF SAME ON ANY WEBSITE, IS RESERVED PENDING BGC'S WRITTEN APPROVAL. IF THIS REPORT IS ISSUED IN AN ELECTRONIC FORMAT, AN ORIGINAL PAPER COPY IS ON FILE AT BGC ENGINEERING INC. AND THAT COPY IS THE PRIMARY REFERENCE WITH PRECEDENCE OVER ANY ELECTRONIC COPY OF THE DOCUMENT, OR ANY EXTRACTS FROM OUR DOCUMENTS PUBLISHED BY OTHERS.

REV.	DATE	REVISION NOTES	DRAWN	CHECK	APPR.

SCALE:	AS SHOWN
DATE:	MAR 2014
DRAWN:	LL, MIB-C
DESIGNED:	MJ
CHECKED:	HW
APPROVED:	MJ

PROFESSIONAL SEAL:

BGC ENGINEERING INC.
AN APPLIED EARTH SCIENCES COMPANY

CLIENT:
TOWN OF CANMORE

PROJECT:
COUGAR CREEK DEBRIS FLOOD HAZARD ASSESSMENT

TITLE:
COUGAR CREEK PROFILE B

PROJECT No.:	DWG No.:	REV.:
1261001	10	

DWG TO BE READ WITH BGC REPORT TITLED "COUGAR CREEK DEBRIS FLOOD HAZARD ASSESSMENT" DATED MARCH 2014

X:\Projects\1261001\Workspace\20131101_Report_Cougar_Creek_Debris_Flood_Hazard_Assessment\10_Cougar_Creek_Profile_B.mxd Date: Thursday, March 06, 2014 Time: 11:55 AM

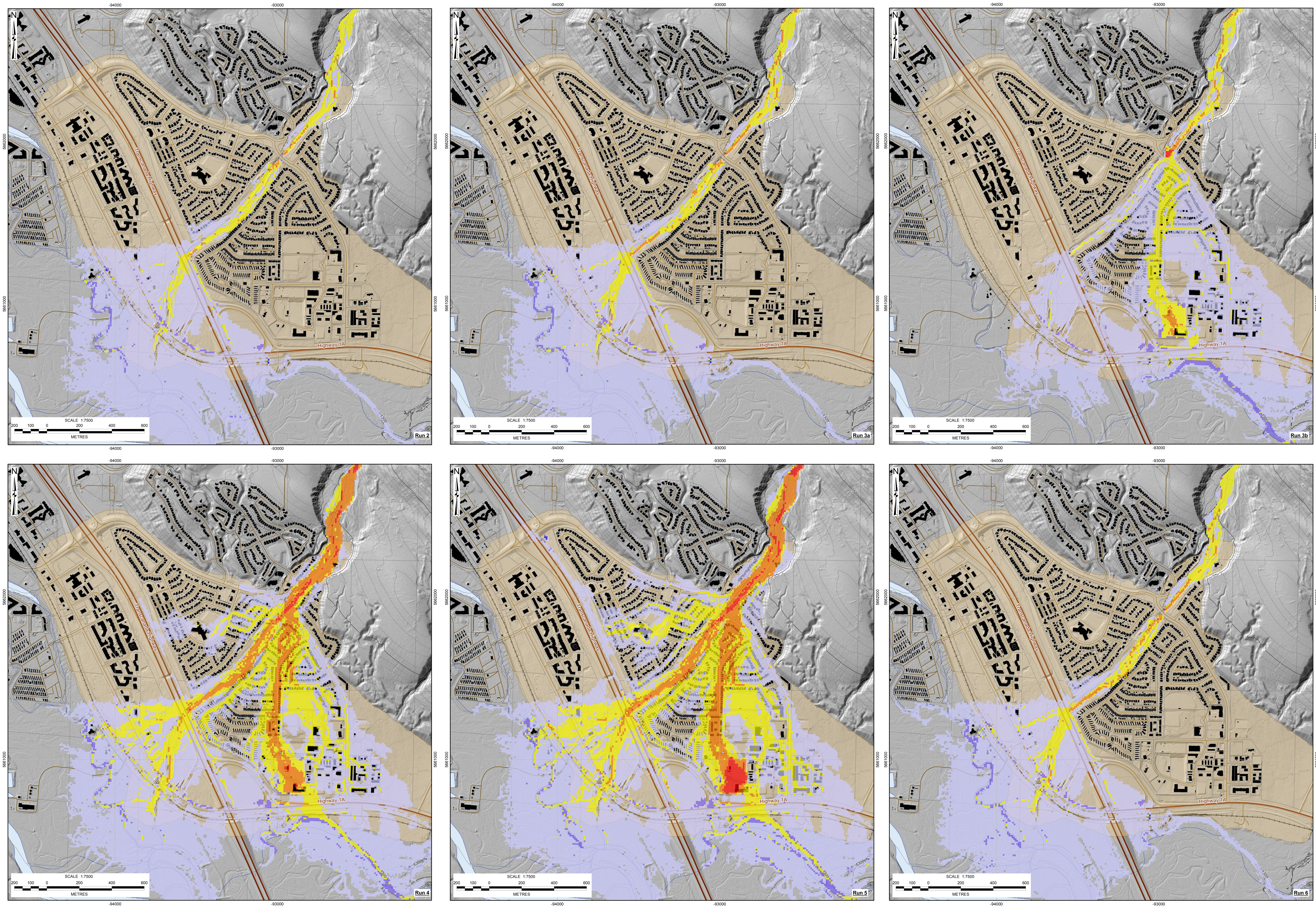

LEGEND

FLOW DEPTH (m) (v < 1 m/s)
- < 1
- 1 to 2.5
- > 2.5

IMPACT INTENSITY (m^2/s^2) (v > 1 m/s)
- < 10
- 10 to 100
- > 100

- PARCELS
- BUILDING
- FAN BOUNDARY
- ROAD
- HIGHWAY
- RAILWAY
- WATERCOURSE
- WATERBODY

NOTES:
1. ROADS, STREAMS AND WATERBODIES FROM NRCAN CANVEC.
2. TOPOGRAPHY DERIVED FROM LIDAR RECEIVED FROM TOWNSHIP OF CANMORE, JULY 2013.
3. PARCELS, ROADS, GAS LINES, SANITARY, STORM AND WATER SYSTEMS OBTAINED FROM TOWN OF CANMORE.

LIMITATIONS:
1. MODELLED DEBRIS FLOOD SCENARIOS ARE LABELLED IN THE LOWER RIGHT HAND CORNER OF EACH MAP INSET.
2. SEE THE REPORT FOR DESCRIPTION OF METHODS AND LIMITATIONS OF MODELLING.

3TM

REV.	DATE	REVISION NOTES	DRAWN	CHECK	APPR.

SCALE:	1:7,500
DATE:	MAR 2014
DRAWN:	GLT
DESIGNED:	MJ, KH
CHECKED:	MJ, HW, KH
APPROVED:	MJ, KH

PROFESSIONAL SEAL:

BGC ENGINEERING INC.
AN APPLIED EARTH SCIENCES COMPANY

CLIENT: TOWN OF CANMORE

PROJECT: COUGAR CREEK DEBRIS FLOOD HAZARD ASSESSMENT

TITLE: DEBRIS FLOOD INTENSITY: SURFACE INFRASTRUCTURE (RUNS 2-6)

PROJECT No.:	DWG No.:	REV.:
1261001	11	

DWG TO BE READ WITH BGC REPORT TITLED "COUGAR CREEK DEBRIS FLOOD HAZARD ASSESSMENT" DATED MARCH 2014